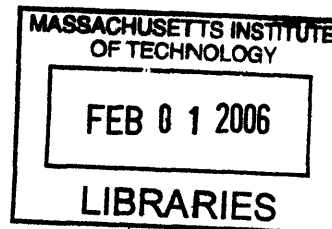# ClpX interactions with ClpP, SspB, protein substrate and nucleotide

by

Greg Louis Hersch

B.S. Biochemistry
University of California at Davis, 2001

*Submitted to the Department of Biology in partial fulfillment
of the requirements for the degree of*

Doctor of Philosophy in Biochemistry

at the

Massachusetts Institute of Technology

February 2006

*The authors hereby grants to MIT permission to reproduce and to distribute publicly
Paper and electronic copies of the thesis document in whole or in part.*

Signature of Author: _____
Department of Biology

Certified by: _____
Robert T. Sauer
Salvador E. Luria Professor of Biology
Thesis Supervisor

Accepted by: _____
Stephen P. Bell
Professor of Biology
Co-Chair, Biology Graduate Committee

ClpX interactions with ClpP, SspB, protein substrate and nucleotide

By

Greg Louis Hersch

Submitted to the Department of Biology on February 6th, 2006 in partial fulfillment of the requirements for the degree of doctor of philosophy in biochemistry

ABSTRACT

ClpXP and related ATP-dependent proteases are implements of cytosolic protein destruction. They couple chemical energy, derived from ATP hydrolysis, to the selection, unfolding, and degradation of protein substrates with the appropriate degradation signals. The ClpX component of ClpXP is a hexameric enzyme that recognizes protein substrates and unfolds them in an ATP-dependent reaction. Following unfolding, ClpX translocates the unfolded substrate into the ClpP peptidase for degradation.

The best characterized degradation signal is the ssrA-degradation tag, which contains a binding site for ClpX and an adjacent binding site for the SspB adaptor protein. I show that the close proximity of these binding elements causes SspB binding to mask signals needed for ssrA-tag recognition by ClpX. The SspB dimer overcomes this signal masking by tethering itself and bound substrate to ClpX, via docking sites located in the dimeric N-terminal domain of ClpX. Because this N-domain dimer binds only a single SspB subunit, the ClpX hexamer can accommodate just one SspB dimer per hexamer. Other adaptor proteins that use these same tethering sites must compete with SspB for access to ClpXP. Substrates bearing ssrA tags with increased spacing between the SspB and ClpX binding elements are degraded more efficiently at low concentrations by ClpXP. This mechanism in which the adaptor first obstructs and then stimulates substrate recognition may have evolved to permit an additional level of regulation of substrate choice. SspB binding to ssrA-tagged substrate is a highly dynamic process, allowing rapid transfer of substrates from SspB to ClpX.

Although the ClpX hexamer is composed of six identical polypeptides, individual subunits assume at least three distinct conformations. Using a hexamer that was engineered to prevent nucleotide hydrolysis, I show that some nucleotide-binding sites in ClpX release ATP rapidly, others release ATP slowly, and at least two sites remain nucleotide free. Occupancy of both the slow sites by ATP and the fast sites by either ATP or ADP is required to bind the degradation tags of protein substrates. The ability of ClpX to retain binding of substrate with ATP or ADP in the fast sites suggests that nucleotide hydrolysis in the fast sites, but not in the slow sites, will allow repeated unfolding attempts without substrate release over multiple ATPase cycles. My results rule out ATPase models including $ClpX_6 \bullet ATP_6$ or ADP_6 and also suggest that the enzyme hydrolyzes only a fraction of bound ATP in a single turnover event.

Short peptide motifs of ClpX, known as IGF loops, interact with ClpP and change conformation as a response to nucleotide binding by ClpX. As ClpX varies its nucleotide content during the ATP hydrolysis cycle, it also varies its affinity for ClpP. Processing of substrates is coupled to the ATP-hydrolysis cycle of ClpX and appears to modulate ClpX's affinity for ClpP by changing how long each ClpX subunit spends in each nucleotide state.

Thesis Supervisor: Robert T. Sauer
Title: Salvador Luria Professor of Biology

TABLE OF CONTENTS

LIST OF FIGURES AND TABLES

Appendix: **Communication between ClpX and ClpP during substrate processing and degradation**

* work of Shilpa A. Joshi

CHAPTER ONE

An introduction to ClpX, ClpP, SspB, and the

AAA+ superfamily of ATPases

Part I: Introduction

The roles of energy dependent proteolysis

Many cytosolic proteins ultimately meet their fate at the hands of ATP-dependent proteases. This destruction is required to remove and recycle proteins that have become damaged by oxidation, heat unfolding and aggregation, or were simply translated from damaged mRNA (Gottesman, 1996). Energy-dependent proteases also destroy folded, native proteins as a signaling event. Examples of this occur as a response to DNA damage. environmental cues, and during the cell cycle (Jenal and Stephens, 2002; Gottesman, 2003; Jenal and Hengge-Aronis, 2003). Some of these same proteases function in quality assurance for the cell. Without quality control, translation of aberrant mRNA messages could result in partial protein products that aggregate or even actively interfere with vital cell processes. Instead, these proteins are recognized and removed by ATP-dependent proteases. Thus, energy dependent proteolysis allows the cell to dynamically control its proteome and respond rapidly to environmental cues. Energy-dependent proteases are all closely related, and belong to a much larger class of proteins called the AAA+ (ATPases associated with a variety of cellular activities) superfamily whose members all function in macromolecular disassembly (Neuwald et al., 1999; Vale, 2000; Glover and Tkach, 2001; Sauer et al., 2004).

E. coli ClpXP is an ATP-dependent protease, which degrades a wide range of substrates (Flynn et al., 2003). The best characterized substrates for ClpXP are those bearing the C-terminal ssrA peptide tag. The eleven-residue ssrA tag (AANDENYALAA), when appended to the C-terminus, can direct any protein to ClpXP for either *in vivo* or *in vitro*

degradation. In the cell, the ssrA tag is co-translationally attached to nascent polypeptides on ribosomes that stall at the end of mRNA lacking a stop codon or stall for other reasons (Keiler et al., 1996). Once tagged, these proteins are recognized by ClpXP and degraded. ClpXP also recognizes other substrates that do not bear the ssrA tag. It has been proposed that there are at least five distinct classes of ClpXP degradation tags, although other substrates which do not appear to fall into these classes have been identified (Flynn et al., 2003).

Below follows a brief introduction of how ClpX, ClpP, and the adaptor protein SspB interact with one another to select and degrade protein substrates. Although much is known about these proteins, many critical, unanswered questions remain. ClpX is a hexameric ATPase and understanding how ATP binding and hydrolysis support its function is an essential step towards understanding how it and related AAA+ proteins operate. How does nucleotide binding affect the conformation and properties of ClpX? Does ATP bind to all six nucleotide-binding sites on a hexamer? Are all bound ATPs equivalent? Do subunits hydrolyze all bound nucleotides simultaneously? Many models have been put forth in an attempt to explain the observed properties of AAA+ enzymes and various mutants. By summarizing what is known about ATP binding and utilization by members of the AAA+ superfamily, I will emphasize commonalities between the members as well as evidence both supporting and contradicting current models. Finally, by discussing the limitations of the experimental methods employed, I hope to highlight the inadequacy of narrow approaches to this problem

Figure 1

A

Native substrate   Strained substrate   Unfolded substrate

ATP hydrolysis   ATP hydrolysis   ATP hydrolysis   degradation

ClpX   ClpX   ClpX   + ClpP

B   ClpX (unfoldase)

ClpP (protease)

C   ClpP cutaway

Sequestered serine active sites
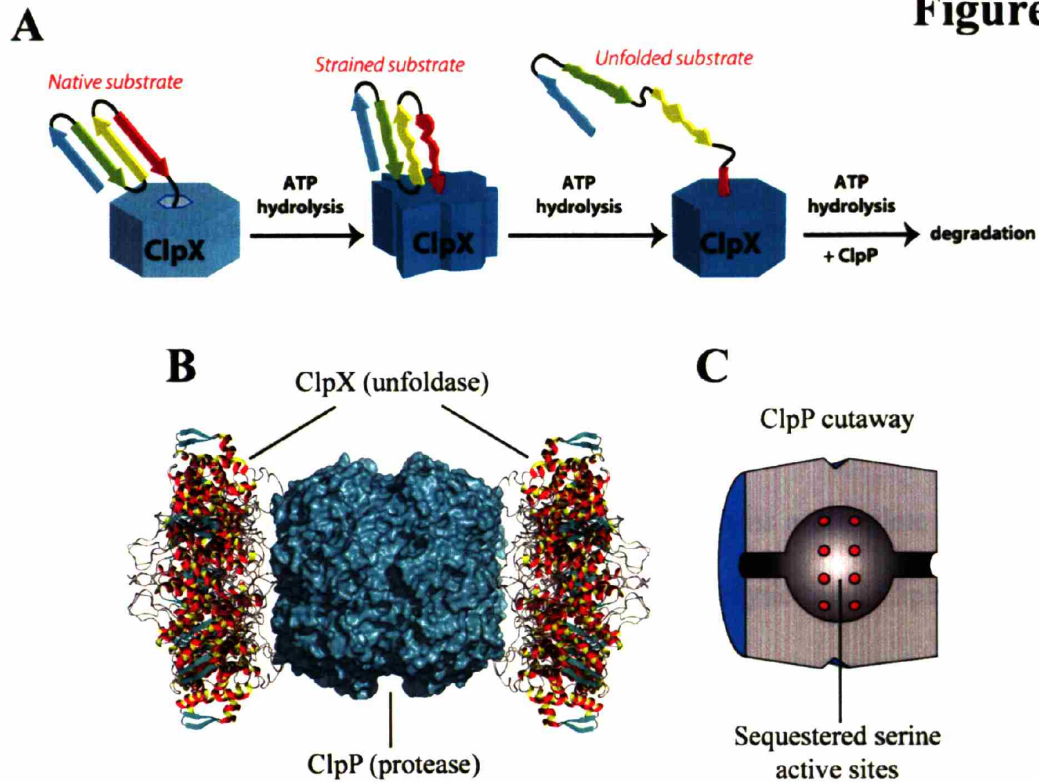
Compartmentalized proteolysis by ClpP

Proteolysis is not inherently energy dependent, as the hydrolysis of peptide bonds is an exergonic process. For instance, chymotrypsin and trypsin require no energy other than thermal energy to degrade substrates. Why do cytoplasmic proteases such as ClpXP require energy? ClpXP is capable of degrading stable substrates that possess significant secondary and tertiary structure and are resistant to proteolysis by non-energy requiring proteases. ClpXP achieves this by using energy from ATP hydrolysis to disrupt the native structure of protein substrates prior to proteolysis. Potential mechanisms for this disruption are discussed below. Importantly, because of ClpXP's unfolding activity, substrate selection is not subject to the same conformational constraints as energy-

independent proteases like chymotrypsin and trypsin. Because ClpXP is capable of destroying any cellular protein, substrate selection must be tightly controlled.

ClpXP is a complex of two proteins, ClpX and ClpP (Wojtkowiak et al., 1993). Substrate selection, unfolding, and ATP hydrolysis are carried out by ClpX. ClpP contains the proteolytic active sites and is made up of 14 subunits which form two seven-subunit rings that stack back-to-back (Fig. 1B). This arrangement results in a barrel-like structure with a large central cavity. Each of ClpP's 14 subunits contains a complete serine active site for peptide hydrolysis with a classical Ser, Asp, His catalytic triad. ClpP sequesters these active sites inside of its barrel-like structure (Fig. 1C). Access to the active sites is restricted by two axial portals on either end of the barrel. These portals have a minimum diameter of about 10 Å, disallowing passage of native, folded proteins (Wang et al., 1997). Consistently, isolated ClpP displays very little proteolytic activity towards even unfolded substrates. Small peptides that are able to diffuse through the axial portals are hydrolyzed efficiently by ClpP, demonstrating that lack of proteolysis for larger substrates is due to limited access rather than active site orientation or activation state (Thompson et al., 1994). Thus, ClpP's robust proteolytic ability is controlled by its small axial portals which restrict proteolysis to substrates that have been translocated into ClpP by ClpX.

ClpX and potential mechanisms of unfolding

As discussed above, ClpX recognizes substrates, unfolds them if needed, and then translocates them into ClpP for proteolysis in an ATP-dependent process. ClpXP's

substrate selection is carried out entirely by ClpX. Six identical polypeptides make up the ClpX hexamer, forming a cylindrical, hex-nut structure with a central pore. In the ClpXP complex, the pores of ClpX and ClpP are aligned, and substrates are translocated through this central pore (Ortega et al., 2000). Like ClpP's axial portals, the central pore of ClpX is too small to allow passage of folded proteins.

ClpXP, like other energy-dependent proteases, disrupts the tertiary structure of protein substrates prior to proteolysis. ATP hydrolysis by ClpX is coupled to the unfolding reaction, although the details of this coupling are far from clear. The most prominent model involves coupling the chemical energy of ATP hydrolysis by ClpX to an exertion of mechanical force on the bound protein, driving disruption of structure. However, other plausible models exist. In one such model, ClpX binds its substrate, but then simply waits to capture or trap a spontaneous unfolding event without exerting any mechanical stress on the protein. In this model, ClpX quickly binds to exposed, unfolded portions of the protein as they become available in a ratchet-like mechanism.

The *ratchet model* seems insufficient to explain ClpXP's potent protease activity. For instance, green fluorescent protein (GFP) with a C-terminal ssrA tag is degraded by ClpXP at a rate 10 million times faster than its spontaneous unfolding rate in solution (Kim et al., 2000). Although this observation makes the *ratchet model* unlikely, it does not render it completely untenable. Proteins in solution may exhibit substantially different properties than those bound to another protein. A substrate bound to ClpX likely experiences a substantially altered local environment, but no evidence exists to suggest

that this local environment is especially conducive to disruption of a protein's structure. Furthermore, if ClpX were quickly capturing unfolded portions of the protein as they were spontaneously exposed, one would expect a significantly higher affinity for unfolded over folded proteins. Contrary to this expectation, ClpX's affinity for an unfolded protein was found to be essentially unchanged with respect to its folded counterpart (Kenniston et al., 2003). One caveat to these experiments is that unfolding of the substrate protein was achieved by chemical modification of cysteines with a negatively charged carboxymethyl group, and thus this modified molecule does not mimic all aspects of a true unfolded, natural substrate. Nonetheless, one would expect some substantial difference in substrate affinity, which was not observed.

Instead, ClpX probably employs an active unfolding mechanism in which ATP binding and hydrolysis is coupled to the unfolding of substrates via mechanical stress. In a simplified version of the most current model, ClpX binds substrate and repeated ATP-hydrolysis cycles drive conformational changes in ClpX that disrupt the bound substrate's native fold (Fig. 1A). Later in chapter 5, I show direct evidence for conformational changes in ClpX that depend on the identity of bound nucleotide. How these conformational changes in ClpX are translated into substrate unfolding is unclear. One possibility is that substrates unfold during ClpX's attempt to engulf them. The pores of ClpX and ClpP are both too small to admit native proteins. In the *steric collision* model, ClpXP recognizes and binds the exposed degradation tag of a folded substrate. Subsequent attempts to translocate this tag and attached peptide sequence through the narrow central channel of ClpXP results in steric collisions of the folded portion of the

substrate with the central pore. In this model, unfolding of the protein substrate occurs when a steric collision occurs with the right geometry to unravel the protein's tertiary structure.

Part II: Interactions between ClpX, ClpP, adaptors, and substrate

ClpX's interactions with ClpP

ClpX must associate with ClpP to form a functional protease. At least one site of interaction between these two proteins has been located. ClpX contains an internal tri-peptide of sequence Ile-Gly-Phe (IGF) which extends from one face of ClpX as part of a surface loop (Fig. 2). Many experiments have suggested that these loops dock with ClpP, likely in seven hydrophobic pockets on either side of ClpP (red, Fig. 2). When the IGF loops of ClpX are mutated or removed, ClpX neither associates with ClpP nor delivers substrates for degradation. Wild-type ClpX associates with ClpP in an ATP-dependent fashion and isolated IGF peptides interact very weakly with ClpP (Joshi et al., 2004; Hersch et al., 2005), suggesting that ClpX hexamers specifically orient IGF loops for interaction with ClpP as a response to ATP binding.

Structural studies suggest that ClpP has seven potential sites of interaction on each face for ClpX's IGF loops (Wang et al., 1997). However, ClpX is a hexamer and thus possesses only six IGF loops. This asymmetry must result in at least one potential IGF docking site on ClpP being unfilled in the complex.

Figure 2
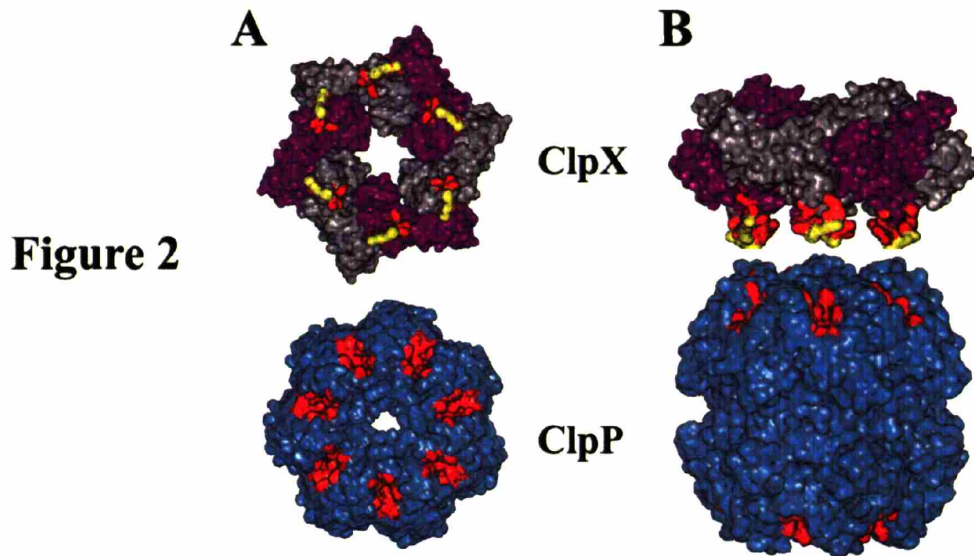
Why would ClpP want to have open docking sites? One possibility is to provide a way for ClpX to rotate with respect to ClpP. This feature was once an attractive model for explaining how ClpX drives translocation of substrates into ClpP. In this model, substrates were translocated by mechanism that resembles the way threaded screws enter a piece of wood when twisted as ClpX rotated with respect to ClpP. However, ClpX is capable of unfolding substrates in the absence of ClpP. Moreover, a full complement of IGF loops appears to be unnecessary for degradation of substrates (Joshi et al., 2004). Consistent with an asymmetric interaction not being an essential feature of the true mechanism, another ATP-dependent protease, HslUV, does not possess this asymmetry (both the ATPase and peptidase are hexamers) but catalyzes the same types of reactions as ClpXP (Sousa et al., 2000). The functional relevance of the asymmetric interaction of ClpX with ClpP remains an unanswered question in the field.

ClpX's interactions with the adaptor molecule, SspB and substrate

Proteins called adaptors can assist proteases in ATP-dependent degradation reactions. Adaptor proteins can bind substrate proteins in solution, and then dock with the protease. Substrate is then transferred to the protease for degradation and the adaptor protein is generally released, and not consumed by the reaction (Fig. 3). SspB is an 18 kDa protein that forms dimers in solution and can bind the ssrA tag of potential ClpXP substrates (Levchenko et al., 2000; Wah et al., 2002). It utilizes flexible C-terminal tails to tether itself to ClpXP and deliver substrates for degradation (Wah et al., 2003). By bringing substrate and protease together, the efficiency of degradation is enhanced. This enhancement is achieved by significantly increasing the apparent affinity of substrate for ClpXP and modestly increasing the speed at which they are degraded.

Figure 3
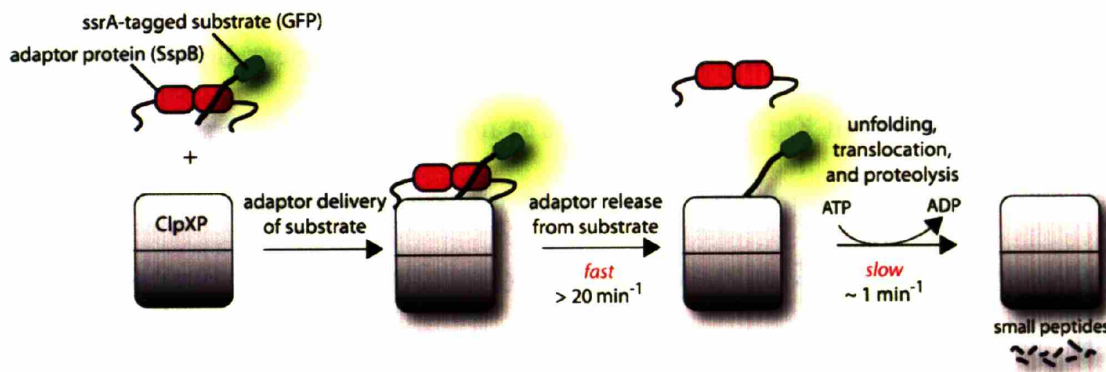
SspB and ClpX bind distinct residues of the ssrA tag. Of the 11 residues composing the ssrA tag, $\underline{A}^1\underline{A}^2\underline{N}^3\underline{D}^4E^5N^6\underline{Y}^7A^8\mathbf{L}^9\mathbf{A}^{10}\mathbf{A}^{11}$, the final $LAA\text{-}CO_2^-$ is the primary motif recognized by ClpXP (bold) (Flynn et al., 2001). The first four residues and the central Tyr^7 are recognized by SspB (underlined). No single residue is crucial for both ClpX and SspB recognition. As I will describe later in this thesis, unfavorable interactions occur when ClpX and SspB simultaneously bind the ssrA tag. Consequently, when proteins

bearing the ssrA tag are bound by SspB, the ssrA tag is obstructed and no longer efficiently recognized by ClpX (Hersch et al., 2004). The inhibitory effect of this masking is overcome by the C-terminal tails of SspB, which tether it to ClpXP. This tethering drives tag engagement by ClpXP by means of a high local concentration. The net effect of this *obstruct-then-stimulate* interaction is a ~20-fold increase in efficiency.

Central to SspB's activity as an adaptor is its ability to tether itself to ClpX. This interaction appears to be highly specific, because SspB does not deliver substrates to other closely related ATP-dependent proteases. ClpX and orthologs contain specialized regions which are not shared by other classes of AAA+ proteins (Neuwald et al., 1999). One such region, the N-terminal domain of ClpX, is essential for the enhancement of degradation by SspB. The isolated N-domain of ClpX forms dimers in solution (Wojtyra et al., 2003). Later in this thesis, I show that an isolated N-domain dimer of ClpX is sufficient for SspB recognition and that all of SspB's contacts with ClpX are made through this N-terminal domain (Bolon et al., 2004). The ClpX hexamer contains three N-domain dimers. Each dimer binds just one subunit of the SspB dimer, explaining why only a single SspB dimer binds efficiently to ClpX (Wah et al., 2002; Bolon et al., 2004).

SspB binds its ssrA-tagged substrates significantly more tightly than ClpX. How then are substrates transferred to ClpXP for degradation? As I discuss in chapter two, substrate dissociates from SspB much more rapidly than the processing (unfolding and degradation) of substrates by ClpXP (Figure 3). Since bound substrates are in a fast, dynamic equilibrium, ClpXP can simply wait for passive dissociation from SspB to

process substrates. In other words, waiting for substrate to dissociate will not perceptibly slow down proteolysis by ClpXP. Additionally, ClpXP could pull substrate from SspB in an active process, but based on the kinetic measurements there seems to be no need for it to do so.

In addition to enhancing substrate recognition, SspB causes a moderate increase in the rate at which substrates are degraded. This phenomenon remains essentially unexplained, although potential models do exist. On its own, ClpX is capable of binding only a single molecule of substrate, likely in the central pore of the hexamer (Piszczek et al., 2005). The turnover increase could be explained if ClpXP were able to degrade both substrate molecules bound to SspB simultaneously. A second way for SspB to increase the rate of substrate degradation would be to destabilize the substrates it delivers. For example, if binding of substrates to SspB resulted in minor disruption of structure near the ssrA tag, the rate at which those substrates are degraded could increase (Kenniston et al., 2003). Later, I show that GFP molecules fused to a C-terminal ssrA tag experience a reduction in fluorescence when bound to SspB in a manner consistent with a structural perturbation. If SspB truly does disrupt the structure of GFP-ssrA, then the perturbation must be minor since no major disruption of GFP's secondary structure is observed by circular dichroism measurements when bound by SspB (unpublished data). Also in conflict with this hypothesis, SspB enhances the rate at which carboxymethylated substrates, which are unstructured as determined by circular dichroism, are degraded (J. Kenniston, personal communication).

Part III: The AAA+ superfamily

The common purpose of AAA+ ATPases

ClpX contains a conserved AAA+ domain of roughly 200 amino acids. Many proteins that contain similar domains perform tasks that all seem to require the application of mechanical force (Vale, 2000; Glover and Tkach, 2001; Sauer et al., 2004). Enzymes of the AAA+ superfamily play important roles in life. They are involved in processive DNA replication, endoplasmic reticulum associated degradation (ERAD), vesicle fusion, cellular transport, viral genome replication, and a host of energy-dependent degradation pathways (Neuwald et al., 1999). The AAA+ domain encodes various elements that make up an ATPase active site. These include the well known Walker A and B sequences that mediate binding and hydrolysis of ATP, as well as two conserved arginine residues that have been implicated in sensing the identity of bound nucleotides. AAA+ proteins are typically hexameric and can contain either one or two copies of the AAA+ domain. Proteins that contain two AAA+ modules form two stacked hexameric rings, with each domain forming a subunit of each ring. In these cases, each ring often possesses distinct catalytic properties (Parsell et al., 1994; Singh and Maurizi, 1994; Nagiec et al., 1995; Seol et al., 1995; Watanabe et al., 2002; Song et al., 2003; Wang et al., 2003).

Useful AAA+ mutants

ClpX and other AAA+ enzymes use ATP hydrolysis to drive molecular disassembly processes that seem to require the exertion of mechanical force. ATP binding, hydrolysis, and product release at the ATPase active site of the enzyme must somehow result in allosteric conformational changes that perform these tasks. Mutations that disrupt the

ATPase cycle and communication network are critical for understanding how AAA+ proteins achieve their functions. Several classes of mutants have been used to probe this mechanism. Below, I outline the mutant classes and their characteristic enzymatic phenotypes which have provided the most information about the mechanism of AAA+ proteins.

Figure 4

The ATPase sites of AAA+ proteins are located at the interfaces between subunits (Fig. 4A). Residues involved in nucleotide sensing and hydrolysis extend from both adjacent subunits. The Walker-A sequence motif is the canonical feature of P-loop ATPases and features residues which loop around the phosphate moiety of the bound nucleotide (Fig. 4A and B). This motif is critical for the binding of nucleotide, whereas residues of the

Walker-B motif are essential for ATP hydrolysis. The extended Walker-B motif contains a highly conserved sequence in ClpX Asp^{184}-Glu^{185}-Ile^{186}-Asp^{187} and many related proteins. Magnesium is an important cofactor of the ATP hydrolysis reaction, and is coordinated by Asp^{184} and Asp^{187}. Glu^{185}, shown in Figure 4A, serves as the catalytic base and activates a water molecule for hydrolysis of the gamma phosphate of ATP.

Mutation of the glutamate to a non-acidic residue is sufficient to disrupt ATP hydrolysis in most AAA+ and related proteins. By preventing hydrolysis, it is possible to study the static ATP-bound form that may normally not be substantially populated. In the wild-type ClpX, the ATP form of the enzyme is highly unstable due to a high basal ATP-hydrolysis rate (over 100 min^{-1} enzyme^{-1}). Hydrolysis of the ATP analog ATPγS occurs about 20-fold more slowly (Burton et al., 2003). Other ATP analogs fail to bind ClpX tightly or at all. Another concern is the possibility that analogs do not faithfully mimic ATP as reported for AMPPNP and GroEL (Rye et al., 1997). However, mutation of the Walker-B glutamate also has the potential to misreport characteristics of the wild-type enzyme. For instance, removal of the negatively charged glutamate from the active site could potentially change the rate at which nucleotide is bound and released or alter the conformational changes that typically accompany ATP binding and hydrolysis.

Arg^{370} and Arg^{307} are important for ClpX activity, and arginines at homologous positions are common in other AAA+ proteins (Song et al., 2000; Hishida et al., 2004; Joshi et al., 2004; Schumacher et al., 2004). Arg^{370} is located in a region of ClpX known as the sensor-II helix and is in close proximity to the gamma phosphate of ATP in some AAA+

structures, including that of *Helicobacter pyrlori* ClpX (Fig. 4A). In most, but not all AAA+ proteins, altering this residue results in a hydrolysis-defective mutant. In contrast to mutations in the Walker-B motif, enzymes lacking the sensor-II arginine do not usually display properties of the ATP state when ATP is bound. This observation suggests that the sensor-II arginine senses bound ATP and helps propagate resulting conformation changes.

Arg^{307} in ClpX is part of the box-VII sequence motif. This position has been described as an arginine finger in many AAA+ proteins, akin to those seen in GTPases (Ahmadian et al., 1997). The hydrolysis activity of GTPases is often activated by protein factors (GAPs) which supply a catalytic arginine to stabilize the transition state of nucleotide hydrolysis (Ahmadian et al., 1997). Similarly, the side chain of Arg^{307} in ClpX is supplied in trans to the ATPase site of the adjacent subunit (Fig. 4A). The "arginine finger" of AAA+ proteins contacts the sensor-II arginine in some crystal structures and contacts the gamma phosphate of ATP in other structures (Bochtler et al., 2000). Rather than participating in catalysis, Arg^{307} in ClpX may serve a sensing function similar to Arg^{370}, except in trans; sensing the identity of the nucleotide bound to the adjacent subunit. As I discuss in chapter four, ATP hydrolysis by ClpX and many other AAA+ enzymes is cooperative. Therefore individual subunits of ClpX must have information about the nucleotide content of other subunits (Hattendorf and Lindquist, 2002; Burton et al., 2003; Hersch et al., 2005). The box-VII arginine seems a likely candidate for this role as mutants behave similarly to sensor-II mutants, although a role in transition state stabilization cannot be ruled out (Hishida et al., 2004).

Nucleotide utilization by AAA+ proteins

Nucleotide content determines the conformation of AAA+ proteins throughout the catalytic cycle. As I discuss in chapter four, ATP binding causes ClpX to adopt a conformation that can bind protein substrates and the ClpP peptidase tightly (Wah et al., 2002; Hersch et al., 2005). I also show that ATP/ATPγS binding to ClpX results in allosteric changes in the central pore, similar to those seen for other AAA+ enzymes (Schlieker et al., 2004; Hersch et al., 2005). Measuring the properties of an all ATP or all ADP form of the enzyme is useful, but does not report on the way energy is used in the enzymatic cycle. For instance, how many nucleotides are hydrolyzed in a single unfolding attempt? As a first step to answering this question, many laboratories have employed both crystallographic and biochemical methods to find the number of nucleotides bound. As a second step, it must be determined whether bound ATPs are hydrolyzed simultaneously or whether only a sub-population of bound ATP is hydrolyzed in a single enzymatic cycle. Data from different experimental systems can be compared to address the possibility that all hexameric AAA+ motor proteins use closely related mechanisms.

In the most straightforward ATP-hydrolysis scheme for ClpX, six ATP molecules are bound at the interface of the six subunits, simultaneously hydrolyzed to ADP + P_I, and then released (Fig. 5A). Some structural results for other AAA+ hexamers appear to support this concerted model of hydrolysis (Gai et al., 2004). However, many biochemical experiments and a few structures are inconsistent with this model and

suggest a significantly different mechanism. For example, several AAA+ and related hexameric proteins bind fewer than six molecules of ATP at saturation. Furthermore, functional as well as single turnover experiments suggest that bound ATPs are not all hydrolyzed at once, but instead are hydrolyzed individually or in other substoichiometric groups. What follows is an assemblage of the current evidence, highlighting unifying principles and the need for clarifying experiments in the hopes of illuminating the details of a shared catalytic mechanism.

Part IV: Nucleotide utilization by AAA+ and related protein*s*

ClpX and HslU – How AAA+ unfoldases utilize nucleotide

Later in this thesis, I examine ClpX's capacity for binding ATP by several methods including isothermal titration calorimetry (ITC). Only a subset of the six potential nucleotide-binding sites in ClpX bound nucleotide. Chromatography and filter-binding experiments confirmed that only 3-4 ATPs bound per ClpX hexamer. The remaining unbound sites could not be filled by ADP at the concentrations tested. Thus, biochemical experiments indicate that at least two of ClpX's subunits assume a conformation that prevents nucleotide binding at μM concentrations. This result is clearly in conflict with a model in which six ATPs are simultaneously hydrolyzed by ClpX. Figure 5B and 5C show the models of ATP hydrolysis consistent with the observed mode of ATP binding by ClpX.

Figure 5

A. Six fold symmetric, concerted ATP hydrolysis model

ATP Hydrolysis → ADP/P$_i$ Release → six ADP

B. Concerted hydolysis model with less than six ATPs bound

ATP Hydrolysis → ADP/P$_i$ Release → four ADP

C. Partial hydrolysis model

ATP Hydrolysis → ADP/P$_i$ Release → two ADP

I   **II**   **III**

Experiments show that ClpX•ATP, but not ClpX•ADP binds tightly to protein substrates and ClpP. This raises an interesting paradox. If a ClpX hexamer were to adopt the ADP state after hydrolysis of ATP (Fig. 5B, intermediate II), it would lose affinity for its

substrate and peptidase. This situation would present problems for a processive protease. Because ClpXP degrades ssrA-tagged proteins from the C-terminus, the degradation tag is degraded first (Lee et al., 2001; Kenniston et al., 2005). If the ClpXP•substrate complex were to prematurely dissociate before completing degradation, the resulting substrate fragment would be resistant to further proteolysis by ClpXP because it would lack a degradation signal. In this case, one would expect a build up of partially proteolyzed products. However, partially proteolyzed products are not normally observed, indicating that proteolysis by ClpXP is processive and rarely disrupted before completion. I discuss evidence for one potential solution to this paradox in chapter four. In short, I found that a hexamer with mixed nucleotide content (ATP/ADP) retained its tight association with substrate (Hersch et al., 2005). This mixed nucleotide intermediate is depicted in Figure 5C, II and suggests that the *partial hydrolysis* model depicted in Figure 5C is most consistent with the current data.

The crystal structure of *Helicobacter pylori* ClpX appears to contradict the *partial hydrolysis* model as every subunit in the crystal has an identical conformation and contains bound ADP (Kim and Kim, 2003). However, the crystal did not contain a ring hexamer of ClpX. Instead, ClpX subunits are related to one another in the crystal by a screw axis (Table 1). This crystallographic arrangement may actually provide subtle evidence against a six-fold symmetric hexamer. With nucleotide bound to all subunits, the structures of the individual protomers may not be able to form a closed ring. Some empty subunits may be essential to provide the required kinks to form a closed ring.

Attempts to crystallize ClpX in the empty state or with bound ATPγS/magnesium produced an identical ADP-bound, helical arrangement (Kim and Kim, 2003).

HslU and ClpX are about 50% homologous and perform similar functions. Like ClpX, HslU is the unfoldase component of a bacterial ATP-dependent protease. Although biochemical testimony is lacking, the literature is rich with structural data for HslU. Unlike ClpX, HslU has been crystallized as a hexamer and in many different nucleotide states (Table 1). Some forms clearly have six nucleotides bound, which seems either to contradict the data for ClpX or possibly to suggest divergent mechanisms. The 1G4A structure of HslU was crystallized with six bound ADP molecules and the 1E94 structure was crystallized with six bound AMP-PNP molecules (Song et al., 2000; Wang et al., 2001a). However, the presence of AMP-PNP in the 1E94 structure has been called into question by showing that density for the gamma phosphate is mising from a recalculated electron-density map (Wang et al., 2001b).

Other HslU structures are not six-fold symmetric. For example, the 1DO0 structure consists of a dimer of trimers with two subunits containing ATP•Mg, two containing ATP, and the last two containing only sulfate ion (Bochtler et al., 2000). Each subunit pair exhibited a distinct conformation, with unique conformations of the pore residues. Another crystal form (1DO2) contained a trimer of dimers with AMP-PNP bound in alternating subunits (Bochtler et al., 2000). This form was reminiscent of the F_1 ATP synthase, in which catalytic and non-catalytic subunits alternate around the hexamer (Abrahams et al., 1994). In this case, differences in the structure and roles of different F_1

subunits arise from differences in the primary sequence (discussed below). The two HslU hexamer structures which deviate from six-fold symmetry seem consistent with the biochemical data described for ClpX.

Unfortunately, some aspects of the HslU structures that deviate from six-fold symmetry are controversial. The identity of the bound nucleotide in the 1DO2 structure has been questioned because the temperature factor for the gamma phosphate is much higher than surrounding atoms (Wang et al., 2001b). This could simply reflect greater flexibility, or more ominously be indicating that the nucleotides are ADP and not ATP. An unusual *syn* conformation of the adenine base in this structure has also caused suspicion. An *anti* orientation of the base is typical, whereas the *syn* form is rarely observed in crystal structures including other HslU structures. If the ATP is incorrectly bound or is actually ADP, the resulting structure might not represent the true "ATP bound" state of the enzyme. A possible exception to the *anti* rule is the D2 AAA+ domain of NSF, which appears to bind ATP is the *syn* conformation (Lenzen et al., 1998; Yu et al., 1998). However, this domain has very low hydrolytic ability, so its relevance is unclear.

HslUV is the only ATP-dependent protease for which the crystal structure of the ATPase•peptidase complex is known. HslUV structure 1G3I clearly shows how HslU aligns with HslV to form a shared central pore (Sousa et al., 2000). Although there are six ATPs bound in this structure, magnesium is not present. Biochemical experiments, some of which I will discuss in chapter four, have shown that magnesium is essential for ClpX, HslU, and likely all AAA+ ATPases to adopt the ATP-bound conformation (Burton et

al., 2005; Hersch et al., 2005). Furthermore, skepticism exists concerning the identity of the bound nucleotide as ATP rather than ADP. No structure of HslU exists with six bound molecules of Mg•ATP or Mg•ATP analogs. However, these structures do seem to show that HslU can form a closed ring with six bound molecules of ADP. Preliminary chromatography experiments with ClpX suggest that it cannot bind six ADP, but again only 3-4, similar to ATP. These data from ClpX seem far more congruent with crystal structures of HslU that deviate from six-fold symmetric nucleotide binding. Further experiments are needed to resolve this apparent contradiction.

F_1F_0 ATP Synthase – the best characterized molecular motor

The F_1F_0 ATP synthase is an important molecular machine found in the membranes of bacteria, chloroplasts, and mitochondria. This machinery is used to generate ATP from ADP and P_I in the presence of an electrochemical gradient. It does this by coupling the downhill conductance of protons across the membrane to the endergonic synthesis of ATP. This complex is composed of two separable units termed F_0 and F_1. The F_0 complex is a membrane-spanning conduit for protons. The F_1 component is composed of nine subunits of composition $\alpha_3\beta_3\gamma\delta\varepsilon$. The $\alpha_3\beta_3$ core of F_1 is highly homologous to AAA+ proteins. Indeed, the ATP-binding P-loop or Walker-A motif was first recognized in these proteins (Walker et al., 1982). Although neither the α nor β subunits contain all of the sequence elements found in the AAA+ superfamily, there is significant structural and sequence homology (Saraste et al., 1981; Abrahams et al., 1994). For instance, $\alpha_3\beta_3$ forms a hexamer and subunits adopt a fold similar to AAA+ proteins including ATP-binding sites at the subunit interfaces. The α and β subunits share 20% sequence identity,

but the α subunits are hydrolytically inactive due to the absence of a catalytic, basic residue in the active side. In the absence of the F_0 channel, F_1 can function as an ATPase. Together with sequence conservation, there is ample reason to believe that mechanistic similarities exist between the F_1 ATPase and AAA+ proteins.

Crystal structures of F_1 ATPase show that a hexamer is formed by alternating α and β subunits which surround a central γ subunit (Bianchet et al., 1991; Abrahams et al., 1994). In structure 1BMF, all three hydrolytically inactive α subunits are bound to AMP-PNP, but only one β subunit is bound to AMP-PNP. A second β subunit was bound to ADP and the final β subunit contained no bound nucleotide (Fig. 6A). Moreover, each β subunit assumed a slightly different conformation.

Figure 6

A

Loose (conformation for ADP/Pi binding)
Open (conformation for ATP release)
Tight (conformation for ATP synthesis)

B
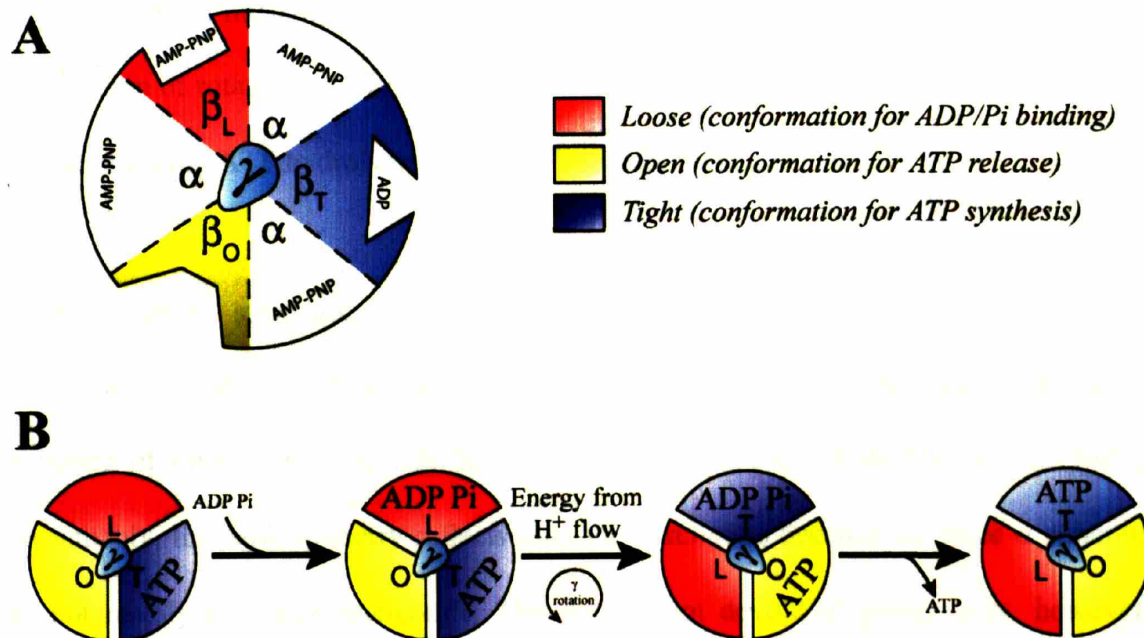
The observation of asymmetry in nucleotide binding by the β subunits was well suited to a postulated cyclical *binding change* mechanism (Cross, 1981; Boyer, 1993). In this mechanism, each β subunit can assume at least three conformations with different affinity for nucleotide called open (β_O), loose (β_L), and tight (β_T). Conversion of the loose site to a tight site requires conversion of the pre-existing tight site to an open site, and the open site to a loose site, all coupled to the orientation of the central γ subunit (Fig. 6B). In this way, subunits changed their affinity for nucleotide in a cyclical fashion during ATP synthesis and prevent hydrolysis of newly synthesized ATP. It is not entirely clear which of the three β subunits in the structure is tight, open, or loose but structural considerations seem to indicate the assignment designated in Figure 6A (Abrahams et al., 1994). The structure also suggested that these conformational changes were driven by rotation of the central γ subunit, with the orientation of the gamma subunit preventing β_O from tight association with nucleotide. The rotation hypothesis was further bolstered by the direct observation of rotation by a fluorescent actin filament which had been cross-linked to the γ subunit during ATP hydrolysis by F_1 ATPase (Noji et al., 1997).

There is ample structural evidence to suggest that F_1 operates by an asymmetric mechanism. In addition, biochemical evidence predating the structure also suggests the presence of only two nucleotide-binding sites per hexamer (Ackerman et al., 1987). Presumably, this stoichiometry reflects only the β subunits because the three α subunits do not readily exchange nucleotide. The field is not devoid of controversy, however. Figure 6B depicts a "bi-site" ATP synthesis mechanism that is likely an oversimplification, as many experiments suggest that F_1 operates via a "tri-site"

mechanism where all sites must be filled with ATP (Weber and Senior, 2001). However, other experiments continue to challenge this notion and indicate that ATP synthesis is possible in a bi-site mechanism (Tomashek et al., 2004). Another interesting point is that F_1 loses its asymmetry in the absence of nucleotide and becomes three-fold symmetric (Bianchet et al., 1991; Shirakihara et al., 1997). This result is important because it suggests that properly bound nucleotide is important for inducing asymmetry in the complex and warns us that the observed symmetry in other systems may not represent the functionally important states of the enzyme.

T7 and SV40 – DNA translocation machines

Many AAA+ and related motor proteins function as helicases to melt polynucleotide complexes. Helicases separate the strands of DNA and RNA in an energy-dependent process to facilitate DNA replication, RNA splicing, etc. Like ClpX and HslU, the T7 DNA helicase is a hexameric ATPase with a canonical P-loop active site. This helicase does not fit a strict definition of a AAA+ protein, but like F_1 shares significant sequence and structural homology with AAA+ family members. In addition to the motor domain, helicases typically have an N-terminal domain responsible for targeting the helicase to the site of strand separation (Hickman and Dyda, 2005). Occasionally this N-terminal domain also helps the helicase to oligomerize, but it is more commonly dispensable for this function.

Like the AAA+ proteins I have discussed, the T7 DNA helicase is a homohexamer with the nucleotide-binding sites located at subunit interfaces. Biochemical experiments have

indicated that the T7 helicase hexamer binds three nucleotides, but structural evidence suggests four are bound (Patel and Hingorani, 1995; Hingorani et al., 1997; Singleton et al., 2000). Distinguishing between three and four bound nucleotides may be critical for a detailed mechanistic understanding, but it seems clear that the hexamer does not bind six nucleotides. Asymmetric nucleotide binding is an essential feature of the *binding change* mechanism suggested for T7 DNA helicase. Whereas F_1 ATP synthase binds the γ subunit in its central channel, T7 helicase binds its substrate DNA. In a reversal of the model for F_1 ATP synthase, different subunits vary their affinity for substrate based on the nucleotide bound. As nucleotide is bound, hydrolyzed, and released, each subunit of the helicase is postulated to vary its affinity for DNA causing the DNA substrate to be bound and translocated by a subset of T7 subunits, and then released. When one set of subunits releases the substrate DNA, another set of T7 subunits binds the DNA to prevent back sliding, as well as to execute the next translocation step. In this way, the helicase could propel itself along DNA. Strand separation likely occurs as a single strand is pulled through the central pore, thereby excluding or peeling off the complementary strand that was formerly bound.

For unknown reasons, T7 DNA helicase hydrolyzes dTTP more efficiently than any other nucleotide (Hingorani and Patel, 1996; Sawaya et al., 1999). Pre-steady state hydrolysis experiments have shown that the T7-helicase hexamer hydrolyzes 1 dTTP in a burst phase during the first ~250 milliseconds of the reaction (Jeong et al., 2002). These data imply that only a single subunit of the T7 DNA helicase hydrolyzes nucleotide at a time. This hydrolysis is detected as a burst phase because ADP release is rate limiting. A

similar burst, but of two nucleotides per hexamer is seen in the RuvAB branch-migration motor protein (Marrione and Cox, 1995; Marrione and Cox, 1996).

An AAA+ helicase is encoded by the genome of simian virus 40 (SV40), a small DNA virus that encodes just two open reading frames (ORF). One ORF produces the capsid proteins and the other encodes an AAA+ helicase called the large tumor antigen (LTag) (Gai et al., 2004; Hickman and Dyda, 2005). Crystal structures are available for hexameric LTag in a variety of bound forms including ATP, ADP•BeF$_3^-$•Mg^{2+}, ADP, and no nucleotide (Gai et al., 2004 and Table 1). All structures were six-fold symmetric, seeming to suggest a *six-fold symmetric, concerted hydrolysis* mechanism (Fig. 5A). In the ATP-bound structure, magnesium was omitted to prevent hydrolysis. Although no biochemical data are available, we can assume by extension from ClpX and HslU that magnesium is essential for SV40 to sense and correctly respond to bound ATP. "ATP-bound" crystal forms in the absence of bound magnesium likely do not represent a biologically relevant conformation, or at least not a true Mg•ATP-bound state.

The LTag structure with ATP and no Mg^{2+} was very similar to a second structure with bound ADP•BeF$_3^-$•Mg^{2+}. Because of this similarity, the authors believe that the ADP•BeF$_3^-$•Mg^2 bound structure represents the ATP-bound state. However, it is unclear what state this nucleotide analog truly induces in ATP-binding proteins. BeF$_3^-$ (like AlF$_3^-$) is a phosphoryl mimic sometimes assumed to mimic the transition state, occasionally the ATP-bound state, and at other times the post-hydrolysis state preceding phosphate release. A second point of contention is that the ADP•BeF$_3^-$•Mg^{2+}-bound structure was

34

obtained by soaking BeF_3^-/Mg^{2+} into a preformed ADP-bound crystal. Soaking techniques often allow crystallographers to identify ligand binding sites, but can also prohibit large structural changes that would result in perturbation of crystal contacts. Thus, both structures must be interpreted with extreme caution. However, like HslU, it seems clear that a ring hexamer with six bound nucleotides can be crystallized. The biological relevance of such structures, however, remains unclear.

The membrane motor - p97 / VCP

In mammals, the AAA protein p97 mediates membrane fusion, is essential for dislocation of proteins from the endoplasmic reticulum, and is required for reassembly of the ER and golgi (Ye et al., 2001; Meyer, 2005). It is found in all mammalian tissue types and has relatives in other species, including flies and yeast. p97 contains two AAA modules (D1 and D2) and assembles into a double hexameric ring. The D1 ring does not hydrolyze ATP at physiological temperatures, but nucleotide binding to this ring promotes hexamer stability (Song et al., 2003).

Small-angle x-ray scattering (SAXS) has provided low-resolution data on the solution geometry of p97. Large conformational changes were observed that depended on the identity of nucleotide bound to the D2 domain (Davies et al., 2005). The low-resolution reconstructions of p97 were largely symmetric, although some deviations from six-fold symmetry were detected. Larger deviations were observed in high-resolution crystal structures of p97, bound to different nucleotides (DeLaBarre and Brunger, 2005). The protein crystallized as a closed hexamer, with multiple subunits in the asymmetric unit of

some crystal forms. For instance, the ADP and ADP•AlF$_3^-$ bound forms crystallized with three subunits in the asymmetric unit, similar to crystals of T7 DNA helicase. Each subunit assumed a different conformation, detected as a rotation of the D2 module with respect to the D1 module, clearly demonstrating a deviation from six-fold symmetry. Analysis of heterogeneity was not possible with the nucleotide-free form, as the hexamer was reconstructed from a single subunit per asymmetric unit. The AMP-PNP-bound protein crystallized with multiple subunits in the asymmetric unit, however only small differences were detectable between individual subunits.

All crystal structures of p97, even those deviating from six-fold symmetry, have nucleotide bound to all subunits. However, this observation has been argued by the authors of the study to be an artifact of the high ionic strength used to crystallize p97 (DeLaBarre and Brunger, 2005). Also, the crystal structures contained no bound magnesium. A nucleotide cross-linking experiment suggested that at some p97 subunits do not bind nucleotide. In this study, sheep brain p97 was cross-linked to labeled benzyl ATP (BzATP). Only a few of the potential nucleotide-binding sites were crosslinked to BzATP (Zalk and Shoshan-Barmatz, 2003). These and other data suggest that only two or three potential nucleotide-binding sites are occupied at any one time during hydrolysis (Zalk and Shoshan-Barmatz, 2003; DeLaBarre and Brunger, 2005).

Heteromeric AAA+ domain proteins – the β-clamp loader and dynein

Is symmetry, or at least the potential for symmetry an essential feature of the mechanisms of AAA+ and related proteins? The β-clamp loader and dynein are examples of AAA+

proteins that are fundamentally asymmetric. In these proteins, domains or subunits of different primary sequence form the AAA+ ring. Can a shared mechanism be extended to these proteins as well? The β-clamp loader of bacteria is a heteromeric enzyme, which contains three distinct AAA+ polypeptides. Unlike most AAA+ proteins, it forms a pentamer rather than a hexamer. The pentamer is constructed from three γ, one δ, and one δ' subunit. This motor protein loads the β-clamp onto DNA for processive replication by DNA-polymerase III. Neither the δ or the δ' subunits are capable of hydrolyzing ATP, although δ' contributes some necessary residues to the adjacent γ subunit active site interface.

In the current model, ATP binding by the γ subunits allows the δ' subunit to open the β-clamp bound by the δ subunit so that it can subsequently encircle DNA. ATP hydrolysis is thought to occur in an ordered mechanism, whereby γ_1 hydrolyzes last after γ_2 and γ_3. It is tempting to speculate that akin to homomeric AAA+ proteins which specialize their subunits at the level of conformation (which is flexible and can change), the clamp loader does so at the fixed level of sequence. Could this difference reflect a different requirement for processivity? ClpX, a homomeric AAA+ protein, performs a processive degradation reaction which requires hundreds of ATP-hydrolysis cycles, all while bound to a single processing substrate (Kim et al., 2000). In contrast, the clamp loader hydrolyzes only two to three ATP molecules per clamp-loading cycle (Turner et al., 1999). Thus, a continuous ordered subunit specification of ATP hydrolysis seems unnecessary, although some firing order for the three γ subunits does exist (Johnson and O'Donnell, 2003; Seybert and Wigley, 2004).

37

Dynein's central motor domain is a eukaryotic member of the AAA family and is responsible for coupling ATP hydrolysis to cargo transport along microtubules (King, 2000). The AAA+ ring forms the head portion of the heavy chain of dynein, and two of these heavy chains associate with intermediate and light chains to form the familiar motor. The AAA+ ring in the head of dynein is constructed from six tandemly linked AAA+ modules, providing an opportunity to study AAA modules in fixed positions (Silvanovich et al., 2003). Attachment to substrate, in this case tubulin, does not occur directly with the pore of the AAA+ ring, but with a stalk that extends laterally from the ring. ATPase activity by the AAA+ ring has been proposed to drive a power stroke in which movement of the stalk drives translocation of the attached microtubule (Burgess et al., 2003). Two of the AAA+ modules do not bind or hydrolyze nucleotide. The four remaining AAA+ modules appear to bind nucleotide, but just two of the nucleotide-binding sites are responsible for the majority of ATP hydrolysis (Kon et al., 2004). Like the β-clamp loader, the function of each subunit appears to be hard-coded in the amino acid sequence.

Like the homomeric AAA+ proteins discussed so far, dynein is a processive motor protein. As discussed above, the individual AAA modules of dynein are not structurally or functionally equivalent. Therefore, a *binding change mechanism* such as that described for the homo-hexameric AAA+ proteins discussed earlier is ruled out as a model. The holoenzyme is composed of two heavy chains and thus two hexamers of AAA+ modules. The coordinate action of these two AAA+ rings may be responsible for the observed processivity – when one stalk releases a microtubule, the other stalk can retain

association. In a recent experiment, a single-headed dynein variant affixed to a glass surface was shown to translocate microtubules, arguing against the hypothesis (Nishiura et al., 2004). However, it is unclear if processivity is damaged in single-headed dynein or whether multiple single-headed variants can cooperate on the surface of the glass slide. Other experiments suggest that the two heads are an essential feature of dynein, and required for microtubule association and translocation (Iyadurai et al., 1999). The role of the two heads of dynein remains an open question in the field of AAA+ motor proteins.

Part V: Interpretations and Conclusions

Interpreting structural and biochemical data

Electron microscopy (EM) is another source of structural data involving AAA+ proteins and their substrates. AAA+ proteins are commonly seen to undergo large structural changes that are dependent upon the identity of bound nucleotide. One might expect these micrographs to reveal the structural asymmetry that has been detected by biochemical experiments and crystallography. Contrarily, the resulting images are usually six-fold symmetric hexamers. One possibility is that the limited resolution offered by EM (~20 Å) is not sufficient to distinguish unique subunit conformations. Furthermore, the final EM image generated is not that of a single molecule. Rather, it is a computer average of thousands of individual molecules. Molecule to molecule variation can be obscured by this homogenization of the data. EM has generated images of AAA+ bound to their substrates. Although ClpX binds only one substrate per hexamer, because of the averaging process described above, they appear only as a ring of extra density that collides at the pore. (Ortega et al., 2000).

Some caveats of interpreting crystallographic data have already been discussed. Many structures with bound ATP or analogs may not represent the true ATP state of the enzyme because magnesium is not present. An additional concern is that nucleotide analogs induce conformations that cannot be reliably ascribed to an unambiguous point in the ATPase cycle. The orientation of the nucleotide (syn vs. anti) has also called into question crystallographic data. Yet another concern is that the high ionic strength used in many crystallography experiments may induce symmetric conformations which are not functionally relevant. How are we to extricate ourselves from this confusion? Substrate bound forms of the enzyme may provide the path towards understanding. For ClpX and many other AAA+ proteins, only the "ATP state" forms tight association with macromolecular substrate. For the enzymes where this is the case, there is as of yet no crystal structure of this enzyme•substrate interaction. Demonstration of a productive substrate interaction would go a long way towards validating it as the ATP state of that enzyme. So far, complexes of AAA+ proteins with their macromolecular substrates have proven very difficult to crystallize. One potential reason for this difficulty may be the inherent heterogeneity that I and others postulate as an essential feature of these enzymes.

The results of biochemical experiments are also not beyond reproach and present ample opportunity for artifacts. All the experiments measuring the stoichiometry of nucleotide-binding rely on accurately knowing the active enzyme concentration. For instance, a stoichiometry of three nucleotides per hexamer could easily arise if 50% of the enzyme were damaged or overestimated. Enzymes can be damaged by oxidation, aggregation, proteolysis, or just misfolding. For the work on ClpX discussed in chapter four, a

substrate that binds tightly only to the ATP state was used. From this assay, I found that nearly all of the enzyme was capable of assuming the ATP state and binding to substrate. Of course, this assay just exchanges one reagent for another and leaves open the possibility that some fraction of the tight-binding substrate used in the assay was somehow under-represented. In addition, distinguishing between three and four bound nucleotides by biochemical methods is nearly impossible given the inherent inaccuracy in methods for determining protein concentration.

Conclusions

The mechanism whereby ClpX, ClpP and SspB cooperate to degrade substrates in the cytoplasm is an interesting problem and a key undertaking for biologists interested in the details of molecular machines. In this first chapter, I have provided an overview of the most prevalent models for interactions between these proteins as well as a brief review of possible models for substrate delivery and disassembly. These models clearly fall short of a complete mechanistic description, as shown by the unanswered questions that I highlighted throughout the chapter. To answer these questions, I believe that experiments involving other members of the AAA+ superfamily must be considered. In the search for a common mechanism, I have summarized experiments and conclusions from many representative AAA+ proteins. Many of these experiments have suggested that asymmetry is a prominent feature of these enzymes. Models including intermediates that deviate from six-fold symmetry seem to explain many of the features of ClpX and other AAA+ proteins (Fig. 5B and 5C).

Further improvements to the models, including the details of ATP utilization can only be solved by applying a combination of structural and biochemical methods. Structural biologists interested in the questions of AAA+ protein mechanism can greatly impact the field if a protein molecule can be crystallized which is unquestionably part of the catalytic cycle. Demonstration of productive interactions with substrate is a necessity in the validation of potential structures of biological relevance. If a clearer picture of substrate recognition emerges, it may be possible to direct these disassembly machines to novel targets including those involved in diseases of aggregation, to which AAA+ proteins seem particularly well suited. AAA+ enzymes are vital workhorses of the cell, and deciphering their detailed molecular mechanisms is an important and challenging goal.

Table I

Description	Nucleotides per Hexamer	Other notes	Space group	Accession code
Helicobacter Pylori ClpX	All ADP	Screw axis	P 6₅	1UM8
Haemophilus influenzae HslU	All dADP		P 3 2 1	1G4A
Haemophilus influenzae HslU	All AMP-PNP(??)	No Mg	P 6₃ 2 2	1E94
Escherichia coli HslU	2 MgATP/ 2 ATP/ 2 Apo	SO4 in Apo	P 2₁ 2₁ 2	1DO0
Escherichia coli HslU	3 AMP-PNP(?) / 3 Apo	No Mg	P 3 2 1	1DO2
Haemophilus influenzae HslUV	All ATP	No Mg Mg with all nucleotide	P 2₁ 2₁ 2	1G3I
Bovine mitochondrial F₁ ATPase	4 AMP-PNP / 1 ADP		P 2₁ 2₁ 2₁	1BMF
Phage T7 Helicase	4 Mg + ADPNP / 2 Apo		P 4₁ 2₁ 2	1E0J
Phage T7 Helicase	All Apo	Nucleotide soaked into apo crystal form	P 4₁ 2₁ 2	1E0K
SV40 LTag Helicase	All Mg ADP BeF₃	Zn and Mg	P 1 2₁ 1	1SVM
SV40 LTag Helicase	All ADP	Zn	C 1 2 1	1SVL
SV40 LTag Helicase	All Apo	Zn	P 3 2 1	1SVO
Mus musculus p97/VCP	All ADP AlF₃	Zn	I 2 2 2	1YQ0
Mus musculus p97/VCP	All ADP	Zn	I 2 2 2	1YQI
Mus musculus p97/VCP	All AMP-PNP in D2 (ADP in D1)		P 3	1YPW
Mus musculus p97/VCP	D1 ADP D2 APO		P 6 2 2	1R7R
Escherichia coli clamp loader (pentamer)	2 ATPγS and 3 apo	PO4 / Zn	P 2₁ 2₁ 2₁	1XXH
Escherichia coli clamp loader (pentamer	2 ADP and 3 apo	PO4 / Zn	P 2₁ 2₁ 2₁	1XXI

43

References

Abrahams, J. P., Leslie, A. G., Lutter, R., and Walker, J. E. (1994). Structure at 2.8 A resolution of F1-ATPase from bovine heart mitochondria. Nature *370*, 621-628.

Ackerman, S. H., Grubmeyer, C., and Coleman, P. S. (1987). Evidence for catalytic cooperativity during ATP hydrolysis by beef heart F1-ATPase. Kinetics and binding studies with the photoaffinity label BzATP. J Biol Chem *262*, 13765-13772.

Ahmadian, M. R., Stege, P., Scheffzek, K., and Wittinghofer, A. (1997). Confirmation of the arginine-finger hypothesis for the GAP-stimulated GTP-hydrolysis reaction of Ras. Nat Struct Biol *4*, 686-689.

Bianchet, M., Ysern, X., Hullihen, J., Pedersen, P. L., and Amzel, L. M. (1991). Mitochondrial ATP synthase. Quaternary structure of the F1 moiety at 3.6 A determined by x-ray diffraction analysis. J Biol Chem *266*, 21197-21201.

Bochtler, M., Hartmann, C., Song, H. K., Bourenkov, G. P., Bartunik, H. D., and Huber, R. (2000). The structures of HsIU and the ATP-dependent protease HsIU-HsIV. Nature *403*, 800-805.

Bolon, D. N., Wah, D. A., Hersch, G. L., Baker, T. A., and Sauer, R. T. (2004). Bivalent tethering of SspB to ClpXP is required for efficient substrate delivery: a protein-design study. Mol Cell *13*, 443-449.

Boyer, P. D. (1993). The binding change mechanism for ATP synthase--some probabilities and possibilities. Biochim Biophys Acta *1140*, 215-250.

Burgess, S. A., Walker, M. L., Sakakibara, H., Knight, P. J., and Oiwa, K. (2003). Dynein structure and power stroke. Nature *421*, 715-718.

Burton, R. E., Baker, T. A., and Sauer, R. T. (2003). Energy-dependent degradation: Linkage between ClpX-catalyzed nucleotide hydrolysis and protein-substrate processing. Protein Sci *12*, 893-902.

Burton, R. E., Baker, T. A., and Sauer, R. T. (2005). Nucleotide-dependent substrate recognition by the AAA+ HslUV protease. Nat Struct Mol Biol *12*, 245-251.

Cross, R. L. (1981). The mechanism and regulation of ATP synthesis by F1-ATPases. Annu Rev Biochem *50*, 681-714.

Davies, J. M., Tsuruta, H., May, A. P., and Weis, W. I. (2005). Conformational changes of p97 during nucleotide hydrolysis determined by small-angle X-Ray scattering. Structure (Camb) *13*, 183-195.

DeLaBarre, B., and Brunger, A. T. (2005). Nucleotide dependent motion and mechanism of action of p97/VCP. J Mol Biol *347*, 437-452.

Flynn, J. M., Levchenko, I., Seidel, M., Wickner, S. H., Sauer, R. T., and Baker, T. A. (2001). Overlapping recognition determinants within the ssrA degradation tag allow modulation of proteolysis. Proc Natl Acad Sci U S A *98*, 10584-10589.

Flynn, J. M., Neher, S. B., Kim, Y. I., Sauer, R. T., and Baker, T. A. (2003). Proteomic discovery of cellular substrates of the ClpXP protease reveals five classes of ClpX-recognition signals. Mol Cell *11*, 671-683.

Gai, D., Zhao, R., Li, D., Finkielstein, C. V., and Chen, X. S. (2004). Mechanisms of conformational change for a replicative hexameric helicase of SV40 large tumor antigen. Cell *119*, 47-60.

Glover, J. R., and Tkach, J. M. (2001). Crowbars and ratchets: hsp100 chaperones as tools in reversing protein aggregation. Biochem Cell Biol *79*, 557-568.

Gottesman, S. (1996). Proteases and their targets in Escherichia coli. Annu Rev Genet *30*, 465-506.

Gottesman, S. (2003). Proteolysis in bacterial regulatory circuits. Annu Rev Cell Dev Biol *19*, 565-587.

Hattendorf, D. A., and Lindquist, S. L. (2002). Cooperative kinetics of both Hsp104 ATPase domains and interdomain communication revealed by AAA sensor-1 mutants. Embo J *21*, 12-21.

Hersch, G. L., Baker, T. A., and Sauer, R. T. (2004). SspB delivery of substrates for ClpXP proteolysis probed by the design of improved degradation tags. Proc Natl Acad Sci U S A *101*, 12136-12141.

Hersch, G. L., Burton, R. E., Bolon, D. N., Baker, T. A., and Sauer, R. T. (2005). Asymmetric interactions of ATP with the AAA+ ClpX6 unfoldase: allosteric control of a protein machine. Cell, (in press).

Hickman, A. B., and Dyda, F. (2005). Binding and unwinding: SF3 viral helicases. Curr Opin Struct Biol *15*, 77-85.

Hingorani, M. M., and Patel, S. S. (1996). Cooperative interactions of nucleotide ligands are linked to oligomerization and DNA binding in bacteriophage T7 gene 4 helicases. Biochemistry *35*, 2218-2228.

Hingorani, M. M., Washington, M. T., Moore, K. C., and Patel, S. S. (1997). The dTTPase mechanism of T7 DNA helicase resembles the binding change mechanism of the F1-ATPase. Proc Natl Acad Sci U S A *94*, 5012-5017.

Hishida, T., Han, Y. W., Fujimoto, S., Iwasaki, H., and Shinagawa, H. (2004). Direct evidence that a conserved arginine in RuvB AAA+ ATPase acts as an allosteric effector for the ATPase activity of the adjacent subunit in a hexamer. Proc Natl Acad Sci U S A *101*, 9573-9577.

Iyadurai, S. J., Li, M. G., Gilbert, S. P., and Hays, T. S. (1999). Evidence for cooperative interactions between the two motor domains of cytoplasmic dynein. Curr Biol *9*, 771-774.

Jenal, U., and Hengge-Aronis, R. (2003). Regulation by proteolysis in bacterial cells. Curr Opin Microbiol *6*, 163-172.

Jenal, U., and Stephens, C. (2002). The Caulobacter cell cycle: timing, spatial organization and checkpoints. Curr Opin Microbiol *5*, 558-563.

Jeong, Y. J., Kim, D. E., and Patel, S. S. (2002). Kinetic pathway of dTTP hydrolysis by hexameric T7 helicase-primase in the absence of DNA. J Biol Chem *277*, 43778-43784.

Johnson, A., and O'Donnell, M. (2003). Ordered ATP hydrolysis in the gamma complex clamp loader AAA+ machine. J Biol Chem *278*, 14406-14413.

Joshi, S. A., Hersch, G. L., Baker, T. A., and Sauer, R. T. (2004). Communication between ClpX and ClpP during substrate processing and degradation. Nat Struct Mol Biol *11*, 404-411.

Keiler, K. C., Waller, P. R., and Sauer, R. T. (1996). Role of a peptide tagging system in degradation of proteins synthesized from damaged messenger RNA. Science *271*, 990-993.

Kenniston, J. A., Baker, T. A., Fernandez, J. M., and Sauer, R. T. (2003). Linkage between ATP consumption and mechanical unfolding during the protein processing reactions of an AAA+ degradation machine. Cell *114*, 511-520.

Kenniston, J. A., Baker, T. A., and Sauer, R. T. (2005). Partitioning between unfolding and release of native domains during ClpXP degradation determines substrate selectivity and partial processing. Proc Natl Acad Sci U S A *102*, 1390-1395.

Kim, D. Y., and Kim, K. K. (2003). Crystal structure of ClpX molecular chaperone from Helicobacter pylori. J Biol Chem *278*, 50664-50670.

Kim, Y. I., Burton, R. E., Burton, B. M., Sauer, R. T., and Baker, T. A. (2000). Dynamics of substrate denaturation and translocation by the ClpXP degradation machine. Mol Cell *5*, 639-648.

King, S. M. (2000). AAA domains and organization of the dynein motor unit. J Cell Sci *113 (Pt 14)*, 2521-2526.

Kon, T., Nishiura, M., Ohkura, R., Toyoshima, Y. Y., and Sutoh, K. (2004). Distinct functions of nucleotide-binding/hydrolysis sites in the four AAA modules of cytoplasmic dynein. Biochemistry *43*, 11266-11274.

Lee, C., Schwartz, M. P., Prakash, S., Iwakura, M., and Matouschek, A. (2001). ATP-dependent proteases degrade their substrates by processively unraveling them from the degradation signal. Mol Cell *7*, 627-637.

Lenzen, C. U., Steinmann, D., Whiteheart, S. W., and Weis, W. I. (1998). Crystal structure of the hexamerization domain of N-ethylmaleimide-sensitive fusion protein. Cell *94*, 525-536.

Levchenko, I., Seidel, M., Sauer, R. T., and Baker, T. A. (2000). A specificity-enhancing factor for the ClpXP degradation machine. Science *289*, 2354-2356.

Marrione, P. E., and Cox, M. M. (1995). RuvB protein-mediated ATP hydrolysis: functional asymmetry in the RuvB hexamer. Biochemistry *34*, 9809-9818.

Marrione, P. E., and Cox, M. M. (1996). Allosteric effects of RuvA protein, ATP, and DNA on RuvB protein-mediated ATP hydrolysis. Biochemistry *35*, 11228-11238.

Meyer, H. H. (2005). Golgi reassembly after mitosis: the AAA family meets the ubiquitin family. Biochim Biophys Acta *1744*, 481-492.

Nagiec, E. E., Bernstein, A., and Whiteheart, S. W. (1995). Each domain of the N-ethylmaleimide-sensitive fusion protein contributes to its transport activity. J Biol Chem *270*, 29182-29188.

Neuwald, A. F., Aravind, L., Spouge, J. L., and Koonin, E. V. (1999). AAA+: A class of chaperone-like ATPases associated with the assembly, operation, and disassembly of protein complexes. Genome Res *9*, 27-43.

Nishiura, M., Kon, T., Shiroguchi, K., Ohkura, R., Shima, T., Toyoshima, Y. Y., and Sutoh, K. (2004). A single-headed recombinant fragment of Dictyostelium cytoplasmic dynein can drive the robust sliding of microtubules. J Biol Chem *279*, 22799-22802.

Noji, H., Yasuda, R., Yoshida, M., and Kinosita, K., Jr. (1997). Direct observation of the rotation of F1-ATPase. Nature *386*, 299-302.

Ortega, J., Singh, S. K., Ishikawa, T., Maurizi, M. R., and Steven, A. C. (2000). Visualization of substrate binding and translocation by the ATP-dependent protease, ClpXP. Mol Cell *6*, 1515-1521.

Parsell, D. A., Kowal, A. S., and Lindquist, S. (1994). Saccharomyces cerevisiae Hsp104 protein. Purification and characterization of ATP-induced structural changes. J Biol Chem *269*, 4480-4487.

Patel, S. S., and Hingorani, M. M. (1995). Nucleotide binding studies of bacteriophage T7 DNA helicase-primase protein. Biophys J *68*, 186S-189S; discussion 189S-190S.

Piszczek, G., Rozycki, J., Singh, S. K., Ginsburg, A., and Maurizi, M. R. (2005). The molecular chaperone, ClpA, has a single high affinity peptide binding site per hexamer. J Biol Chem *280*, 12221-12230.

Rye, H. S., Burston, S. G., Fenton, W. A., Beechem, J. M., Xu, Z., Sigler, P. B., and Horwich, A. L. (1997). Distinct actions of cis and trans ATP within the double ring of the chaperonin GroEL. Nature *388*, 792-798.

Saraste, M., Gay, N. J., Eberle, A., Runswick, M. J., and Walker, J. E. (1981). The atp operon: nucleotide sequence of the genes for the gamma, beta, and epsilon subunits of Escherichia coli ATP synthase. Nucleic Acids Res *9*, 5287-5296.

Sauer, R. T., Bolon, D. N., Burton, B. M., Burton, R. E., Flynn, J. M., Grant, R. A., Hersch, G. L., Joshi, S. A., Kenniston, J. A., Levchenko, I., *et al.* (2004). Sculpting the proteome with AAA(+) proteases and disassembly machines. Cell *119*, 9-18.

Sawaya, M. R., Guo, S., Tabor, S., Richardson, C. C., and Ellenberger, T. (1999). Crystal structure of the helicase domain from the replicative helicase-primase of bacteriophage T7. Cell *99*, 167-177.

Schlieker, C., Weibezahn, J., Patzelt, H., Tessarz, P., Strub, C., Zeth, K., Erbse, A., Schneider-Mergener, J., Chin, J. W., Schultz, P. G., *et al.* (2004). Substrate recognition by the AAA+ chaperone ClpB. Nat Struct Mol Biol *11*, 607-615.

Schumacher, J., Zhang, X., Jones, S., Bordes, P., and Buck, M. (2004). ATP-dependent transcriptional activation by bacterial PspF AAA+protein. J Mol Biol *338*, 863-875.

Seol, J. H., Baek, S. H., Kang, M. S., Ha, D. B., and Chung, C. H. (1995). Distinctive roles of the two ATP-binding sites in ClpA, the ATPase component of protease Ti in Escherichia coli. J Biol Chem *270*, 8087-8092.

Seybert, A., and Wigley, D. B. (2004). Distinct roles for ATP binding and hydrolysis at individual subunits of an archaeal clamp loader. Embo J *23*, 1360-1371.

Shirakihara, Y., Leslie, A. G., Abrahams, J. P., Walker, J. E., Ueda, T., Sekimoto, Y., Kambara, M., Saika, K., Kagawa, Y., and Yoshida, M. (1997). The crystal structure of the nucleotide-free alpha 3 beta 3 subcomplex of F1-ATPase from the thermophilic Bacillus PS3 is a symmetric trimer. Structure *5*, 825-836.

Silvanovich, A., Li, M. G., Serr, M., Mische, S., and Hays, T. S. (2003). The third P-loop domain in cytoplasmic dynein heavy chain is essential for dynein motor function and ATP-sensitive microtubule binding. Mol Biol Cell *14*, 1355-1365.

Singh, S. K., and Maurizi, M. R. (1994). Mutational analysis demonstrates different functional roles for the two ATP-binding sites in ClpAP protease from Escherichia coli. J Biol Chem *269*, 29537-29545.

Singleton, M. R., Sawaya, M. R., Ellenberger, T., and Wigley, D. B. (2000). Crystal structure of T7 gene 4 ring helicase indicates a mechanism for sequential hydrolysis of nucleotides. Cell *101*, 589-600.

Song, C., Wang, Q., and Li, C. C. (2003). ATPase activity of p97-valosin-containing protein (VCP). D2 mediates the major enzyme activity, and D1 contributes to the heat-induced activity. J Biol Chem *278*, 3648-3655.

Song, H. K., Hartmann, C., Ramachandran, R., Bochtler, M., Behrendt, R., Moroder, L., and Huber, R. (2000). Mutational studies on HslU and its docking mode with HslV. Proc Natl Acad Sci U S A *97*, 14103-14108.

Sousa, M. C., Trame, C. B., Tsuruta, H., Wilbanks, S. M., Reddy, V. S., and McKay, D. B. (2000). Crystal and solution structures of an HslUV protease-chaperone complex. Cell *103*, 633-643.

Thompson, M. W., Singh, S. K., and Maurizi, M. R. (1994). Processive degradation of proteins by the ATP-dependent Clp protease from Escherichia coli. Requirement for the multiple array of active sites in ClpP but not ATP hydrolysis. J Biol Chem *269*, 18209-18215.

Tomashek, J. J., Glagoleva, O. B., and Brusilow, W. S. (2004). The Escherichia coli F1F0 ATP synthase displays biphasic synthesis kinetics. J Biol Chem *279*, 4465-4470.

Turner, J., Hingorani, M. M., Kelman, Z., and O'Donnell, M. (1999). The internal workings of a DNA polymerase clamp-loading machine. Embo J *18*, 771-783.

Vale, R. D. (2000). AAA proteins. Lords of the ring. J Cell Biol *150*, F13-19.

Wah, D. A., Levchenko, I., Baker, T. A., and Sauer, R. T. (2002). Characterization of a specificity factor for an AAA+ ATPase: assembly of SspB dimers with ssrA-tagged proteins and the ClpX hexamer. Chem Biol *9*, 1237-1245.

Wah, D. A., Levchenko, I., Rieckhof, G. E., Bolon, D. N., Baker, T. A., and Sauer, R. T. (2003). Flexible linkers leash the substrate binding domain of SspB to a peptide module that stabilizes delivery complexes with the AAA+ ClpXP protease. Mol Cell *12*, 355-363.

Walker, J. E., Saraste, M., Runswick, M. J., and Gay, N. J. (1982). Embo J *1*, 945-951.

Wang, J., Hartling, J. A., and Flanagan, J. M. (1997). The structure of ClpP at 2.3 A resolution suggests a model for ATP-dependent proteolysis. Cell *91*, 447-456.

Wang, J., Song, J. J., Franklin, M. C., Kamtekar, S., Im, Y. J., Rho, S. H., Seong, I. S., Lee, C. S., Chung, C. H., and Eom, S. H. (2001a). Crystal structures of the HslVU peptidase-ATPase complex reveal an ATP-dependent proteolysis mechanism. Structure (Camb) *9*, 177-184.

Wang, J., Song, J. J., Seong, I. S., Franklin, M. C., Kamtekar, S., Eom, S. H., and Chung, C. H. (2001b). Nucleotide-dependent conformational changes in a protease-associated ATPase HsIU. Structure (Camb) *9*, 1107-1116.

Wang, Q., Song, C., Yang, X., and Li, C. C. (2003). D1 ring is stable and nucleotide-independent, whereas D2 ring undergoes major conformational changes during the ATPase cycle of p97-VCP. J Biol Chem *278*, 32784-32793.

Watanabe, Y. H., Motohashi, K., and Yoshida, M. (2002). Roles of the two ATP binding sites of ClpB from Thermus thermophilus. J Biol Chem *277*, 5804-5809.

Weber, J., and Senior, A. E. (2001). Bi-site catalysis in F1-ATPase: does it exist? J Biol Chem *276*, 35422-35428.

Wojtkowiak, D., Georgopoulos, C., and Zylicz, M. (1993). Isolation and characterization of ClpX, a new ATP-dependent specificity component of the Clp protease of Escherichia coli. J Biol Chem *268*, 22609-22617.

Wojtyra, U. A., Thibault, G., Tuite, A., and Houry, W. A. (2003). The N-terminal zinc binding domain of ClpX is a dimerization domain that modulates the chaperone function. J Biol Chem *278*, 48981-48990.

Ye, Y., Meyer, H. H., and Rapoport, T. A. (2001). The AAA ATPase Cdc48/p97 and its partners transport proteins from the ER into the cytosol. Nature *414*, 652-656.

Yu, R. C., Hanson, P. I., Jahn, R., and Brunger, A. T. (1998). Structure of the ATP-dependent oligomerization domain of N-ethylmaleimide sensitive factor complexed with ATP. Nat Struct Biol *5*, 803-811.

Zalk, R., and Shoshan-Barmatz, V. (2003). ATP-binding sites in brain p97/VCP (valosin-containing protein), a multifunctional AAA ATPase. Biochem J *374*, 473-480.

CHAPTER TWO

SspB Delivery of Substrates for ClpXP Proteolysis Probed by the Design of

Improved Degradation Tags

Abstract

The ssrA-degradation tag sequence contains contiguous binding sites for the SspB adaptor and the ClpX component of the ClpXP protease. Although SspB normally enhances ClpXP degradation of ssrA-tagged substrates, it inhibits proteolysis under conditions that prevent tethering to ClpX. By increasing the spacing between the protease and adaptor binding determinants in the ssrA tag, substrates were obtained that displayed improved SspB-mediated binding to and degradation by ClpXP. These extended-tag substrates also showed significantly reduced conditional inhibition but bound SspB normally. Both wild-type and mutant tags showed highly dynamic SspB interactions. Together, these results strongly support delivery models in which SspB and ClpX bind concurrently to the ssrA tag but also suggest that clashes between SspB and ClpX weaken simultaneous binding. During substrate delivery, this signal masking is overcome by tethering SspB to ClpX, which ensures local concentrations high enough to drive tag engagement. This obstruct-then-stimulate mechanism may have evolved to allow additional levels of regulation and could be a common trait of adaptor-mediated protein degradation.

key words: energy-dependent degradation; degradation specificity; degradation signals; AAA+ ATPase; ClpP; compartmental protease; RssB; adaptor proteins

Introduction

Proteases destroy other proteins. As a consequence, precise and regulated substrate selection is critical in all cells. In organisms from bacteria to humans, ATP-dependent proteases, consisting of at least one AAA+ family ATPase and a compartmental peptidase, are the major machines of cytoplasmic protein destruction (Gottesman, 1996; Gottesman et al., 1997b; Gottesman et al., 1997a; Pickart and Cohen, 2004). Substrate choice for these proteases is mediated by the ATPase and frequently by additional adaptor or delivery proteins (Kondo et al., 1997; Levchenko et al., 2000; Zhou et al., 2001; Dougan et al., 2002b; Dougan et al., 2002a; Schlothauer et al., 2003). Adaptor proteins can also modulate substrate selection by AAA+ ATPases that function independently of proteases to dismantle macromolecular complexes and resolubilize aggregates (Schlothauer et al., 2003).

The ClpXP-SspB system is a paradigm for energy-dependent degradation and adaptor-mediated target recognition (Levchenko et al., 2000; Flynn et al., 2001; Wah et al., 2002; Dougan et al., 2003; Levchenko et al., 2003; Wah et al., 2003; Wojtyra et al., 2003; Song and Eck, 2003; Bolon et al., 2004). Ring hexamers of the ClpX ATPase recognize protein substrates, unfold these molecules, and translocate the denatured polypeptides through a central pore and into ClpP for degradation (Gottesman et al., 1993; Wojtkowiak et al., 1993; Wawrzynow et al., 1995; Gottesman, 1996). Processing of a single substrate can require hundreds of cycles of ATP hydrolysis and conformational change in the ClpXP machine (Kim et al., 2000; Kenniston et al., 2003; Burton et al., 2003). ClpX binds degradation tags in substrates. For example, the ssrA tag—a peptide added to the C terminus of nascent polypeptides on stalled bacterial ribosomes—targets proteins to ClpXP or ClpAP, a related AAA$^+$ protease (Keiler et al., 1996; Gottesman et

al., 1998). The SspB adaptor also binds to the ssrA tags of substrates, lowering K_M and enhancing substrate degradation by ClpXP but inhibiting proteolysis by ClpAP (Flynn et al., 2001). An SspB dimer brings two ssrA-tagged substrates and a ClpX hexamer together in a delivery complex that is more stable than the binary enzyme-substrate complex (Wah et al., 2002; Levchenko et al., 2003; Wah et al., 2003).
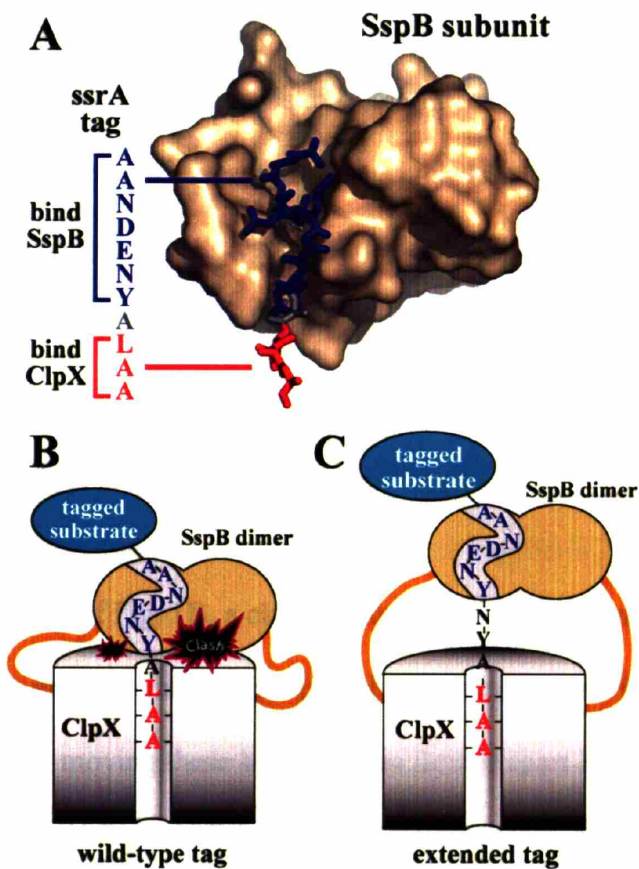

Figure 1. SspB delivery of ssrA-tagged substrates to ClpXP. (**A**) Structure of SspB subunit with bound ssrA tag (Levchenko et al., 2003). SspB and ClpX contact residues in the blue and red portions of the ssrA tag, respectively (Flynn et al., 2001). (**B**) Cartoon showing how SspB delivery of a substrate with a wild-type ssrA tag could result in a steric or electrostatic clash. (**C**) This clash could be relieved during delivery of a substrate with an extended ssrA tag in which the SspB and ClpX binding sites are farther apart.

Three distinct sets of protein-peptide interactions link ClpX, SspB, and the ssrA tags of substrates (11, 13-18): (*i*) ClpX binds C-terminal residues of the ssrA tag; (*ii*) the substrate-binding domain (SBD) of SspB contacts N-terminal residues in the tag (Fig. 1A); and (*iii*) an XB peptide motif at the C-terminus of SspB binds the N-terminal domain of ClpX, mediating

flexible tethering of these molecules. If the XB tethering motifs are removed or their binding sites on ClpX are blocked by XB peptide or other adaptors, then SspB binding inhibits ClpXP degradation of ssrA-tagged substrates instead of enhancing this reaction (Wah et al., 2003). One attractive model for this conditional inhibition involves the close spacing of binding determinants in the ssrA tag. Because the tag residues that bind ClpX and SspB are very close (Levchenko et al., 2003; Song and Eck, 2003), concurrent binding could result in modest steric or electrostatic clashes between ClpX and SspB (Fig. 1B). Such clashes would weaken binding and thus inhibit degradation of SspB-bound substrates in the absence of the tethering interactions. In tethered delivery complexes, by contrast, the high local concentration of the ssrA tag and ClpX could drive tag engagement despite the clashes. Alternatively, conditional inhibition could arise because breaking the protein-peptide interactions between SspB and the ssrA tag creates a kinetic barrier to degradation in a manner that is overcome in tethered but not in non-tethered complexes with ClpX.

In the model of Fig. 1B, a clash occurs between SspB and ClpX because their binding sites in the ssrA tag are too close. This model predicts that the inhibitory clash could be diminished or relieved by moving these binding sites farther apart in the tag as shown in Fig. 1C. To probe the mechanism of SspB delivery, we therefore constructed and tested the degradation properties of substrates with extended-spacing ssrA tags. Substrates bearing these mutant tags displayed improved SspB-mediated ClpXP degradation and significantly reduced conditional SspB inhibition. We find that interactions between the ssrA tag and SspB are highly dynamic and do not create a major kinetic barrier to degradation. These results support a "direct handoff" model in which SspB and ClpX bind simultaneously but with clashes to the wild-type ssrA tag (Fig.

1B). Hence, SspB binding changes the ssrA tag from a strong to a weak degradation signal but also functions to overcome this weakened binding by tethering the substrate to ClpX. The improved performance of the mutant ssrA tags in promoting SspB-mediated degradation shows that this tag-masking mechanism is not an obligate feature of the activation mechanism. Tag masking may have evolved to allow the SspB adaptor to function either as an enhancer or as an inhibitor of ssrA-tagged substrate degradation. The biological function of SspB may therefore depend on cellular conditions and the menu or abundance of competing ClpXP substrates and adaptor proteins.

Materials and Methods

Solutions. PD buffer contains 25 mM HEPES-KOH (pH 7.6), 5 mM KCl, 5 mM MgCl$_2$, 0.032% NP-40, and 10% glycerol. ATP regeneration mix consists of 16 mM creatine phosphate, 0.32 mg/mL creatine kinase, and 5 mM ATP. Buffer A contains 10 mM Tris (pH 7.6) and 50 mM KCl.

Proteins and Peptides. An overexpression plasmid for GFP-ssrA (pMS30) was provided by Julia Flynn (Flynn et al., 2001). Plasmids GH7 (encoding GFP-ssrA^{NYNY}) and GH8 (encoding GFP-ssrA^{NYGSNY}) were constructed by replacing the cassette between the *Stu*I and *Hind*III restriction sites in the 3′ portion of the *gfp-ssrA* gene in pMS30. The presence of the expected mutations in the genes encoding GFP-ssrA^{NYNY} and GFP-ssrA^{NYGSNY} were confirmed by DNA sequencing. *E. coli* ClpX, *E. coli* ClpP, GFP-ssrA and variants, *E. coli* SspB-SBD (residues 1-117), and *E. coli* SspB were expressed and purified by published procedures (Levchenko et al., 1997; Yakhnin et al., 1998; Kim et al., 2000; Wah et al., 2002; Wah et al., 2003). GFP-ssrA and

variants were further purified on a MonoQ 10/10 column (Amersham Biosciences). The ssrA

peptide (NH$_2$-NKKGRHGAANDENYALAA-COOH) and a derivative containing an N-terminal

fluorescein were synthesized by the MIT Biopolymers Laboratory and purified on a Shimadzu

LC-10AD-VP HPLC column. Concentrations were determined by UV absorbance at 280 nM

using extinction coefficients of 19770 M^{-1}cm^{-1} (GFP-ssrA and variants), 84480 M^{-1}cm^{-1} (ClpX$_6$),

125160 M^{-1}cm^{-1} (ClpP$_{14}$), 12090 M^{-1}cm^{-1} (SspB and SspB-SBD), and 1280 M^{-1}cm^{-1} (ssrA

peptide). The concentration of fluorescent ssrA peptide was determined in basic ethanol (pH

~10) using an extinction coefficient at 500 nM of 92300 M^{-1}cm^{-1} (Seybold et al., 1969). Note

that concentrations of SspB are reported in monomer equivalents.

Activity and binding assays. Degradation assays were performed at 30 °C as described (Kim et

al., 2000). ClpXP degradation of GFP-ssrA or variants in PD buffer plus an ATP regeneration

system was monitored using a Photon Technology International QM-2000-4SE

spectrofluorometer (excitation 467 nm; emission 511 nm; 0.3 cm cuvette). Degradation rates

were calculated from the initial linear loss of fluorescence. ClpXP-mediated degradation of [35]S-

GFP-ssrA was assayed by the release of radioactive peptides soluble in ice-cold trichloroacetic

acid (Kim et al., 2000). Curve fitting was performed using Kaleidagraph (Synergy Software).

Binding of tagged GFP to SspB at 30 °C was assayed by isothermal titration calorimetry using a

Microcal VP-ITC calorimeter. After degassing, SspB (60 µM) was loaded into the 300 µL

syringe and injected in 7.5 µL aliquots at 320 s intervals into a 1.4 mL cell containing 7 µM

GFP-ssrA or GFP-ssrA[NYNY]. Integration and least-squares fitting was performed using Origin

(Microcal) software, after discarding the first data point. The absorbance spectrum of GFP-ssrA in the presence and absence of SspB was taken on a HP-8452a UV-Vis spectrophotometer.

The kinetics of ssrA peptide or GFP-ssrA binding to SspB at 30 °C were assayed by changes in fluorescence (excitation 467 nM; emission > 495 nm) using an Applied Photophysics SX.18MV stopped-flow instrument. Stopped-flow samples were equilibrated at 30 °C for 10 min before injection. Mixing ratios of 1:1 or 1:5 were used for association and dissociation experiments, respectively. For association assays, different amounts of SspB were used and the concentrations, after mixing, of the fluorescent ssrA peptide or GFP-ssrA were 330 nM and 250 nM, respectively. For dissociation assays, SspB and fluorescent ssrA peptide were mixed (1 μM each) and diluted 6-fold into buffer containing 20 μM unlabeled peptide. For all stopped-flow experiments, at least 10 kinetic trajectories were collected, averaged, and fit to a single exponential function using Applied Photophysics software.

Results

Design of extended-spacing ssrA tags. ClpX recognizes the three C-terminal residues of the 11-residue ssrA tag, whereas SspB contacts determinants in the seven N-terminal residues (11; Fig. 1A). To move the ClpX and SspB binding sites farther apart, we designed an altered tag in which the NY sequence was repeated to generate a 13-residue variant (ssrA^{NYNY}) with the sequence AANDENYNYALAA. We also created a 15-residue tag (ssrA^{NYGSNY}) with the sequence AANDENYGSNYALAA. To ensure that the altered ssrA tags were functional, we fused them to the C terminus of green fluorescent protein (GFP) and determined K_M and V_{max} values for degradation by ClpXP (Table 1; data not shown). The mutant tags caused only minor changes in

these kinetic parameters, usually within experimental error, demonstrating that the mutations do not significantly alter tag interactions with ClpXP.

Table 1. Constants for ClpXP degradation and SspB binding to ssrA-tagged molecules.

ClpXP degradation (no SspB; 30 °C; PD buffer)

substrate	K_M (μM)	V_{max} (min^{-1} $ClpX_6^{-1}$)
GFP-ssrA	1.1 ± 0.1	0.9 ± 0.1
NYNY	0.8 ± 0.2	1.0 ± 0.1
NYGSNY	1.0 ± 0.3	1.0 ± 0.2

ClpXP degradation (with [SspB] = [substrate]; 30 °C; PD buffer)

substrate	K_M (nM)	V_{max} (min^{-1} $ClpX_6^{-1}$)
GFP-ssrA	75 ± 15	1.2 ± 0.1
NYNY	20 ± 4	1.2 ± 0.1
NYGSNY	15 ± 3	1.2 ± 0.1

ClpXP degradation (with [SspB SBD] = 20 μM; 30 °C; PD buffer)

substrate	K_M (μM)	V_{max} (min^{-1} $ClpX_6^{-1}$)
GFP-ssrA	48 ± 4[a]	1.0[a]
NYNY	2.3 ± 0.5	1.0 ± 0.1
NYGSNY	3.0 ± 0.7	1.0 ± 0.1

SspB binding (30 °C; buffer A)

substrate	K_D (nM)	ΔH ($kcal/mol$)	k_{on} ($\mu M^{-1}s^{-1}$)	k_{off} (s^{-1})
GFP-ssrA	48 ± 9	20 ± 1	ND	ND
NYNY	52 ± 11	17 ± 1	ND	ND
NYGSNY	92 ± 18	22 ± 1	ND	ND
ssrA peptide	650 ± 43[b]	ND	4.8 ± 0.1	3.1 ± 0.2

SspB binding (30 °C; PD buffer)

substrate	K_D (nM)	ΔH ($kcal/mol$)	k_{on} ($\mu M^{-1}s^{-1}$)	k_{off} (s^{-1})
GFP-ssrA	75 ± 30	22 ± 1	4.6 ± 0.3	0.3 ± 0.1[c]
NYNY	ND	ND	4.4 ± 0.4	ND
NYGSNY	ND	ND	ND	ND
ssrA peptide	450 ± 14	ND	4.0 ± 0.1	1.8 ± 0.1

[a] K_M value calculated by fitting with assumed V_{max} of 1.0 min^{-1}.
[b] K_D value calculated as ratio of k_{off}/k_{on}.
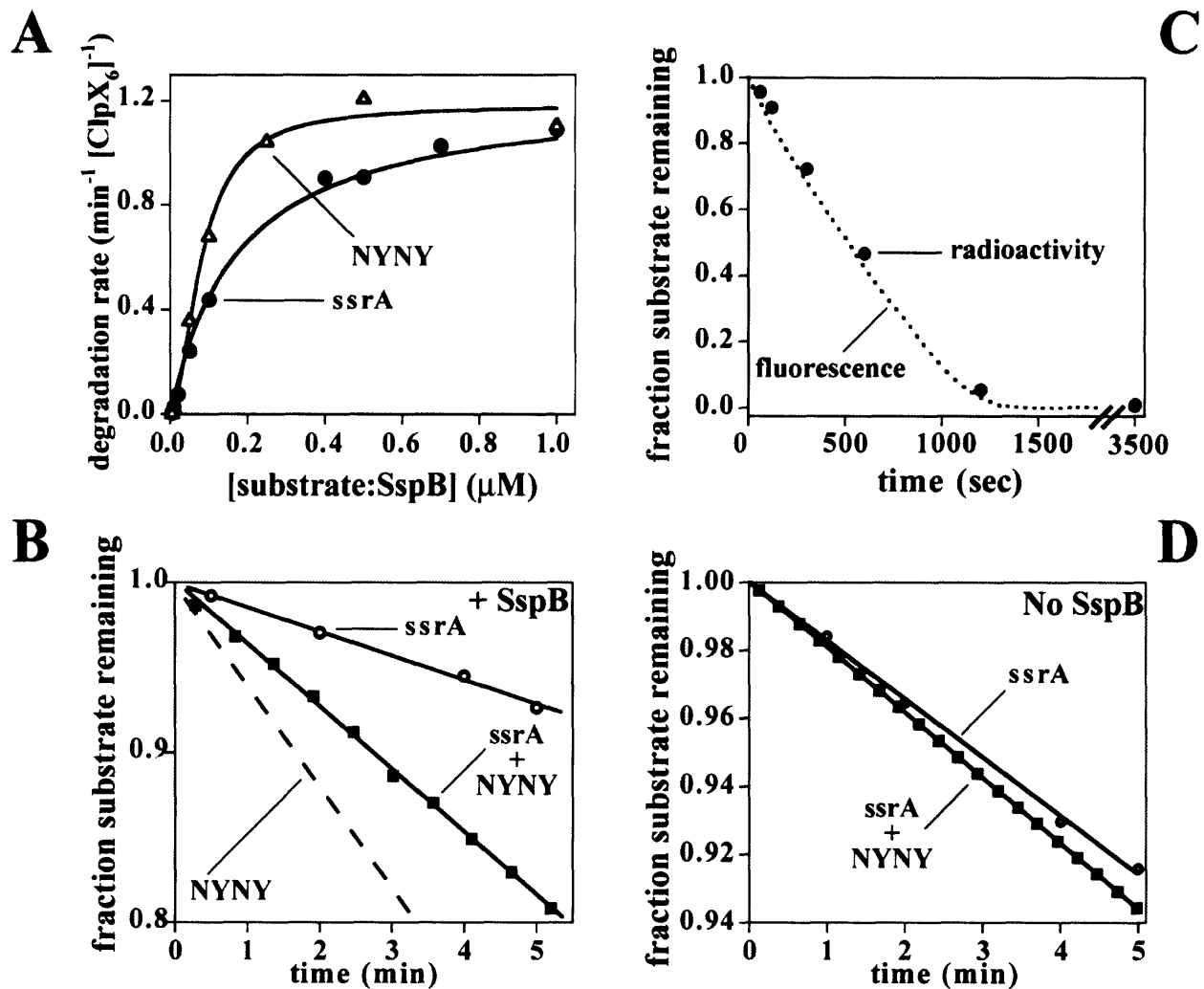[c] k_{off} calculated as $K_D \cdot k_{on}$.

Figure 2. ClpXP degradation of ssrA-tagged GFP variants in the presence of SspB. (A) Rates of degradation of tagged GFP in the presence of equimolar concentrations of SspB by ClpXP (50 nM $ClpX_6$; 300 nM $ClpP_{14}$) are plotted as a function of substrate concentration. (B) ^{35}S-GFP-ssrA (2 μM) and GFP-ssrA^{NYNY} (2 μM) were degraded by ClpXP in the same reaction in the presence of SspB (4 μM). Degradation reactions were monitored by changes in fluorescence (total degradation) and by release of acid-soluble radioactive peptides from ^{35}S-GFP-ssrA. The degradation of GFP-ssrA^{NYNY} (dashed line) was calculated by subtracting the degradation of ^{35}S-GFP-ssrA from the total degradation. (C) Kinetics of degradation of ^{35}S-GFP-ssrA (2 μM) by ClpXP (100 nM $ClpX_6$; 300 nM $ClpP_{14}$) in the presence of SspB (2 μM) were the same when monitored by loss of fluorescence (dotted line) or by release of acid-soluble radioactivity (circles). (D) ^{35}S-GFP-ssrA (2 μM) and GFP-ssrA^{NYNY} (2 μM) were degraded by ClpXP in the same reaction in the absence of SspB. The rate of degradation of ^{35}S-GFP-ssrA (open circles) is only slightly slower than the combined rate of degradation of both proteins (closed squares).

Improved SspB delivery to ClpXP. To test whether the mutant tags improved SspB-mediated delivery to ClpXP, we measured degradation rates at different substrate concentrations in the

presence of SspB. At saturating substrate concentrations, GFP-ssrA, GFP-ssrA^{NYNY}, and GFP-ssrA^{NYGSNY} were all degraded with comparable maximal velocities (Fig. 2A; Table 1). At low substrate concentrations, however, GFP-ssrA^{NYNY} (Fig. 2A) was degraded more efficiently than the wild-type substrate, as expected if the mutant tag reduced K_M for degradation. K_M for SspB-mediated degradation of GFP-ssrA was calculated to be 75 nM, after correcting for the concentration of enzyme bound SspB•GFP-ssrA and for the concentration of GFP-ssrA not bound to SspB. However, K_M values for the extended-spacing substrates could not be determined from these experiments because the concentrations of ClpXP•SspB•substrate and total SspB•substrate were too close to obtain a reliable value of the free SspB•substrate concentration.

To quantify differences in susceptibility to degradation, equal quantities of ^{35}S-GFP-ssrA and unlabeled GFP-ssrA^{NYNY} were mixed and SspB-mediated degradation was assayed under conditions where the two substrates compete for ClpXP (Fig. 2B). The overall degradation rate (GFP-ssrA^{NYNY} plus GFP-ssrA) was determined by changes in fluorescence, and the degradation rate of ^{35}S-GFP-ssrA was determined by release of acid-soluble radioactivity, allowing calculation of the GFP-ssrA^{NYNY} degradation rate. Under these conditions, GFP-ssrA^{NYNY} was degraded about 4-fold faster than GFP-ssrA (Fig. 2B) and GFP-ssrA^{NYGSNY} was degraded 5-fold faster (data not shown). Control experiments showed the same rate of ClpXP degradation of ^{35}S-GFP-ssrA assayed by fluorescence or acid-soluble radioactivity (Fig. 2C) and revealed similar rates of ^{35}S-GFP-ssrA and GFP-ssrA^{NYNY} degradation without SspB (Fig. 2D). When equal concentrations of two substrates compete for limiting enzyme, the ratio of V_{max}/K_M for processing of each substrate determines their relative degradation rates. This allows calculation of K_M values of 15-20 nM for ClpXP degradation of SspB-bound GFP-ssrA^{NYNY} and GFP-

ssrA^{NYGSNY} (Table 1). Thus the K_M's observed for substrates bearing the mutant tags are substantially lower than the wild-type value. Because $K_M \approx K_D$ for ClpXP degradation of ssrA-tagged substrates (24), the extended-spacing ssrA tags must mediate stronger binding to the enzyme in ternary complexes with the SspB adaptor.

Reduced conditional inhibition. The isolated substrate-binding domain of SspB inhibited ClpXP degradation of the extended-tag substrates less than degradation of GFP-ssrA (Fig. 3A). When substrate concentrations were varied in the presence of 20 μM SspB-SBD (Fig. 3B), roughly 20-fold higher concentrations of GFP-ssrA ($K_M \approx 50$ μM) were required to attain the same rates of degradation observed for the extended-tag GFP substrates (K_M 2-3 μM). Thus, moving the ClpX and SspB recognition determinants farther apart in the ssrA tag improves binding to ClpX in the presence of intact SspB or its substrate-binding domain. The importance of the tethering interactions for both the wild-type and mutant substrates is illustrated by the fact that K_M values for ClpXP degradation are at least 100-fold lower in the presence of SspB than in the presence of its tethering-defective SBD.

Can GFP-ssrA bound to the isolated SspB SBD actually be degraded by ClpXP or does the observed proteolysis result from degradation of adaptor-free substrate? The dashed line in Fig. 3B shows the calculated contribution of free GFP-ssrA to degradation observed in the presence of 20 μM SspB-SBD. Because the observed degradation is significantly higher than that expected from free substrate alone, we conclude that GFP-ssrA bound to the SspB-SBD is a substrate for ClpXP degradation.
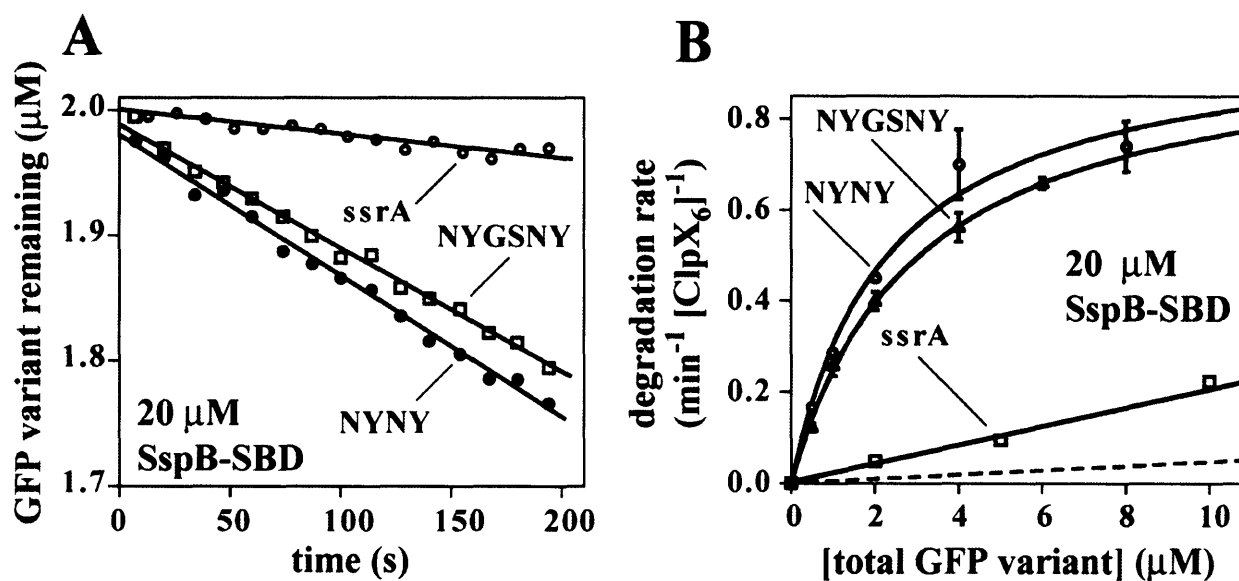
Figure 3. ClpXP degrades the extended-tag substrates significantly faster than GFP-ssrA in the presence of the substrate-binding domain of SspB. **(A)** Degradation of tagged GFP substrates (2 μM) by ClpXP (130 nM ClpX$_6$; 300 nM ClpP$_{14}$) in the presence of the SspB SBD (20 μM). **(B)** Michaelis-Menten plots of degradation rates at different substrate concentrations in the presence of 20 μM SspB SBD (same conditions as panel A). The dashed line is the calculated contribution from free GFP-ssrA degradation (i.e., substrate not bound to the SspB SBD) using K_D = 75 nM for SspB-SBD•GFP-ssrA binding, K_M = 1.1 μM, V_{max} = 0.9 min^{-1} ClpX$_6^{-1}$ (Table 1). Previous studies show that SspB and its SBD bind ssrA tagged substrates with essentially the same affinity (Wah et al., 2003). Kinetic parameters from Michaelis-Menten fits of the data are listed in Table 1. Because saturable kinetics was not observed for GFP-ssrA, the fit was constrained by assuming a V_{max} of 1 min^{-1}.

Binding of extended-tag substrates to SspB. To ensure that the mutations in the extended-spacing ssrA tags did not cause major changes in SspB interactions, isothermal titration calorimetry was used to assay binding (Table 1; Fig. 4). SspB bound GFP-ssrA and the mutants with equilibrium dissociation constants of roughly 50-90 nM (30 °C; buffer A or PD buffer). Hence, the extended tag mutations do not significantly perturb equilibrium binding to SspB.
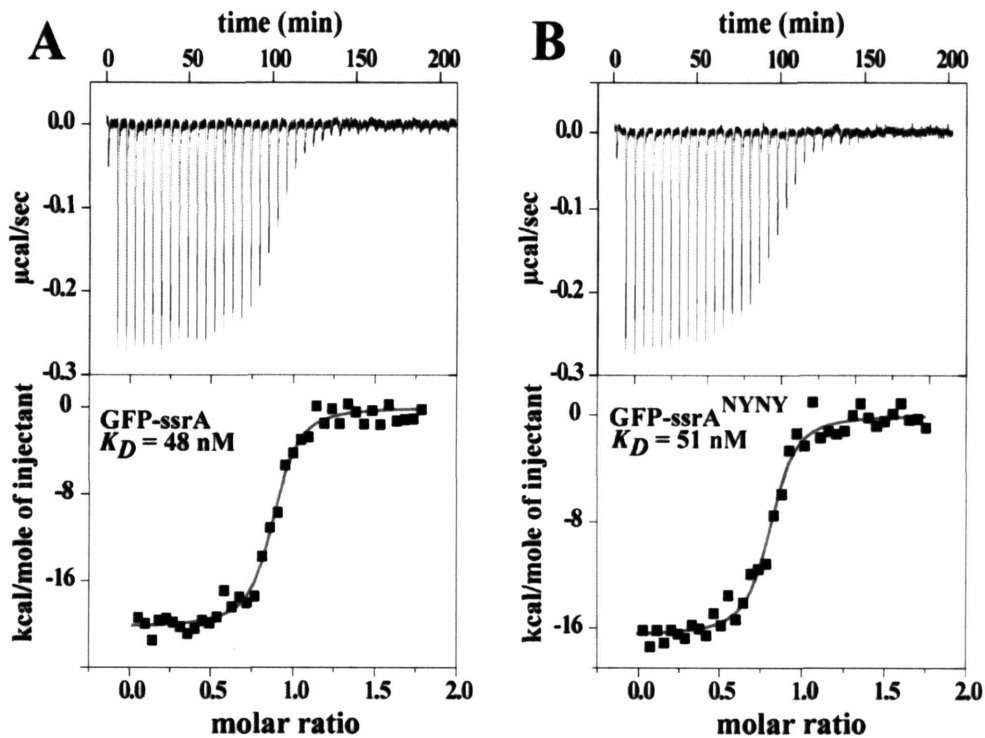
Figure 4. Equilibrium binding of SspB to GFP-ssrA (**A**) or GFP-ssrA^{NYNY} (**B**) assayed by isothermal titration calorimetry at 30 °C in buffer A. Thermodynamic parameters for these and additional binding experiments are listed in Table 1.

Dynamic interactions between SspB and ssrA tags. Successful substrate delivery for degradation must involve dissociation of ssrA-tagged substrates from SspB because the tag and attached substrate are translocated through the ClpX pore and into ClpP. To determine whether tag dissociation might be a slow step in degradation, we used stopped-flow experiments to measure the kinetics of interactions between SspB and an ssrA peptide or ssrA-tagged GFP. Fig. 5A shows a time course, assayed by changes in fluorescence, for dissociation of an SspB complex with an ssrA peptide containing an N-terminal fluorescein. The rate constant for dissociation (k_{off}) was 3.1 s^{-1} (30 °C, buffer A). Association also takes place in the sub-second time regime. Pseudo first-order rate constants (k_{obs}) for SspB-peptide association conditions were
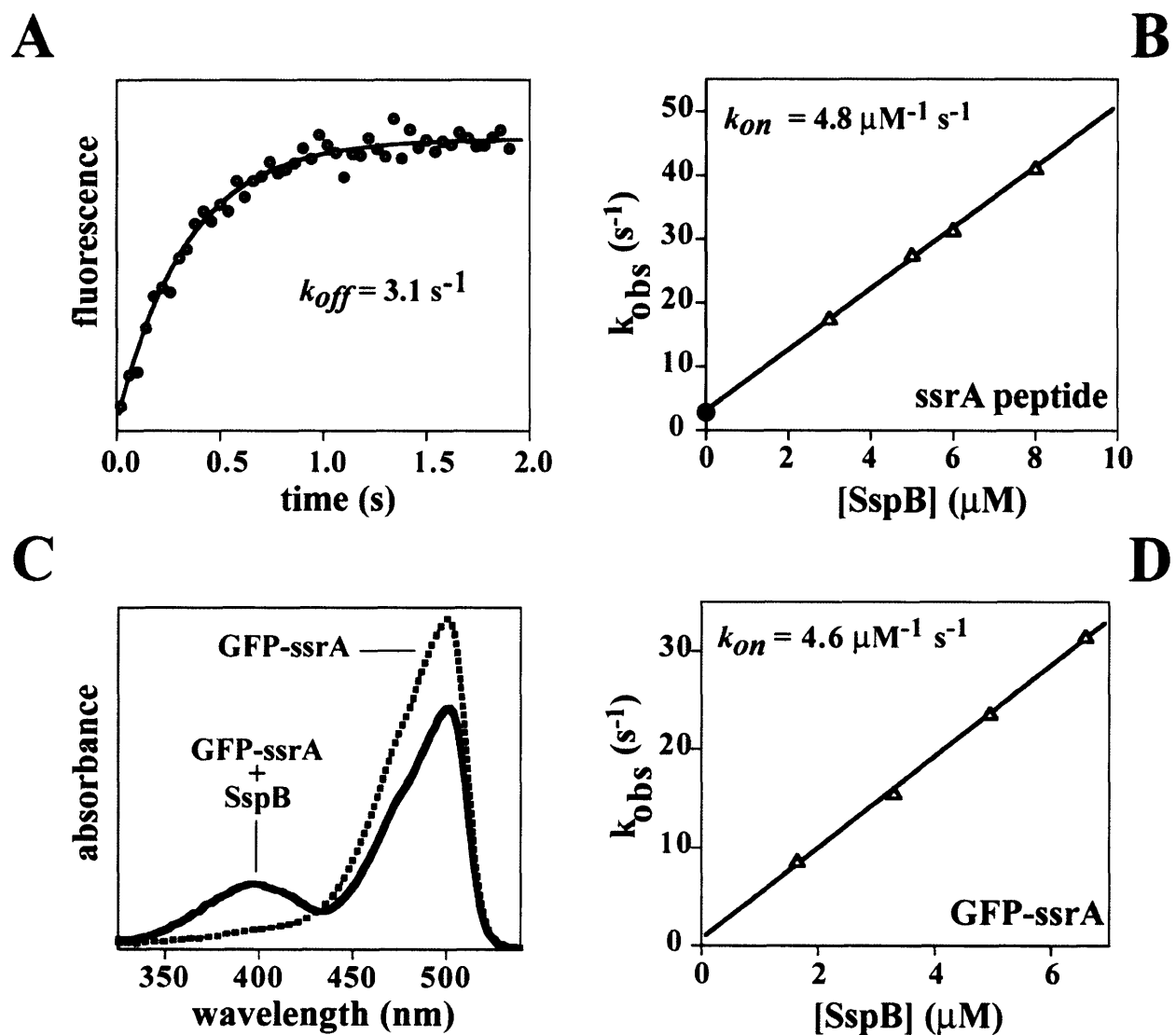
69

Figure 5. Kinetics of dissociation and association of ssrA-tagged molecules with SspB. (A) Dissociation kinetics; SspB (1 μM) was pre-bound to an ssrA peptide with a N-terminal fluorescein (1 μM) and, at time zero, was diluted 6-fold into buffer containing excess unlabelled peptide (20 μM). The solid line is a single exponential fit with a dissociation rate constant of 3.1 s^{-1}. (B) Association kinetics; the fluorescent ssrA peptide (330 nM) was mixed with different excess concentrations of SspB at time zero and pseudo-first order rate constants (k_{obs}) were determined by single exponential fits of the kinetic trajectories. These rate constants (open triangles) show a linear dependence on the total SspB concentration (R = 0.999), with a slope equal to the association rate constant. The y-intercept of the fit is very close to the k_{off} value (closed circle) as expected for relaxation kinetics (Fersht, 1985). (C) Absorbance spectra of GFP-ssrA (10 μM) in the presence (10 μM) or absence of SspB taken at room temperature in 10 mM Tris•HCl (pH 7.6). Under these conditions, SspB binding reduces the GFP-ssrA absorbance peak centered near 500 nM and results in a new peak ($\lambda_{MAX} \approx 400$ nm). The intensity of this new peak was diminished in a hyperbolic fashion as the KCl concentration was raised (50% decrease at 16 mM KCl; data not shown). (D) GFP-ssrA (250 nM) was mixed with different concentrations of SspB and pseudo-first order rate constants were determined by fits of kinetic trajectories measured by changes in fluorescence. The solid line is a linear fit (R = 0.999) with a slope of 4.6 μM^{-1}s^{-1} and a y-intercept of 0.73 ± 0.5 s^{-1}.

determined at different SspB concentrations and are plotted in Fig. 5B. The slope of this plot (4.8 $\mu M^{-1}s^{-1}$) is the association rate constant (k_{on}). Hence, both association and dissociation of the ssrA peptide and SspB occur rapidly. Similar rate constants for the SspB•ssrA-peptide interaction were obtained in PD buffer (Table 1). K_D values for SspB•peptide binding (450-650 nM), calculated from the kinetic constants, were similar to values determined directly for binding of the ssrA peptide to SspB or its substrate-binding domain at a lower temperature (Wah et al., 2002; Wah et al., 2003) but were about 10-fold higher than K_D for the binding of SspB to GFP-ssrA (Table 1).

Studies of the kinetics of the SspB•GFP-ssrA interaction were facilitated by the finding that SspB binding causes spectral changes in the GFP chromophore, including appearance of an absorbance peak near 400 nm (Fig. 5C) and reduction in the fluorescence emission peak near 510 nm (data not shown). The circular-dichroism spectrum of native GFP-ssrA was not altered upon SspB binding (data not shown), showing that GFP denaturation, which also results in an absorbance peak near 400 nM, is not the cause of the absorbance change. Assays of the kinetics of GFP-ssrA binding at different concentrations of SspB (Fig. 5D) yielded an association rate constant of 4.6 $\mu M^{-1}s^{-1}$ (30 °C; PD buffer). Dissociation could not be monitored directly because of hysteresis; changes in the environment of the GFP-ssrA chromophore apparently persist after dissociation of SspB. However, a dissociation rate constant of 0.3 s^{-1} was calculated from the association rate constant and equilibrium constant, indicating that the SspB•GFP-ssrA interaction is still highly dynamic with a half-life of roughly 2 sec. Because the maximal rate of SspB-mediated ClpXP degradation of GFP-ssrA is about 1 min^{-1}, dissociation of GFP-ssrA from SspB does not appear to be a significant kinetic barrier in the overall degradation reaction.

Discussion

SspB enhances ClpXP degradation of ssrA-tagged substrates by helping to bring the substrate and enzyme together (6, 12) but it has not been clear whether all three sets of peptide-protein interactions (ClpX•SspB, SspB•ssrA, and ssrA•ClpX) all form simultaneously in a true ternary complex or whether only binary contacts (ClpX•SspB and SspB•ssrA) are made. In the former case, SspB would directly hand the ssrA-tagged substrate to ClpX, whereas the latter model would require substrate dissociation from SspB prior to engagement by ClpX. The results reported here support the "direct handoff" model and suggest that ClpX and SspB can bind ssrA-tagged substrates concurrently albeit with modest clashes that weaken the ternary interaction (Fig. 1B). As a consequence, efficient handoff only occurs in tethered delivery complexes where the local concentrations of the degradation tag and its docking site on ClpX are very high. This model explains why SspB binding conditionally inhibits ClpXP degradation of ssrA-tagged substrates when the tethering interactions between SspB and ClpX are blocked or removed (Wah et al., 2003).

The extended-spacing ssrA tags had little effect on degradation by ClpXP in the absence of SspB, but mediated improved binding and degradation when either SspB or its isolated substrate binding domain were present. These results support the idea that clashes between ClpX and SspB occur when these molecules bind concurrently to the wild-type ssrA tag but are relieved in the mutant tags because the ClpX and SspB binding sites are farther apart (Fig. 1C). Concurrent binding of SspB and ClpX to the ssrA tag is required for "direct handoff" and is consistent with studies showing that complexes of SspB and ssrA-tagged substrates bind ClpX more tightly than either SspB or the substrates alone (Wah et al., 2002; Wah et al., 2003; Bolon et al., 2004).

Finally, we note that direct handoff is also supported by the finding that ClpXP degrades GFP-ssrA bound to the tethering defective substrate-binding domain of SspB.

The extended-spacing degradation tags lower K_M for SspB-mediated ClpXP degradation by 4 to 5-fold relative to the wild-type ssrA tag but lower K_M in the presence of the SspB substrate-binding domain by 16 to 20-fold (Table 1). Both results demonstrate improved ClpX interaction and therefore are consistent with tag-dependent relief of unfavorable interactions between SspB and ClpX, but the effect is clearly larger in the context of the isolated substrate-binding domain. The added sequences in extended tags may hinder binding to a small degree specifically in tethered complexes, whereas they relieve unfavorable interactions between SspB and ClpX in both tethered and untethered complexes.

To complete the process of substrate delivery, ssrA-tagged substrates must dissociate from SspB to allow full engagement and processing by ClpXP. We find that the complex of SspB with GFP-ssrA dissociates with a half-life of a few seconds in solution. This rate is much faster than the overall rate of SspB-mediated ClpXP degradation, and thus dissociation of the complex between SspB and the ssrA-tagged substrate should not limit the overall rate of degradation. Whether ClpX simply waits for spontaneous dissociation of the tagged substrate from SspB in ternary complexes or accelerates dissociation by pulling on the C-terminal end of the ssrA tag remains to be determined. The rapid dynamics of association and dissociation of the ssrA tag from SspB also ensures that the system equilibrates rapidly. Indeed, all of the peptide-protein interactions (ClpX•SspB, SspB•ssrA, and ssrA•ClpX) involved in SspB-mediated delivery of ssrA-tagged substrates to ClpXP are relatively weak and highly dynamic. The conformation of the ClpX

machine must change during the ATPase-cycle, which takes place on the sub-second time scale. Moreover, hydrolysis of hundreds of ATP molecules can be required for ClpXP to denature a single native substrate (Kim et al., 2000; Burton et al., 2001; Kenniston et al., 2003). The use of multiple weak and dynamic peptide-protein interactions presumably allows individual contacts to be broken easily but then to reform rapidly during the conformational excursions of the ATPase. This may allow delivery complexes to remain intact for many cycles of ATP hydrolysis, while ClpX is attempting to denature native ssrA-tagged substrates.

Most of the energy for binding ssrA-tagged substrates to SspB comes from interactions between the tag and SspB, but GFP-ssrA binding was about 10-fold tighter than ssrA-peptide binding to SspB. This difference could arise because native GFP makes a few favorable contacts with SspB (≈ 1 kcal/mol) or because the non-ssrA portions of the peptide make a few unfavorable contacts of the same magnitude. We favor the former model because the absorbance and fluorescence properties of GFP-ssrA are perturbed upon binding to SspB, indicating that there is, in fact, interaction between these two proteins. These spectral changes were more prominent at low ionic strength, consistent with the interaction having an electrostatic component. SspB binding may perturb the GFP chromophore, which is buried in the hydrophobic core (Ormo et al., 1996), by stabilizing a slightly altered GFP conformation. Distinct equilibrium populations of GFP with spectral properties similar to those described here have been previously observed (Chattoraj et al., 1996).

Evolution has not optimized the ssrA tag for maximal rates of SspB-mediated ClpXP degradation. Our results show that substrates bearing the extended-spacing mutant tags are

degraded 4-5 fold faster than substrates with the wild-type tag under competitive conditions. Why has the efficiency of SspB-mediated ClpXP degradation of ssrA-tagged substrates not been maximized by natural selection? The design of the natural ssrA tag could be constrained because it must be added by the co-translational machinery of the tmRNA system (Keiler et al., 1996) or because it also serves as a degradation signal for other proteases (Keiler et al., 1996; Herman et al., 1998). There is, however, no significant support for either of these possibilities. We prefer the idea that SspB has important biological roles both as an enhancer and as an inhibitor of ClpXP degradation of ssrA-tagged substrates. Because SspB binding changes the wild-type ssrA tag from a "strong" to a "weak" degradation signal, ClpXP degradation of bound substrates is dependent on the tethering interactions. As a result, ClpXP degradation of complexes of SspB with ssrA-tagged substrates could be blocked in the cell by other substrates, adaptors, or regulatory proteins that prevented tethering of SspB to ClpX. Recent studies have shown that the UmuD/D′ substrate competes with SspB for the tethering sites in the N-terminal domain of ClpX (Neher et al., 2003). Moreover, the RssB adaptor has been proposed to interact with ClpX in a manner similar to SspB (Dougan et al., 2003).

Interestingly, *E. coli* has many ways to prevent or slow degradation of ssrA-tagged substrates, which arise from aberrant translation and therefore represent a form of intracellular debris. For example, both SspB and the ClpS adaptor inhibit ClpAP degradation of ssrA-tagged substrates (Dougan et al., 2002b). Why would a cell add a very efficient degradation tag to proteins it wants to degrade and then repress proteolysis of these same polypeptides? Because the number of ClpXP and ClpAP proteases are limited in the cell (roughly 100 copies each (Ortega et al., 2004)), these enzymes may be easily saturated when substrates are abundant. Under such

conditions, delaying proteolysis of ssrA-tagged proteins could allow ClpAP and ClpXP to degrade more critical substrates such as key transcription factors including stress regulators. The inhibitory activities of SspB could be especially important under adverse conditions, where translational mistakes and the level of ssrA tagging were high and ClpAP or ClpXP degradation of specific substrates was needed for an efficient stress response. Indeed, the main function of proteolytic adapters may be to prioritize the proteolysis of different substrates under conditions where the degradation capacity of the cell is stressed.

The RssB adaptor, which delivers σ^S for ClpXP degradation, also functions as an inhibitor of σ^S function under some conditions (Zhou and Gottesman, 1998; Becker et al., 1999; Becker et al., 2000; Zhou et al., 2001). Becker et al. (Becker et al., 2000) have speculated that the inhibition function of adaptors may have evolved before their recruitment as enhancers of protein degradation. Thus, SspB may initially have functioned largely as a degradation inhibitor. This proposal is consistent with the obstruct-then-stimulate mechanism, which SspB uses for delivery of ssrA-tagged substrates to ClpXP, and with the fact that SspB inhibits ClpAP degradation of ssrA-tagged substrates (Levchenko et al., 2000; Flynn et al., 2001). Can inhibitors be turned into enhancers by tethering the inhibition complex to an appropriate protease? Inhibition of ClpAP degradation has been ascribed to overlap between ClpA and SspB binding determinants in the ssrA tag (Levchenko et al., 2000; Flynn et al., 2001). Because ClpA does not contain tethering sites for SspB, any clash that substantially weakened concurrent ClpA and SspB binding to the tag would obviously be inhibitory in a manner analogous to inhibition of ClpXP degradation by tethering-defective SspB. In this regard, however, it would be interesting to determine whether

SspB could deliver substrates to ClpA variants bearing the ClpX N-domain, which contains the tethering sites for SspB.

REFERENCES

Becker, G., Klauck, E., and Hengge-Aronis, R. (1999). Regulation of RpoS proteolysis in *Escherichia coli*: the response regulator RssB is a recognition factor that interacts with the turnover element in RpoS. Proc Natl Acad Sci U S A *96*, 6439-6444.

Becker, G., Klauck, E., and Hengge-Aronis, R. (2000). The response regulator RssB, a recognition factor for sigmaS proteolysis in Escherichia coli, can act like an anti-sigmaS factor. Mol Microbiol *35*, 657-666.

Bolon, D. N., Wah, D. A., Hersch, G. L., Baker, T. A., and Sauer, R. T. (2004). Bivalent tethering of SspB to ClpXP is required for efficient substrate delivery: a protein-design study. Mol Cell *13*, 443-449.

Burton, R. E., Baker, T. A., and Sauer, R. T. (2003). Energy-dependent degradation: Linkage between ClpX-catalyzed nucleotide hydrolysis and protein-substrate processing. Protein Sci *12*, 893-902.

Burton, R. E., Siddiqui, S. M., Kim, Y. I., Baker, T. A., and Sauer, R. T. (2001). Effects of protein stability and structure on substrate processing by the ClpXP unfolding and degradation machine. EMBO J *20*, 3092-3100.

Chattoraj, M., King, B. A., Bublitz, G. U., and Boxer, S. G. (1996). Ultra-fast excited state dynamics in green fluorescent protein: multiple states and proton transfer. Proc Natl Acad Sci U S A *93*, 8362-8367.

Dougan, D. A., Mogk, A., Zeth, K., Turgay, K., and Bukau, B. (2002a). AAA+ proteins and substrate recognition, it all depends on their partner in crime. FEBS Lett *529*, 6-10.

Dougan, D. A., Reid, B. G., Horwich, A. L., and Bukau, B. (2002b). ClpS, a substrate modulator of the ClpAP machine. Mol Cell *9*, 673-683.

Dougan, D. A., Weber-Ban, E., and Bukau, B. (2003). Targeted delivery of an ssrA-tagged substrate by the adaptor protein SspB to its cognate AAA+ protein ClpX. Mol Cell *12*, 373-380.

Fersht, A. (1985). Enzyme Structure and Mechanism, 2nd edn, W. H. Freeman and Company).

Flynn, J. M., Levchenko, I., Seidel, M., Wickner, S. H., Sauer, R. T., and Baker, T. A. (2001). Overlapping recognition determinants within the ssrA degradation tag allow modulation of proteolysis. Proc Natl Acad Sci U S A *98*, 10584-10589.

Gottesman, S. (1996). Proteases and their targets in Escherichia coli. Annu Rev Genet *30*, 465-506.

Gottesman, S., Clark, W. P., de Crecy-Lagard, V., and Maurizi, M. R. (1993). ClpX, an alternative subunit for the ATP-dependent Clp protease of Escherichia coli. Sequence and in vivo activities. J Biol Chem *268*, 22618-22626.

Gottesman, S., Maurizi, M. R., and Wickner, S. (1997a). Regulatory subunits of energy-dependent proteases. Cell *91*, 435-438.

Gottesman, S., Roche, E., Zhou, Y., and Sauer, R. T. (1998). The ClpXP and ClpAP proteases degrade proteins with carboxy-terminal peptide tails added by the SsrA-tagging system. Genes Dev *12*, 1338-1347.

Gottesman, S., Wickner, S., and Maurizi, M. R. (1997b). Protein quality control: triage by chaperones and proteases. Genes Dev *11*, 815-823.

Herman, C., Thevenet, D., Bouloc, P., Walker, G. C., and D'Ari, R. (1998). Degradation of carboxy-terminal-tagged cytoplasmic proteins by the Escherichia coli protease HflB (FtsH). Genes Dev *12*, 1348-1355.

Keiler, K. C., Waller, P. R., and Sauer, R. T. (1996). Role of a peptide tagging system in degradation of proteins synthesized from damaged messenger RNA. Science *271*, 990-993.

Kenniston, J. A., Baker, T. A., Fernandez, J. M., and Sauer, R. T. (2003). Linkage between ATP consumption and mechanical unfolding during the protein processing reactions of an AAA+ degradation machine. Cell *114*, 511-520.

Kim, Y. I., Burton, R. E., Burton, B. M., Sauer, R. T., and Baker, T. A. (2000). Dynamics of substrate denaturation and translocation by the ClpXP degradation machine. Mol Cell *5*, 639-648.

Kondo, H., Rabouille, C., Newman, R., Levine, T. P., Pappin, D., Freemont, P., and Warren, G. (1997). p47 is a cofactor for p97-mediated membrane fusion. Nature *388*, 75-78.

Levchenko, I., Grant, R. A., Wah, D. A., Sauer, R. T., and Baker, T. A. (2003). Structure of a delivery protein for an AAA+ protease in complex with a peptide degradation tag. Mol Cell *12*, 365-372.

Levchenko, I., Seidel, M., Sauer, R. T., and Baker, T. A. (2000). A specificity-enhancing factor for the ClpXP degradation machine. Science *289*, 2354-2356.

Levchenko, I., Yamauchi, M., and Baker, T. A. (1997). ClpX and MuB interact with overlapping regions of Mu transposase: implications for control of the transposition pathway. Genes Dev *11*, 1561-1572.

Neher, S. B., Sauer, R. T., and Baker, T. A. (2003). Distinct peptide signals in the UmuD and UmuD' subunits of UmuD/D' mediate tethering and substrate processing by the ClpXP protease. Proc Natl Acad Sci U S A *100*, 13219-13224.

Ormo, M., Cubitt, A. B., Kallio, K., Gross, L. A., Tsien, R. Y., and Remington, S. J. (1996). Crystal structure of the Aequorea victoria green fluorescent protein. Science *273*, 1392-1395.

Ortega, J., Lee, H. S., Maurizi, M. R., and Steven, A. C. (2004). ClpA and ClpX ATPases bind simultaneously to opposite ends of ClpP peptidase to form active hybrid complexes. J Struct Biol *146*, 217-226.

Pickart, C. M., and Cohen, R. E. (2004). Proteasomes and their kin: proteases in the machine age. Nat Rev Mol Cell Biol *5*, 177-187.

Schlothauer, T., Mogk, A., Dougan, D. A., Bukau, B., and Turgay, K. (2003). MecA, an adaptor protein necessary for ClpC chaperone activity. Proc Natl Acad Sci U S A *100*, 2306-2311.

Seybold, P. G., Gouterman, M., and Callis, J. (1969). Calorimetric, photometric and lifetime determinations of fluorescence yields of fluorescein dyes. Photochem Photobiol *9*, 229-242.

Song, H. K., and Eck, M. J. (2003). Structural basis of degradation signal recognition by SspB, a specificity-enhancing factor for the ClpXP proteolytic machine. Mol Cell *12*, 75-86.

Wah, D. A., Levchenko, I., Baker, T. A., and Sauer, R. T. (2002). Characterization of a specificity factor for an AAA+ ATPase: Assembly of SspB dimers with ssrA-tagged proteins and the ClpX hexamer. Chem Biol *9*, 1237-1245.

Wah, D. A., Levchenko, I., Rieckhof, G. E., Bolon, D. N., Baker, T. A., and Sauer, R. T. (2003). Flexible linkers leash the substrate binding domain of SspB to a peptide module that stabilizes delivery complexes with the AAA+ ClpXP protease. Mol Cell *12*, 355-363.

Wawrzynow, A., Wojtkowiak, D., Marszalek, J., Banecki, B., Jonsen, M., Graves, B., Georgopoulos, C., and Zylicz, M. (1995). The ClpX heat-shock protein of *Escherichia coli*, the ATP-dependent substrate specificity component of the ClpP-ClpX protease, is a novel molecular chaperone. Embo J *14*, 1867-1877.

Wojtkowiak, D., Georgopoulos, C., and Zylicz, M. (1993). Isolation and characterization of ClpX, a new ATP-dependent specificity component of the Clp protease of Escherichia coli. J Biol Chem *268*, 22609-22617.

Wojtyra, U. A., Thibault, G., Tuite, A., and Houry, W. A. (2003). The N-terminal zinc binding domain of ClpX is a dimerization domain that modulates the chaperone function. J Biol Chem *278*, 48981-48990.

Yakhnin, A. V., Vinokurov, L. M., Surin, A. K., and Alakhov, Y. B. (1998). Green fluorescent protein purification by organic extraction. Protein Expr Purif *14*, 382-386.

Zhou, Y., and Gottesman, S. (1998). Regulation of proteolysis of the stationary-phase sigma factor RpoS. J Bacteriol *180*, 1154-1158.

Zhou, Y., Gottesman, S., Hoskins, J. R., Maurizi, M. R., and Wickner, S. (2001). The RssB response regulator directly targets σ^S for degradation by ClpXP. Genes Dev *15*, 627-637.

CHAPTER THREE

Binding of the XB module of SspB to the

N-domain dimer of ClpX

Greg L. Hersch, David A. Wah, Tania A. Baker, and Robert T. Sauer

Abstract

Assembly of stable SspB-substrate-ClpX delivery complexes requires the coupling of weak tethering interactions between ClpX and the XB modules of the SspB dimer as well as interactions between ClpX and the substrate degradation tag. The ClpX hexamer contains three XB binding sites, one per N-domain dimer, and thus binds strongly to just one SspB dimer at a time. Because different adaptor proteins use the same tethering sites in ClpX, those which employ bivalent tethering, like SspB, will compete more effectively for substrate delivery to ClpXP.

Introduction

In the ClpXP protease, ClpX binds protein substrates and unfolds and translocates these molecules into the degradation chamber of ClpP (Hoskins et al., 2001). ClpX recognizes target proteins via peptide signals such as the ssrA tag, an 11 residue sequence added to the C terminus of nascent proteins on stalled ribosomes (Keiler et al., 1996; Gottesman et al., 1998; Flynn et al., 2003). SspB, a dimeric adaptor protein, also binds ssrA-tagged proteins and enhances their degradation by ClpXP (Levchenko et al., 2000; Wah et al., 2002). Each SspB subunit contains a substrate-binding domain (SBD) and a flexible C-terminal tail (Levchenko et al., 2003; Song and Eck, 2003; Wah et al., 2003). An XB module at the end of each SspB tail mediates tethering interactions with ClpX (Wah et al., 2003). SspB does not deliver ssrA-tagged substrates to ClpX variants lacking the N domain (Dougan et al., 2003; Wojtyra et al., 2003), suggesting that this domain plays either a direct or indirect role in SspB-mediated delivery. Biochemical studies and an NMR structure have shown that the isolated N domain of ClpX is a dimer (Donaldson et al., 2003; Wojtyra et al., 2003).

The mechanism by which SspB stimulates ClpXP degradation of ssrA-tagged substrates is only partially understood. It is clear that the tails of SspB form tethering interactions with ClpX, thereby increasing the local concentration of ssrA-tagged substrates relative to the enzyme. In principle, several SspB dimers could bind one ClpX hexamer. Indeed experiments in which full-length and N-terminal truncations of ClpX were mixed have been interpreted as evidence that SspB binding and efficient substrate delivery require only a single N domain of ClpX (Dougan et al., 2003). If true, this result suggests that as many as six SspB dimers might bind ClpX. Other studies, however, indicate that

substrate-delivery complexes contain just one SspB dimer and two ssrA-tagged substrates per ClpX hexamer (Wah et al., 2002). This result suggests that more than one dimer of SspB does not interact with ClpX.

To ask if the N domain of ClpX is directly responsible for binding SspB, we performed binding experiments and found that the purified N domain bound an XB peptide as well as intact ClpX. Interestingly, one N-domain dimer bound only one XB peptide. This stoichiometry suggests that a ClpX hexamer contains just three tethering sites for the XB module of SspB, and thus could bind strongly to only one SspB dimer at a time. These results shed light on the mechanism of substrate delivery by SspB and suggest a way in which different intracellular adaptors could compete for ClpXP, thereby determining the priority of substrate selection.

Interactions of SspB with the ClpX N Domain

To assay for potential interactions with the XB peptide of SspB, N-domain fragments consisting of ClpX residues 1–61 with no His_6 tag or residues 1–64 with a C-terminal His_6 tag were purified and studied. As expected (Wojtyra et al., 2003), the untagged N domain formed a stable dimer as assayed by analytical equilibrium centrifugation (data not shown).

As monitored by fluorescence anisotropy (Fig. 1), the XB peptide bound the untagged N domain with a K_D (20 ± 5 μM) within error of that for intact ClpX (23 ± 7 μM). This results shows that the N domain mediates all of the energetically significant contacts between ClpX and the XB peptide.
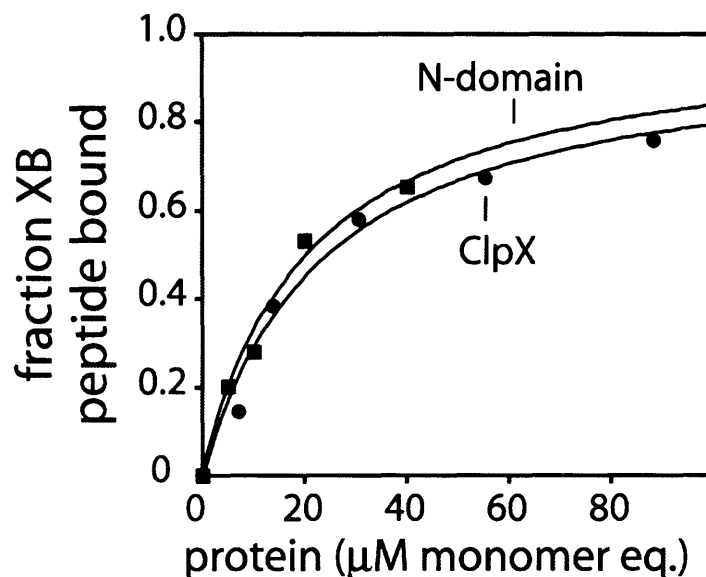
Figure 1. Binding of the N Domain of ClpX and XB modules of SspB (A) Equilibrium binding of untagged N domain or ClpX to fluorescent-XB peptide assayed by changes in anisotropy at 20°C. ClpX binding data is from Wah et al., (2003).

When binding experiments were performed using concentrations of the XB peptide (200 µM) much higher than the K_D, a stoichiometry of approximately 1 XB peptide per untagged N-domain dimer was obtained (Fig. 2A). A stoichiometry of 1.1 XB peptides per His_6-tagged N-domain dimer also provided the best fit in binding experiments assayed by isothermal titration calorimetry (Fig. 2B and 2C). Because untagged and His_6-tagged N-domain dimers, purified by different methods, were used for the two experiments, it seems unlikely that the reduced stoichiometry results from an equal mixture of fully active and inactive protein in both cases. The N domain forms a symmetric homodimer (Donaldson et al., 2003). Therefore, any tethering site present in one subunit should also be present in the other subunit, and there should be two equivalent binding sites for the XB peptide. We assume that the observed half-of-the-sites binding occurs because the tethering sites in both subunits overlap the 2-fold axis of the N domain, and thus that binding of one XB module occludes binding of a second.
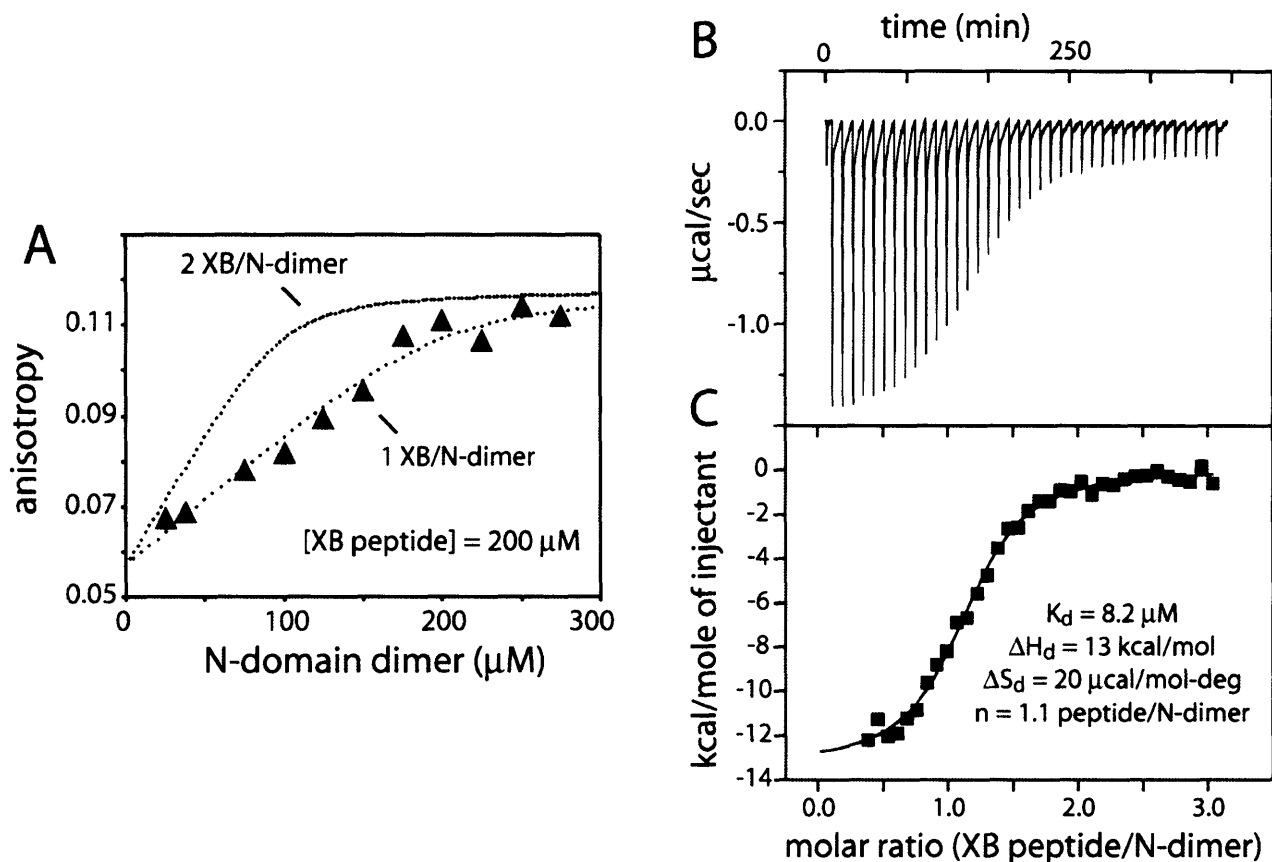
Figure 2. Binding stoichiometry of the N Domain of ClpX to XB modules of SspB (A) Stoichiometric binding of untagged N domain to XB peptide assayed by fluorescence anisotropy at 4°C. Theoretical curves for binding stoichiometries of 1 or 2 XB peptides per N domain dimer are shown. (B) Binding assayed by ITC. Aliquots (7.5 µl) of an XB peptide (1.1 mM) were injected into a 1.4 ml solution containing the His-tagged N domain dimer of *E. coli* ClpX (80 µM dimer) at 25°C (pH 7.6, 50 mM KCl). (C) Single-species fit of the data shown in (B) gave the K_D, ΔH, ΔS, and n values listed.

Discussion

Two groups have shown that deleting the N domain of ClpX prevents SspB stimulation of ClpXP degradation of ssrA-tagged substrates (Dougan et al., 2003; Wojtyra et al., 2003), suggesting that this domain is required directly or indirectly for SspB interactions. The results presented here show that this interaction is direct and also show that N domains in isolation or intact ClpX bind the XB peptide equally well. Notably, however,

only a single XB peptide binds to the N-domain dimer. This stoichiometry indicates that a ClpX hexamer contains just three potential tethering sites for the two XB peptides of a SspB dimer. Moreover, other studies have shown that both XB modules of the SspB dimer are required for full adaptor activity (Bolon et al., 2004). Taken together, these results are consistent with a model in which the two tails of the SspB dimer bind to two of the three tethering sites on ClpX, leaving one tethering site unoccupied (Fig. 3). This model accounts for the finding that delivery complexes contain one ClpX hexamer, one SspB dimer, and two ssrA-tagged substrates (Wah et al., 2002).
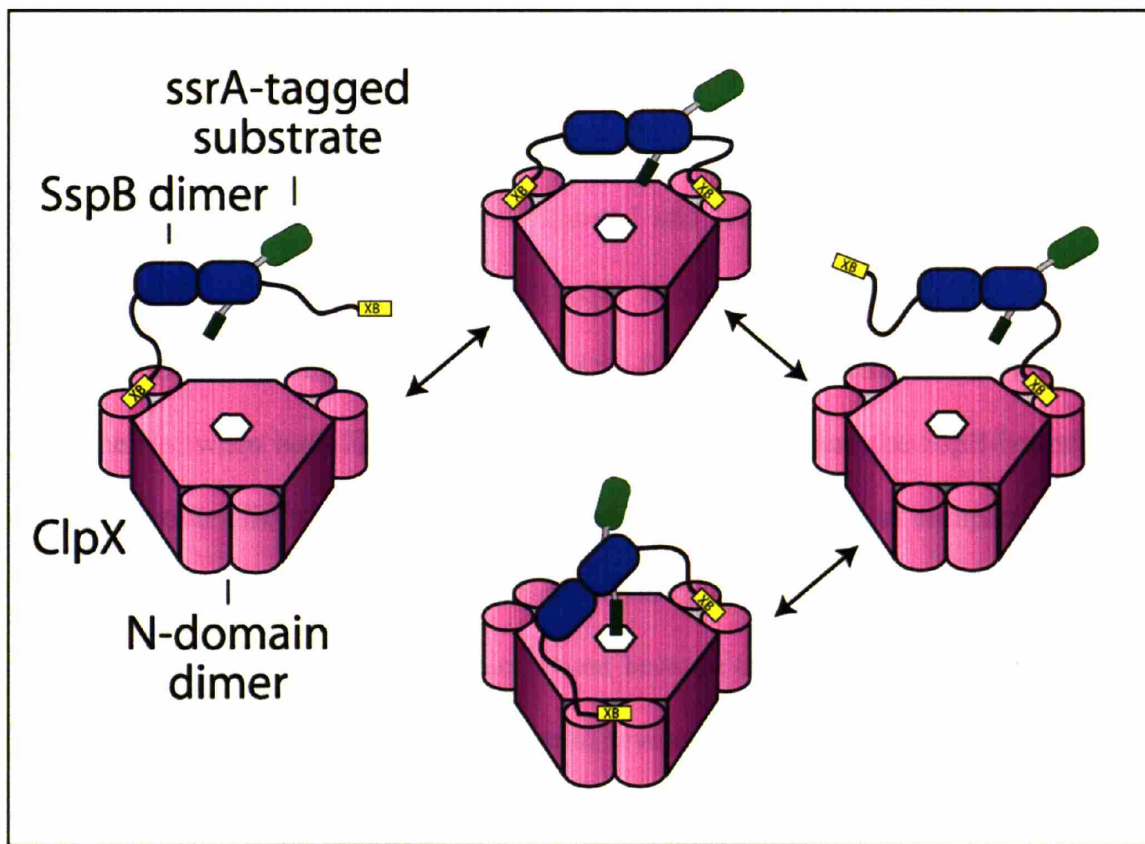

Figure 3. Cartoon representation of SspB, one bound ssrA-tagged substrate, and ClpX, showing how interactions between the XB modules and different ClpX N domains could be shuffled.

Binding of the XB modules of SspB to ClpX is probably a highly dynamic process. Once two tails dock with different N domains, a single tail could be released but then rebind to the same N domain or the other unoccupied N domain before the second tethering contact was broken. Indeed, the approximate 10-fold difference in the ClpX binding affinity of two-tailed and single-tailed SspB variants suggests that one tail is disengaged roughly 10% of the time. By this model, the SspB tails would constantly be detaching from and reattaching to the three N domain tethering sites of ClpX during substrate delivery (Fig. 3). This type of dynamic shuffling of XB tails and tethering sites may aid in substrate delivery.

SspB-mediated delivery of ssrA-tagged substrates to ClpXP involves the use of multiple weak interactions to generate a specific interaction of significantly stronger avidity. As determined from experiments shown in Figures 1 and 2, a single XB tethering interaction between SspB and ClpX is weak ($K_D \approx 20$ µM). Moreover, ClpX recognition of the ssrA tag bound to the substrate binding domain of SspB is also very weak (Bolon et al., 2004). Nevertheless, when both XB tethering interactions are made and the SspB-bound ssrA-tagged substrate also interacts with ClpX, then the overall affinity of complex formation increases to a K_D of roughly 70 nM. This strategy of coupling a number of weak interactions would result in a dynamic system because each individual contact could be broken relatively easily. Moreover, the use of several weak interactions which need to be coupled for strong binding would also permit substrate delivery to be regulated by blocking any of the weak contacts between the delivery complex and ClpX.

The XB binding site in the N domain of ClpX is also used to tether other adaptors. For example, degradation of UmuD/D′ by ClpXP requires tethering by the UmuD subunit which can be blocked by the SspB XB peptide (Neher et al., 2003a). Moreover, the RssB adaptor —which delivers σ^S to ClpXP (Zhou and Gottesman, 1998)— requires the N domain of ClpX and can also be inhibited by the SspB XB peptide (S. Siddiqui, J. Flynn, and S. Ebrahim personal communication). The existence of one tethering site that is shared by different adaptors sets up the possibility of competition when adaptor-substrate complexes are present in excess. Our results show that dimeric adaptors like SspB, which utilize two ClpX tethering sites, compete more effectively for ClpXP than those that use only one tethering interaction of comparable strength. Hence, the number and strength of these tethering interactions, as well as the accessibility and strength of the degradation signal in the substrate bound to the adaptor, would all be important factors in prioritizing the intracellular degradation of different substrates.

Where does the XB peptide bind on the N-Domain?

Although these experiments provide ample evidence that SspB binds to the N domain of ClpX, the site of this interaction has not been determined. The stoichiometry reported here (1 SspB tail (XB peptide) per N-domain dimer) implies that binding of one SspB tail somehow precludes binding of a second. One possibility is that only a single accessible binding site overlaps the two-fold symmetry axis of the N-domain dimer. A second possibility is that binding of the first XB peptide to one subunit of the dimer results in conformational changes in the second subunit that preclude further binding. No experimental evidence is available to support either mechanism, but I favor the single-binding site model out of simplicity.

Many experimental techniques have the potential to locate this binding interface. Because an NMR structure has been solved, it should be possible to locate the general site of XB peptide binding by HSQC experiments (Donaldson et al., 2003). A second possibility is to crystallize the N domain with bound XB peptide. My attempts to crystallize the N domain resulted in small crystals that I was not able to significantly improve through salt titrations or by using anaerobic conditions. When peptide was present in the crystallization solution, no crystals appeared in crystal screens or conditions resulting in crystals of N domain alone. Before crystallization, the N domain (which contains multiple cysteine residues) was treated with high concentrations of DTT at pH 8.8 and then desalted to remove the DTT. Small crystals were seen in Hampton Crystal Screen^{TM} condition 22: 0.2 M sodium acetate trihydrate; 0.1 M Tris•HCL (pH 8.5), 30% PEG 4000. No crystals formed below 23% PEG, and higher concentrations of PEG gave better results. Acetate variations showed that 0.2 M was optimal.

A final possibility for defining the N-domain•XB interface is to examine the binding properties of mutant N-domain proteins. The XB peptide sequence is Leu-Arg-Val-Val-Lys-CO_2^-. Functional experiments showed that only the leucine and penultimate valine, when mutated to alanine, showed any binding impairment (Wah et al., 2003). Other adaptor proteins that share the same docking site on the N-domain also contain a conserved leucine (Neher et al., 2003b). This suggests that the binding interface has significant hydrophobic character. A sequence search for exposed hydrophobic patches yielded ten potential targets distributed throughout the N domain (Fig. 4). Many of these

hydrophobic residues are also near the dimerization interface. Mutating these residues to alanine and then assaying the mutant protein's ability to bind the XB peptide should help to define the interaction interface.
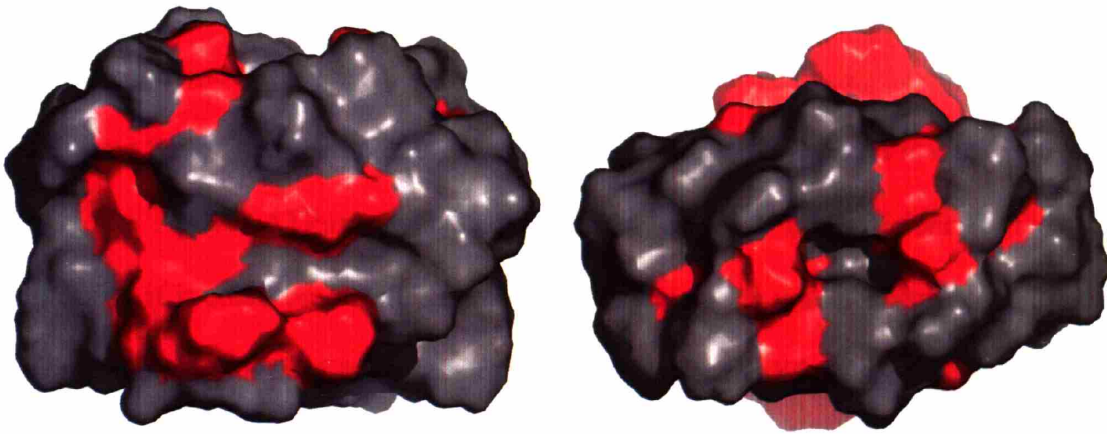

Figure 4. Perpendicular views of the N-domain dimer of ClpX (PDB ID 1OVX). Residues L12, F16, Q21, L27, I28, Y34, V40, L42, I46 and I47 are shown in red.

Is SspB a ClpX-specific adaptor protein?

In the absence of other evidence, the N domain appears to serve the limited function of bringing ClpX and its adaptor protein, SspB together. This interaction appears uncomplicated by allosteric interactions with the AAA+ domain of ClpX or other N domains. Furthermore, SspB's contacts with ClpX are thought to be limited only to the docking platform provided by the N domain. The absence of more extensive contacts with the AAA+ domain of ClpX suggest that these interactions may be transferable to another ATP-dependent protease that does not normally interact with SspB or degrade the substrates of ClpXP.

HslUV is an ATP dependent protease that does not degrade substrates with an ssrA tag and presumably does not interact with SspB (Burton et al., 2005). To investigate the role of the N domain in adaptor function further, the N domain of ClpX could be relocated to the N-terminus of HslUV. Known substrates of HslUV would be modified to include SspB's recognition sequence (A-A-N-D-E-N-Y) and then used in degradation assays with and without SspB (Flynn et al., 2001). If the purpose of the N domain is simply to tether SspB to a AAA+ ATPase, then SspB should enhance the efficiency of HslUV degradation if it could bind HslU. Particularly interesting is whether SspB increases the HslUV degradation rate of these substrates as it does for ClpXP. If so, it would offer the first solid evidence that SspB is "preparing" substrates for degradation rather than specifically activating the protease, as discussed in chapter one.

Experimental Procedures

Plasmid encoding *E. coli* ClpX N domain residues 1–61 or 1–64 with a C-terminal EH_6 tag were gifts from I. Levchenko and R. Burton. *E. coli* SspB and its SBD, GFP-ssrA, *E. coli* ClpX, *E. coli* ClpP, and fluorescein-labeled ssrA and XB peptides were purified or prepared as described (Wah et al., 2002; Wah et al., 2003). The synthetic XB peptide used for ITC was NH_2-CYRGGRPALRVVK-COOH. Peptide binding assays, degradation assays, and biophysical characterization by spectroscopy, sedimentation, and denaturation were performed essentially as described (Wah et al., 2002; Wah et al., 2003).

Bolon, D. N., Wah, D. A., Hersch, G. L., Baker, T. A., and Sauer, R. T. (2004). Bivalent tethering of SspB to ClpXP is required for efficient substrate delivery: a protein-design study. Mol Cell *13*, 443-449.

Burton, R. E., Baker, T. A., and Sauer, R. T. (2005). Nucleotide-dependent substrate recognition by the AAA+ HslUV protease. Nat Struct Mol Biol *12*, 245-251.

Donaldson, L. W., Wojtyra, U., and Houry, W. A. (2003). Solution structure of the dimeric zinc binding domain of the chaperone ClpX. J Biol Chem *278*, 48991-48996.

Dougan, D. A., Weber-Ban, E., and Bukau, B. (2003). Targeted delivery of an ssrA-tagged substrate by the adaptor protein SspB to its cognate AAA+ protein ClpX. Mol Cell *12*, 373-380.

Flynn, J. M., Levchenko, I., Seidel, M., Wickner, S. H., Sauer, R. T., and Baker, T. A. (2001). Overlapping recognition determinants within the ssrA degradation tag allow modulation of proteolysis. Proc Natl Acad Sci U S A *98*, 10584-10589.

Flynn, J. M., Neher, S. B., Kim, Y. I., Sauer, R. T., and Baker, T. A. (2003). Proteomic discovery of cellular substrates of the ClpXP protease reveals five classes of ClpX-recognition signals. Mol Cell *11*, 671-683.

Gottesman, S., Roche, E., Zhou, Y., and Sauer, R. T. (1998). The ClpXP and ClpAP proteases degrade proteins with carboxy-terminal peptide tails added by the SsrA-tagging system. Genes Dev *12*, 1338-1347.

Hoskins, J. R., Sharma, S., Sathyanarayana, B. K., and Wickner, S. (2001). Clp ATPases and their role in protein unfolding and degradation. Adv Protein Chem *59*, 413-429.

Keiler, K. C., Waller, P. R., and Sauer, R. T. (1996). Role of a peptide tagging system in degradation of proteins synthesized from damaged messenger RNA. Science *271*, 990-993.

Levchenko, I., Grant, R. A., Wah, D. A., Sauer, R. T., and Baker, T. A. (2003). Structure of a delivery protein for an AAA+ protease in complex with a peptide degradation tag. Mol Cell *12*, 365-372.

Levchenko, I., Seidel, M., Sauer, R. T., and Baker, T. A. (2000). A specificity-enhancing factor for the ClpXP degradation machine. Science *289*, 2354-2356.

Neher, S. B., Flynn, J. M., Sauer, R. T., and Baker, T. A. (2003a). Latent ClpX-recognition signals ensure LexA destruction after DNA damage. Genes Dev *17*, 1084-1089.

Neher, S. B., Sauer, R. T., and Baker, T. A. (2003b). Distinct peptide signals in the UmuD and UmuD' subunits of UmuD/D' mediate tethering and substrate processing by the ClpXP protease. Proc Natl Acad Sci U S A *100*, 13219-13224.

Song, H. K., and Eck, M. J. (2003). Structural basis of degradation signal recognition by SspB, a specificity-enhancing factor for the ClpXP proteolytic machine. Mol Cell *12*, 75-86.

Wah, D. A., Levchenko, I., Baker, T. A., and Sauer, R. T. (2002). Characterization of a specificity factor for an AAA+ ATPase: assembly of SspB dimers with ssrA-tagged proteins and the ClpX hexamer. Chem Biol *9*, 1237-1245.

Wah, D. A., Levchenko, I., Rieckhof, G. E., Bolon, D. N., Baker, T. A., and Sauer, R. T. (2003). Flexible linkers leash the substrate binding domain of SspB to a peptide module that stabilizes delivery complexes with the AAA+ ClpXP protease. Mol Cell *12*, 355-363.

Wojtyra, U. A., Thibault, G., Tuite, A., and Houry, W. A. (2003). The N-terminal zinc binding domain of ClpX is a dimerization domain that modulates the chaperone function. J Biol Chem *278*, 48981-48990.

Zhou, Y., and Gottesman, S. (1998). Regulation of proteolysis of the stationary-phase sigma factor RpoS. J Bacteriol *180*, 1154-1158.

CHAPTER FOUR

Asymmetric interactions of ATP with the AAA+ ClpX$_6$ unfoldase:

allosteric control of a protein machine

Published: Greg L. Hersch, Randall E. Burton, Daniel N. Bolon, Tania A. Baker, and

Robert T. Sauer (2005). Asymmetric interactions of ATP with the AAA+ ClpX$_6$

unfoldase: allosteric control of a protein machine. Cell *121*, 1017-1027.

Abstract

ATP hydrolysis by AAA+ ClpX hexamers powers protein unfolding and translocation during ClpXP degradation. Although ClpX is a homo-hexamer, positive and negative allosteric interactions partition six potential nucleotide-binding sites into three classes with asymmetric properties. Some sites release ATP rapidly, others release ATP slowly, and at least two sites remain nucleotide free. Recognition of the degradation tag of protein substrates requires ATP binding to one set of sites and ATP or ADP binding to a second set of sites, suggesting a mechanism that allows repeated unfolding attempts without substrate release over multiple ATPase cycles. Our results rule out concerted hydrolysis models involving $ClpX_6 \bullet ATP_6$ or $ClpX_6 \bullet ADP_6$, and highlight structures of hexameric AAA+ machines with 3 or 4 nucleotides as likely functional states. These studies further emphasize commonalities between distant AAA+ family members, including protein and DNA translocases, helicases, motor proteins, clamp loaders, and other ATP-dependent enzymes.

AAA+ ATPases use the chemical energy of ATP hydrolysis to fuel diverse biological processes that require mechanical work on macromolecular substrates (Vale, 2000; Glover and Tkach, 2001; Sauer et al., 2004). For example, these enzymes act as protein unfoldases in energy-dependent proteases, as DNA and RNA helicases, as protein and DNA translocases, and as molecular machines that dismantle macromolecular complexes and resolubilize aggregated proteins. AAA+ machines also function as replication factors that load processivity clamps onto DNA, as microtubule motor proteins, and as transcription factors. Despite these diverse functions, AAA+ enzymes share homologous ATPase domains and their active form is often a ring-shaped hexamer.

ClpXP is an ATP-dependent bacterial protease that consists of $ClpX_6$, a homo-hexameric AAA+ ATPase, and $ClpP_{14}$, an associated peptidase (Ortega et al., 2000). The crystal structure of ClpP reveals a barrel-shaped enzyme with a central degradation chamber and entry portals too small to admit folded protein substrates (Wang et al., 1997). ClpX plays several essential roles in degradation (for review, see Sauer et al., 2004). It recognizes protein substrates by binding to peptide tags, unfolds these proteins, and translocates the denatured polypeptide through a central pore and into ClpP for degradation. The ssrA tag is one of the best-studied targeting peptides for ClpXP and mediates the initial binding of proteins containing this sequence to the central pore of ClpX in an ATP-dependent fashion (Gottesman et al., 1998; Flynn et al., 2001; Wah et al., 2002; Bolon et al., 2004a; Siddiqui et al., 2004; Piszczek et al., 2005). How ATP binding to ClpX is linked to conformational changes and/or to interactions with the ssrA tag is poorly understood.

Structural information is available for ClpX (Kim and Kim, 2003) and for HslU, a highly related ATPase (Bochtler et al., 2000; Sousa et al., 2000; Wang et al., 2001a). Like other AAA+ enzymes, each of the six potential nucleotide-binding sites in ClpX and HslU is situated at an interface between two subunits, potentially allowing ATP binding and/or

hydrolysis to control enzyme conformation and activity (Wang et al., 2001b). In most structures of these ATPases, each subunit has an identical conformation and interacts with bound nucleotide. However, in a few structures, only some subunits bind nucleotide, and individual subunits can assume distinct conformations. At present, it is not known which of these structures are functional and/or interact with macromolecular substrates. The studies presented in this paper address this issue and additional questions by probing how nucleotide binding to ClpX mediates function. Does each subunit of a hexamer bind ATP? Does binding of ATP to one subunit affect the affinity of other subunits for nucleotide? How is nucleotide binding linked to interactions with protein substrates?

Here, we present evidence for distinct classes of nucleotide-binding sites in $ClpX_6$ and for communication between these sites. Binding of ATP to one class of sites drives conformational changes in the central pore and occupancy of subsequent sites by either ATP or ADP activates binding to the ssrA tag of protein substrates. Our results are inconsistent with concerted models in which six ATPs are hydrolyzed by $ClpX_6$ but support important roles for partially liganded species, as proposed for some AAA+ translocases and related helicases (Marrione and Cox, 1995; Singleton et al., 2000). Thus, AAA+ protein unfoldases like ClpX and HslU may operate by mechanisms similar to those used to remodel nucleic acids. Some subunits of $ClpX_6$ do not bind ATP and therefore function as regulatory or structural subunits, emphasizing similarities with heteromeric AAA+ enzymes, in which only some subunits serve catalytic roles (Jeruzalmi et al., 2001; Schwacha and Bell, 2001).

Results

An ATP-hydrolysis defective ClpX variant

Characterization of the ATP-bound state of ClpX has been difficult because the enzyme hydrolyzes ATP rapidly and constantly cycles through different nucleotide states. ClpX

also hydrolyzes ATPγS, although more slowly than ATP (Burton et al., 2003). To obtain a mutant likely to prevent ATP hydrolysis, we constructed the Glu185→Gln substitution in the Walker-B motif of *E. coli* ClpX (Fig. 1a). This motif forms part of the nucleotide-binding site in all P-loop ATPases, and the Glu side chain is thought to activate a water for attack on the γ-phosphate of bound ATP (Smith et al., 2002; Orelle et al., 2003).
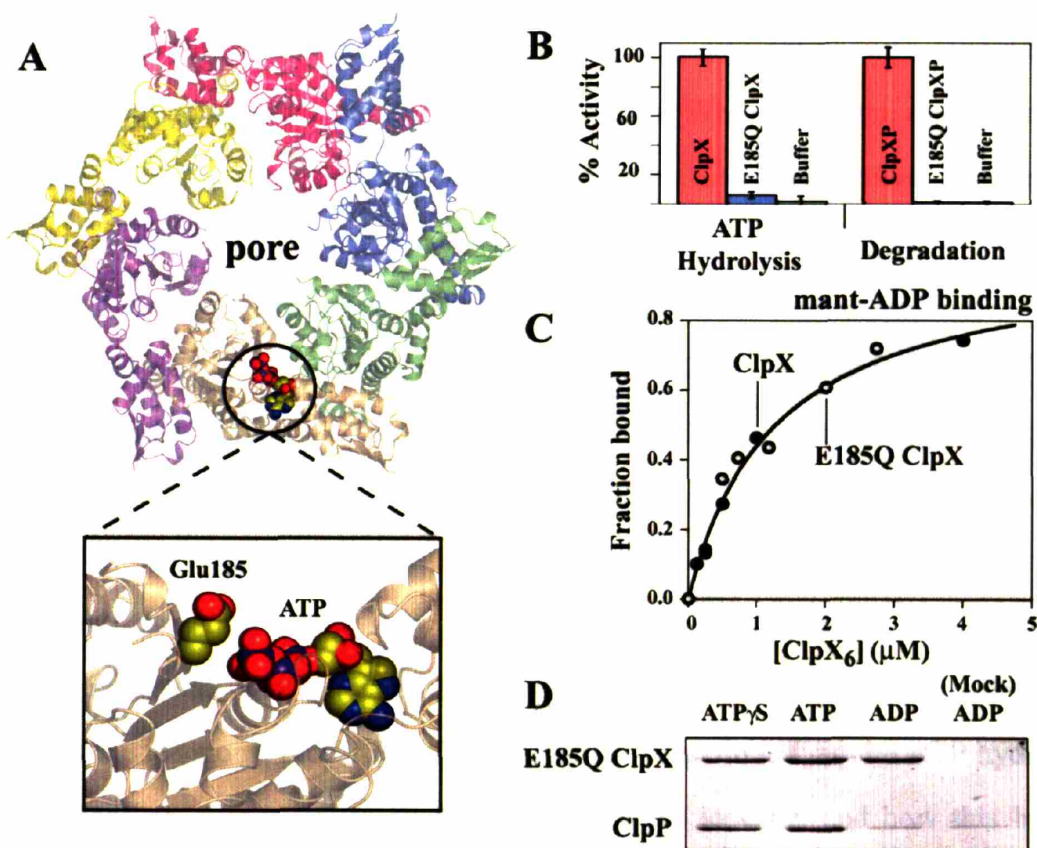

Figure 1. A ClpX variant defective in ATP-hydrolysis. (**A**) Top–axial view of a ClpX hexamer (Kim and Kim, 2003). Bottom–Glu185 in the Walker B motif is close to the γ-phosphate of ATP. (**B**) Relative to wild-type ClpX, the E185Q ClpX mutant hydrolyzes ATP within error of buffer and does not support degradation of GFP-ssrA. Assays contained mutant or wild-type $ClpX_6$ (300 nM) and 2.5 mM ATP; degradation assays also contained $ClpP_{14}$ (900 nM) and GFP-ssrA (2 μM). The wild-type ATPase and degradation rates were 102 min^{-1} $ClpX_6^{-1}$ and 0.7 min^{-1} $ClpX_6^{-1}$, respectively. (**C**) ClpX and E185Q ClpX bind mant-ADP equally well. The fitted curve represents binding of a ClpX hexamer to this nucleotide with a K_D of 1.3 μM. (**D**) His_6-E185Q-ClpX binds ClpP in the presence of ATPγS (lane 1) or ATP (lane 2). With ADP, the same low level of ClpP was recovered in the bound fraction when His_6-E185Q-ClpX was present (lane 3) or absent (lane 4).

The E185Q mutant behaved like wild-type ClpX during purification and formed hexamers as assayed by gel filtration (data not shown). UV spectra of the E185Q protein purified under native or denaturing conditions were very similar, ruling out contamination at levels greater than 0.3 nucleotides per hexamer (data not shown). As expected from the mutant design, the E185Q protein displayed little ATP-hydrolysis activity (within error of the buffer control) and was inactive in degradation of native or denatured substrates in the presence of ClpP (Fig. 1b; data not shown). However, the mutant enzyme retained the ability to bind nucleotide. When either the mutant or wild-type ClpX was titrated against mant-ADP, a fluorescent nucleotide analog, half maximal binding was observed at a hexamer concentration of 1.3 ± 0.3 µM (Fig. 1c; Burton et al., 2003). In pull-down assays, E185Q ClpX bound ClpP in the presence of Mg^{++}/ATP or Mg^{++}/ATPγS but showed no binding over control levels in the presence of Mg^{++}/ADP (Fig. 1d). Wild-type ClpX behaves similarly in this ClpP-binding assay (Joshi et al., 2004).

Experiments presented below show that E185Q ClpX also binds to the ssrA tag of peptide and protein substrates in an Mg^{++}/ATP dependent fashion. Hence, E185Q ClpX maintains the functional properties of wild-type ClpX that do not require ATP hydrolysis and provides an opportunity to study how ATP binds to ClpX and how this binding controls conformational and substrate-binding properties.

Strength and stoichiometry of ATP binding

Binding of ^{32}P-ATP to E185Q ClpX was assayed using nitrocellulose-filter retention. Based on a titration of increasing E185Q $ClpX_6$ against a constant amount of Mg^{++}/ATP, the equilibrium constant for dissociation of E185Q $ClpX_6$•ATP to free hexamer and ATP was 0.5 ± 0.2 µM (Fig. 2a). In this assay, only one molecule of ATP binds to a hexamer. To study whether additional nucleotides bind more strongly, increasing ATP was titrated
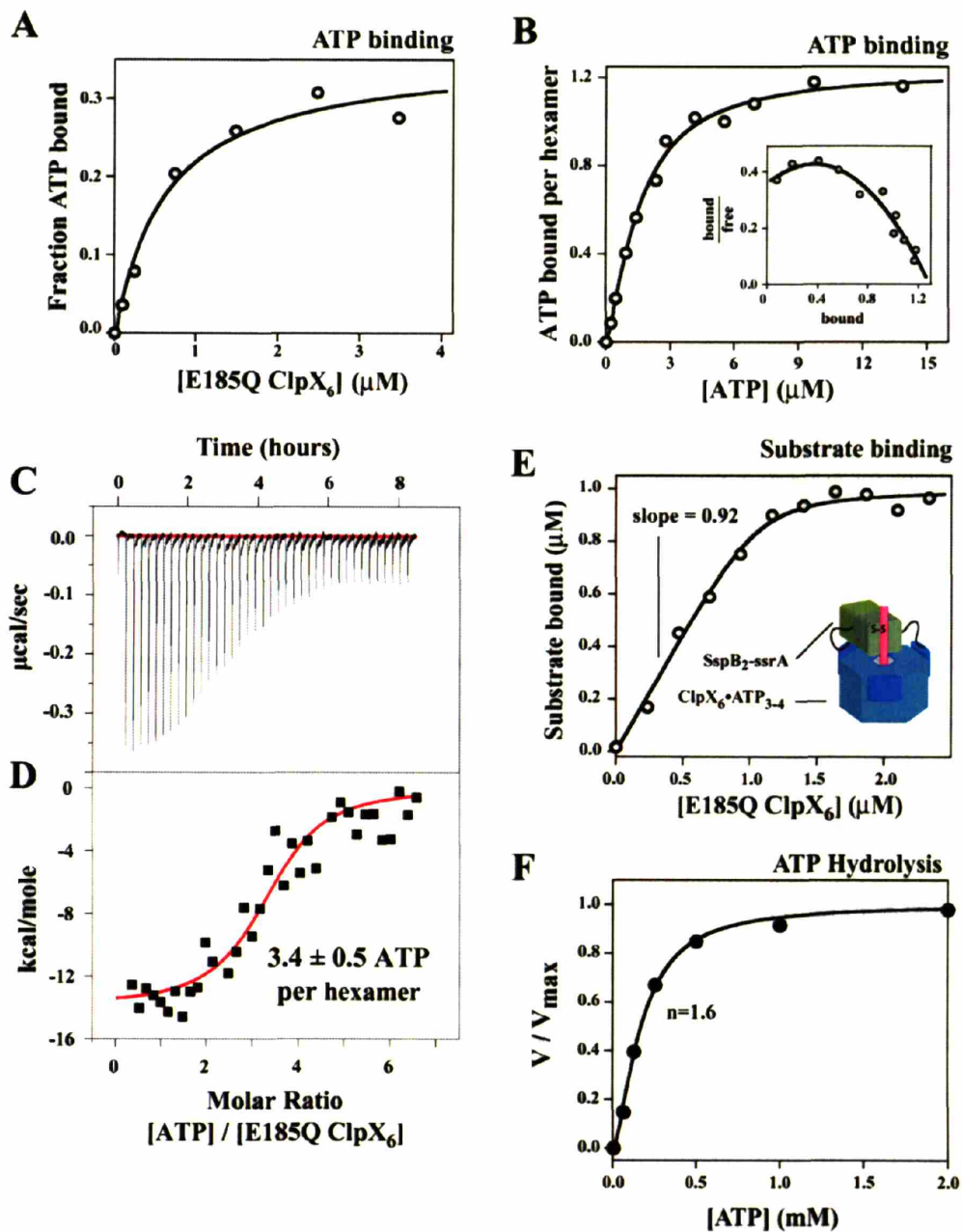
Figure 2. ATP binding. (**A**) Increasing E185Q ClpX$_6$ was titrated against 200 nM [^{32}P]-γ-ATP, and radioactivity retained on a nitrocellulose filter was assayed. The line is a fit with a K_D of 0.5 $\pm$ 0.2 μM and maximum retention of 35% of the total counts. (**B**) Increasing [^{32}P]-γ-ATP was titrated against 0.4 μM E185Q ClpX$_6$. The solid line represents half-maximal binding at a total ATP concentration of 1.4 $\pm$ 0.2 μM, with a Hill constant of 1.5 $\pm$ 0.2, and maximal retention of 1.2 ATP molecules per hexamer. **INSET**–same data plotted in Scatchard form to emphasize positive cooperativity. (**C**) Equilibrium binding assayed by isothermal titration calorimetry. Aliquots of ATP were injected into a solution containing 3.6 μM E185Q ClpX$_6$. (**D**) Integrated heats of binding from panel C fit well to a reaction model in which the E185Q hexamer binds 3.4 $\pm$ 0.5 ATP molecules with an affinity of 0.6 $\pm$ 0.3 μM. (**E**) Increasing E185Q ClpX$_6$ was titrated against 1 μM of the SspB$_2$-ssrA adaptor-substrate complex. The solid line is the curve expected if 92 $\pm$ 5% of the E185Q hexamers are active in binding SspB$_2$-ssrA. (**F**) Positive cooperativity in ATP hydrolysis by wild-type ClpX. Half-maximal velocity required an ATP concentration of 170 $\pm$ 20 μM and the Hill constant was 1.6 $\pm$ 0.3.

105

against a fixed concentration of E185Q ClpX$_6$ (Fig. 2b). ATP binding showed modest positive cooperativity (Hill constant 1.5 ± 0.2), which was also evident from the downward curvature of the Scatchard plot shown in the Fig. 2b inset. This result indicates that initial binding of ATP facilitates binding of subsequent ATPs. Consistent with this model, half-maximal binding was observed at a lower ATP concentration than would have been expected if ATP interacted identically and independently with each subunit in the E185Q ClpX hexamer. The affinity of E185Q ClpX for ATP was similar to that estimated for ATPγS binding to wild-type ClpX (Burton et al., 2003).

Isothermal titration calorimetry (ITC) was used to determine ATP-binding stoichiometry (Fig. 2c). Fitting of these data (Fig. 2d) gave 3.4 ± 0.5 ATPs bound per hexamer and an apparent affinity (0.6 ± 0.3 μM) similar to that observed using filter binding. The ITC stoichiometry is higher than the value of 1.2 ATPs per ClpX hexamer observed by filter binding (Fig. 2b). However, filter assays can underestimate stoichiometry because some ligand dissociates too rapidly to be captured, some ligand dissociates during filtration. and/or some proteins may denature upon binding to nitrocellulose. Indeed, only 35 ± 5% of the radioactive ATP was retained on the filter when saturating protein was present (Fig. 2a), even though thin-layer chromatography confirmed that all radioactivity was present as ATP (data not shown). We assume that 35% represents the efficiency of filter retention (i.e., 65% of ATP bound to E185Q ClpX is not captured). Correcting the filter-binding stoichiometry by dividing by 0.35 gives a value between 3 and 4 ATPs per hexamer, consistent with the ITC results. We also chromatographed E185Q ClpX on a monoQ ion-exchange column in buffers containing excess ATP (100 or 300 μM) and calculated the number of bound ATPs from the UV difference spectra of fractions with and without ClpX. Both experiments gave a value of 3.3 ± 0.5 ATPs per ClpX hexamer (data not shown). Thus, three different experiments indicate that a ClpX hexamer binds 3

or 4 molecules of ATP. Additional chromatography studies using ADP/ATP mixtures gave the same 3 or 4 nucleotides per hexamer suggesting that ADP cannot fill the remaining ATP-free sites (data not shown).

A stoichiometry of 3 or 4 ATPs per ClpX hexamer could potentially arise if approximately 60% of hexamers bound six ATPs, whereas the rest were damaged and bound no ATP. To determine the fraction of E185Q ClpX hexamers that bind ATP, we assayed binding to an adaptor-substrate molecule (SspB$_2$-ssrA) that interacts strongly only with ATP-bound ClpX (Bolon et al., 2004a; Bolon et al., 2004b). This molecule is a heterodimeric variant of the SspB adaptor with an ssrA peptide cross-linked to the peptide-binding groove of one subunit and a fluorescein attached to the tail of the other subunit. SspB$_2$-ssrA was used at a concentration 20-fold above the K_D to ensure that each E185Q hexamer capable of binding would be detected. A fit of the resulting binding data (Fig. 2e), indicated that $92 \pm 5\%$ of the E185Q ClpX was active. This result is inconsistent with a model in which 60% of E185Q hexamers bind six ATPs. We conclude that a hexamer of E185Q ClpX binds 3 or 4 molecules of ATP under saturating conditions with affinities that lead to half-maximal binding near 0.6 μM ATP. Because ClpX hexamers contain six potential nucleotide-binding sites, our results indicate that certain subunits adopt conformations that bind nucleotide strongly, whereas other subunits adopt a non-binding conformation.

Cooperative interactions in wild-type ClpX

To test for positive cooperativity in ATP interactions with wild-type ClpX, we assayed initial rates of hydrolysis as a function of ATP concentration (Fig. 2f). Fitting these data gave a Hill constant of 1.6 ± 0.3, indicative of positive cooperativity. As expected, the ATP concentration required for half-maximal hydrolysis (170 ± 10 μM) was significantly higher than the concentration required for half-maximal binding of ATP to E185Q ClpX

($\approx$1 μM), because most ATP that binds wild-type ClpX exits via hydrolysis and ADP dissociation rather than by ATP dissociation (Burton et al., 2003). As a consequence, K_M for ATP hydrolysis is much larger than K_D for ATP binding.

Multiple classes of ATP sites

In the experiments discussed above, it was established that only a subset of ClpX subunits bind ATP. To ask whether these ATP-binding sites were equivalent, we measured the kinetics of nucleotide dissociation, reasoning that a single exponential phase would support the presence of identical ATP-binding sites, whereas multiple phases would favor distinct classes of sites. For these experiments, E185Q ClpX was first mixed with enough ^{32}P-ATP to ensure 90-95% saturation, excess unlabeled nucleotide was added to block rebinding, and dissociation kinetics were measured using the filter-binding assay. With unlabeled ATP or ADP as competitor, ^{32}P-ATP dissociation was biphasic (Fig. 3, top and middle panels). A fast phase occurred over the first 15 s, and a slow phase occurred over the course of minutes. As a second, independent assay we bound the fluorescent analogue mant-ATP to E185Q ClpX and assayed dissociation by changes in fluorescence following addition of unmodified ATP. Fast and slow kinetic phases were also observed in this experiment (Fig. 3, bottom panel). Because of uncertainties in the efficiency of filter retention and the fluorescence change upon mant-ATP dissociation from each type of site, we cannot use the amplitudes of the two kinetic phases to estimate the numbers of each type of site. Nevertheless, these kinetic results suggest the existence of at least two classes of ATP-binding sites in addition to the third class of non-binding sites. We will refer to ATP-binding sites that release nucleotide rapidly as "fast sites" and those that release nucleotide slowly as "slow sites".
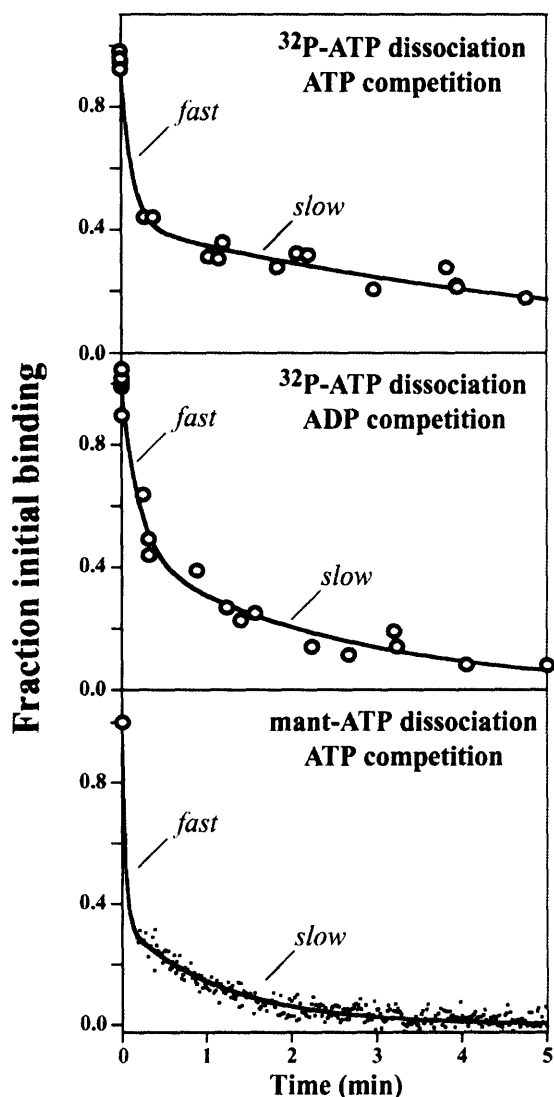
Figure 3. Dissociation kinetics reveals two classes of sites. **(A)** [^{32}P]-γ-ATP (5 μM) was mixed with E185Q ClpX$_6$ (0.4 μM), unlabeled ATP (1.5 mM) was added at time zero, and bound radioactivity was assayed by filter binding. The curve is a double-exponential fit (k_{fast} = 8 ± 4 min^{-1}; k_{slow} = 0.18 ± 0.02 min^{-1}. The fast phase was 56% of the total amplitude). **(B)** Same experiment as top panel except 1.5 mM unlabeled ADP was used as the competitor (k_{fast} = 5 ± 1 min^{-1}; k_{slow} = 0.39 ± 0.01 min^{-1}). The fast phase was 55% of the total amplitude. **(C)** Mant-ATP (12 μM) was mixed with E185Q ClpX$_6$ (1.6 μM), unmodified ATP (3.3 mM) was added at time zero, and mant-ATP dissociation was assayed by changes in fluorescence (k_{fast} > 8 min^{-1}, amplitude = 65% of total change; k_{slow} = 1.0 ± 0.1 min^{-1}).

Linkage between ClpX binding to the ssrA tag and to Mg^{++}/ATP

Previous studies indicate that nucleotide binding controls ClpX binding to the ssrA tag of substrates (Wah et al., 2002; Bolon et al., 2004a). To explore this linkage, binding of a fluorescein-labeled ssrA peptide to E185Q or wild-type ClpX was assayed by fluorescence anisotropy using nucleotide concentrations sufficient to saturate ClpX whether Mg^{++} was present or absent (Burton et al., 2003). E185Q ClpX bound the ssrA peptide equally well with Mg^{++}/ATP or Mg^{++}/ATPγS but did not show significant binding without Mg^{++}, without nucleoside triphosphate, or with Mg^{++}/ADP (Fig. 4a). Wild-type ClpX showed the same pattern, but ssrA-peptide binding was weaker with

Mg^{++}/ATP than with $Mg^{++}/ATP\gamma S$, presumably because rapid ATP-dependent translocation of peptide through ClpX causes faster release (Kenniston et al., 2004). The important result, however, is that ClpX binding to the ssrA tag is thermodynamically linked to both ATP and Mg^{++} binding.

A ClpX hexamer binds only one ssrA-tagged substrate (Piszczek et al., 2005). To ask how many subunits of the hexamer need to bind ATP to allow stable binding to the ssrA tag, we assayed the ATP-dependence of E185Q ClpX binding to the ssrA peptide or the cross-linked $SspB_2$-ssrA molecule (Fig. 4b). If hexamers bound these peptide or protein substrates equally well irrespective of the number of bound ATPs, then binding isotherms should largely reflect ATP occupancy and have a Hill constant of approximately 1.5 (see Fig. 2b). Instead, Hill constants calculated from the Fig. 4b binding curves were > 2.5. Because Hill constants reflect the minimum number of subunits involved in a process (Segel, 1976), these results suggest that three or more ATP-bound subunits of E185Q ClpX must cooperate to bind ssrA-tagged molecules tightly. Apparently, both the nucleotide-binding sites that release ATP rapidly and the sites that release ATP slowly must be occupied to promote ssrA-tag binding. Cooperativity was also observed in the $ATP\gamma S$-dependence of wild-type ClpX binding to $SspB_2$-ssrA (data not shown).

ATP binding and structural changes in the ClpX pore

The central pore of the ClpX hexamer has been implicated in binding the ssrA tag by studies showing that the V154F pore mutation dramatically weakens recognition of ssrA-tagged substrates (Siddiqui et al., 2004). Reasoning that a V154W mutation might act as a fluorescent reporter of pore conformation, we constructed and purified ClpX E185Q/V154W and recorded spectra with different nucleotides (Fig. 4c). Tryptophan fluorescence increased by about 25% and was red-shifted in response to Mg^{++}/ATP binding but was unaffected by Mg^{++}/ADP. Because Trp154 is the only tryptophan in the

protein, these data suggest that ATP binding leads to structural changes in the central pore. In principle, changes in tryptophan fluorescence could also reflect assembly of subunits into hexamers. However, our results are inconsistent with the formation of hexamers because binding of either ADP or ATP stabilizes hexamers. Moreover, the red shift indicates that ATP binding increases the accessibility of pore residues, as expected for a pore-opening model but not for hexamer assembly.
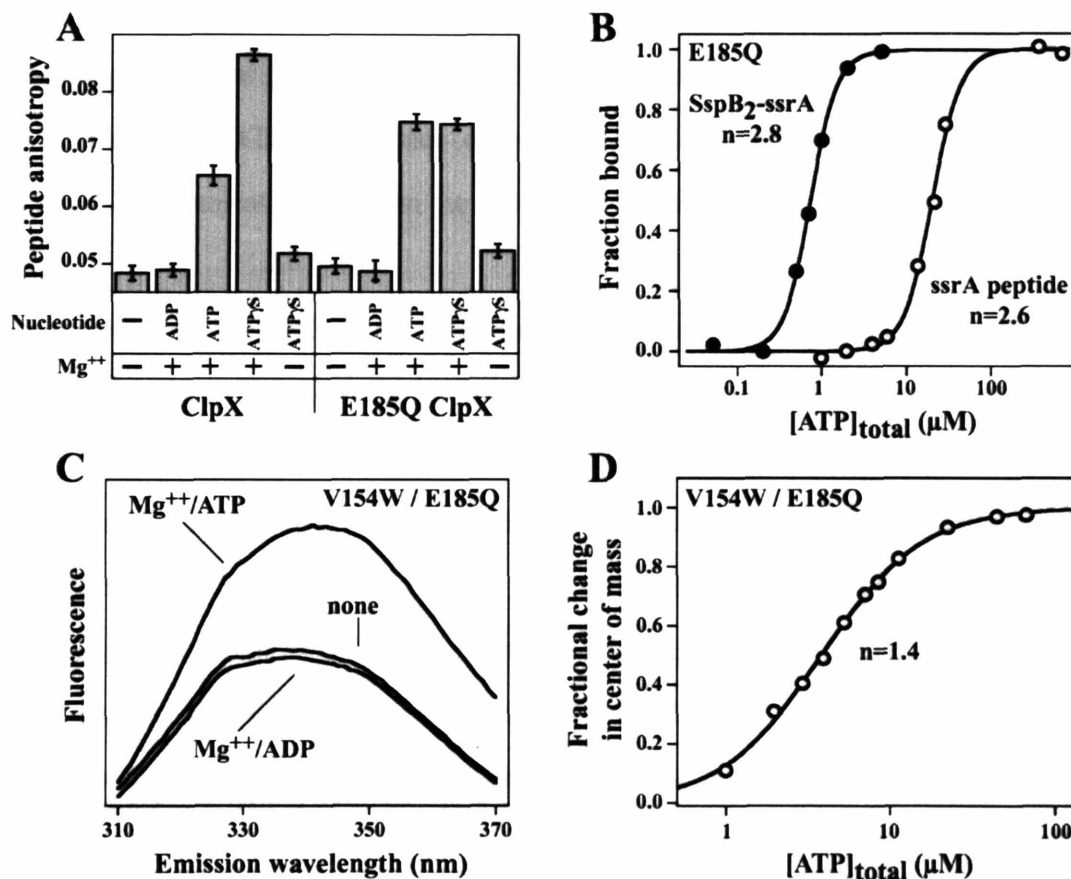

Figure 4. Nucleotide dependence of ClpX substrate binding and conformation. (**A**) Binding of fluorescein-ssrA peptide (200 nM) to wild type or E185Q ClpX$_6$ (5 μM) was assayed by fluorescence anisotropy without nucleotide or Mg^{++}, with 6 mM Mg^{++}/ADP, 6 mM Mg^{++}/ATP, 6 mM Mg^{++}/ATPγS, or 6 mM ATPγS without Mg^{++} (depleted by EDTA). (**B**) ATP dependence of the binding of fluorescein-labeled ssrA peptide (200 nM) or SspB$_2$-ssrA (50 nM) to E185Q ClpX$_6$ (10 μM for the ssrA peptide; 200 nM for SspB$_2$-ssrA). The Hill constants (2.6-2.8) indicate strong positive cooperativity. (**C**) Fluorescence emission spectrum of Y154W/E185Q ClpX$_6$ (1 μM) with no nucleotide, 0.5 mM Mg^{++}/ATP, or 0.5 mM Mg^{++}/ADP. (**D**) Assay of ATP binding to V154W/E185Q ClpX$_6$ (0.8 μM). The fitted curve shows half-maximal binding at an ATP concentration of 3.4 ± 0.3 μM with a Hill constant of 1.4 ± 0.1.

When tryptophan fluorescence was used to assay ATP binding to the E185Q/V154W mutant, the binding curve had a Hill coefficient of 1.4 ± 0.1 with a midpoint at a free ATP concentration of 3-4 μM (Fig. 4d). The latter value is about 5-fold higher than expected based on the properties of the E185Q mutant, suggesting that the V154W mutation weakens interaction of ClpX with ATP. This result is not surprising if binding of ATP is allosterically linked to the structure of the central pore. The V154W mutation, like V154F, effectively abolished binding of ClpX to the ssrA peptide (data not shown), precluding studies of peptide binding on the fluorescence of the E185Q/V154W mutant. Nevertheless, the ATP-dependence of pore fluorescence provides direct evidence for allosteric communication between the nucleotide-binding sites and central pore of ClpX.

ADP substitutes for ATP in "fast" nucleotide binding sites

The existence of two classes of ATP-binding sites in ClpX raises the possibility that ATP could be preferentially hydrolyzed in a subset of these sites, giving rise to ClpX molecules in which some subunits have ATP bound and others have ADP bound. To probe the properties of hexamers with a mixture of bound nucleotides, we incubated ClpX$_6$ E185Q with enough ATP to promote partial binding of the ssrA peptide and then added excess ADP (Fig. 5a). Addition of ADP initially increased peptide binding, which then decreased slowly to a low equilibrium level. The increase in binding indicates that the added ADP must support peptide binding, probably by binding to unoccupied "fast" sites. We assume that the subsequent slow loss of peptide-binding activity results from dissociation of ATP from the "slow" class of binding sites, filling of these sites by ADP, and relaxation to the inactive conformation observed with ADP alone. Consistent with this model, adding excess ATP at the end of this experiment restored full peptide binding (Fig. 5a). As expected for a reaction under "kinetic" control, the order of nucleotide addition was important. When excess ADP was added first and ATP was added second, no significant binding of the ssrA peptide to the enzyme was observed (Fig. 5b). These

results taken with those presented above suggest that binding of one or two ATP molecules places ClpX in a "pore-open" conformation in which filling of additional sites by either ADP or ATP can support a "tag-binding" conformation.
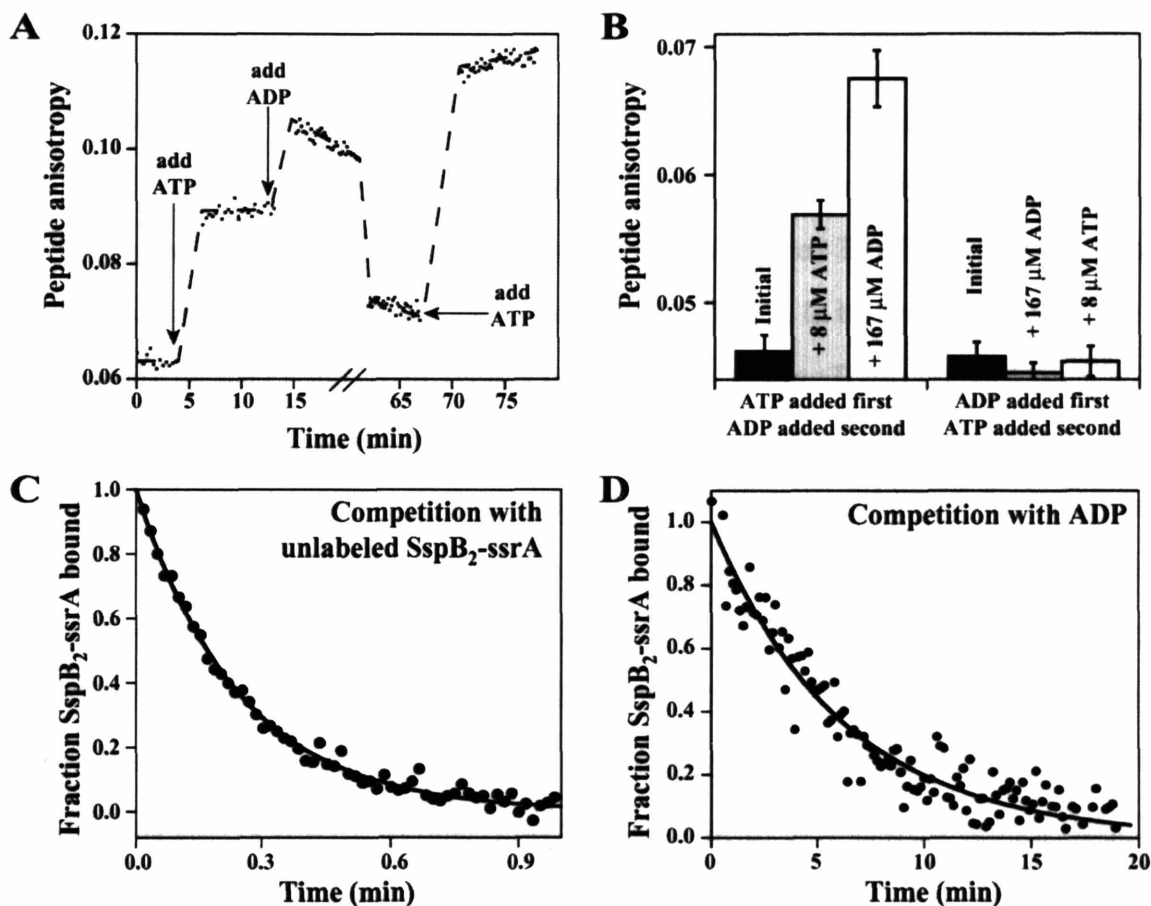

Figure 5. ADP and substrate binding. (**A**) Binding of fluorescein-ssrA peptide (200 nM) to E185Q ClpX (8.5 μM) after addition of 15 μM ATP, after addition of 45 μM ADP, and after final addition of 65 μM ATP. (**B**) ATP (8 μM) and then ADP (167 μM) or *vice versa* were added to E185Q ClpX (4 μM) and fluorescein-ssrA peptide (200 nM) and fluorescence anisotropy was recorded after each nucleotide addition. (**C**) Fluorescein-SspB$_2$-ssrA (125 nM), E185Q ClpX (0.4 μM), and ATP (5 μM) were mixed and dissociation of ClpX•SspB$_2$-ssrA complex was assayed after addition of excess unmodified SspB$_2$-ssrA (5 μM). The curve is a single-exponential fit (k = 4.1 min^{-1}). (**D**) Fluorescein-SspB$_2$-ssrA (125 nM) was mixed with E185Q ClpX (0.4 μM) and ATP (5 μM). At time zero, ADP (1.5 mM) was added and dissociation of the ClpX•SspB$_2$-ssrA complex was assayed. The curve is a single-exponential fit (k = 0.16 ± 0.03 min^{-1}).

Further studies of mixed-nucleotide hexamers were made possible by the finding that complexes of E185Q ClpX•SspB$_2$-ssrA and ATP are highly dynamic. For example, dissociation of fluorescent SspB$_2$-ssrA from E185Q-ClpX•ATP$_{3-4}$ occurred with a half-

life of 10 s after unlabeled $SspB_2$-ssrA was added as a competitor (Fig. 5c). This result shows that $SspB_2$-ssrA dissociates and rebinds ClpX•ATP_{3-4} rapidly under equilibrium conditions and permits $SspB_2$-ssrA binding to be used as a probe of the slower nucleotide exchange transitions discussed below.

In the presence of sufficient ADP, mixtures of ClpX and ATP eventually lose the ability to bind $SspB_2$-ssrA. To investigate whether the kinetics of this transition mirror replacement of ATP by ADP in "slow" sites, we formed E185Q ClpX•$SspB_2$-ssrA complexes with ATP and then added excess ADP (Fig. 5d). In this experiment, ClpX lost the ability to bind $SspB_2$-ssrA with a half-life of $\approx$ 5 min. These kinetics were much slower than ATP dissociation from "fast" sites and on the same time scale as ATP dissociation from "slow" sites (see Fig. 3). Control experiments showed that $SspB_2$-ssrA binding did not cause substantial changes in the rate at which mant-ATP dissociated from "fast" or "slow" sites (data not shown). Thus, these results support the model that ClpX hexamers with ADP in "fast" sites and ATP in "slow" sites retain the ability to bind ssrA-tagged substrates. In an ATPase cycle, this property could be important in allowing hydrolysis of ATP to ADP in "fast" sites without causing the enzyme to lose its "grip" on an ssrA-tagged substrate (see below).

Discussion

AAA+ and related ATP-dependent enzymes unfold, dismantle, and remodel macromolecules and their complexes. How these machines couple the chemical energy stored in ATP to mechanical work is an important unsolved problem. Many AAA+ enzymes are rings of identical subunits (usually hexamers), whereas others assemble and function using non-identical subunits. It is not clear if different ATP-dependent machines use a common underlying mechanism or whether individual family members have evolved distinct mechanisms to bind and remodel specific macromolecular substrates.

Distinct ATP-binding sites in ClpX

Using the E185Q mutant of *E. coli* ClpX, which is defective in ATP hydrolysis, we have studied how nucleotides bind and affect the conformation and macromolecular interactions of this protein. The E185Q protein is similar to wild-type ClpX in its purification properties, ability to form hexamers, and its binding affinity for ADP and ATP/ATPγS. Both the mutant and wild-type proteins display cooperativity in ATP interactions, show ATP-dependent binding to the ClpP peptidase, and bind to ssrA-tagged proteins in an Mg^{++}/ATP-dependent fashion. Thus, we believe that the nucleotide binding properties of the mutant are the same or very similar to those of wild-type ClpX. Our results show that subsets of the six potential nucleotide-binding sites in the E185Q hexamer have distinct ATP-binding properties. Because only 3 or 4 ATP molecules bind to the hexamer under saturating conditions, one set of sites appears unable to bind ATP with detectable affinity when the remaining sites are filled. Moreover, the sites to which ATP binds also have different properties. For example, ATP dissociates rapidly from some sites and slowly from other sites. Thus, at a minimum, any model for ClpX activity needs to consider discrete subunit conformations that bind ATP tightly, less tightly, and not at all.

Because the distinct properties of different classes of ATP-binding sites must arise from conformational differences in individual subunits, it follows that ClpX hexamers saturated with Mg^{++}/ATP cannot be six-fold symmetric. Indeed, as discussed below, some crystal structures of the ClpX homolog, HslU, contain only 3 or 4 bound nucleotides and show distinct subunit conformations (Bochtler et al., 2000). Nevertheless, other HslU structures as well as structures of ClpX and related Clp/Hsp100 ATPases often show ATP symmetrically bound to each subunit (Bochtler et al., 2000; Sousa et al., 2000; Putnam et al., 2001; Guo et al., 2002; Kim and Kim, 2003; Lee et al., 2003). How

can these findings be reconciled? Some of these structures contain no Mg^{++}, which is required for protein-substrate binding by HslU (Burton et al., 2005) and by ClpX. In other structures, the protein crystallizes as a helical array rather than as a hexameric ring. These Mg^{++}-free and/or helical structures clearly represent real conformational states, but we suspect that they are not part of the functional ATPase cycle.

Cooperativity

ATP binding to ClpX is positively cooperative. Our results can be best explained by a model where ATP-binding stabilizes sequential structural changes that create higher-affinity ATP-binding sites and the ability to bind to ssrA-tagged substrates. We assume that nucleotide-free ClpX is a six-fold symmetric structure and that the first ATP could bind to any of the six subunits. Conformational changes caused by this and successive ATP-binding events would then result in the structural asymmetry that leads to the distinct properties of different nucleotide-binding sites.

Binding of one or a few Mg^{++}/ATPs appears to propagate structural changes to the ClpX pore and creates higher-affinity ATP sites but does not support binding to the ssrA tag of substrates (Fig. 6a). ATP-dependent formation of this "pore-open" hexamer from an unbound hexamer in a positively cooperative reaction explains the Hill constants between 1 and 2 that we observe for ATP binding, for ATP hydrolysis, and for the ATP-dependent fluorescence changes in the E185Q/V154W mutant. Filling additional nucleotide-binding sites stabilizes a subsequent structural transition from the "pore-open" to the "tag-binding" conformation of the hexamer (Fig. 6a). The requirement for 3 or 4 bound ATPs to achieve significant populations of this "tag-binding" hexamer explains Hill constants >2.5 that we observe for ATP-dependent binding of E185Q ClpX to ssrA-tagged molecules.
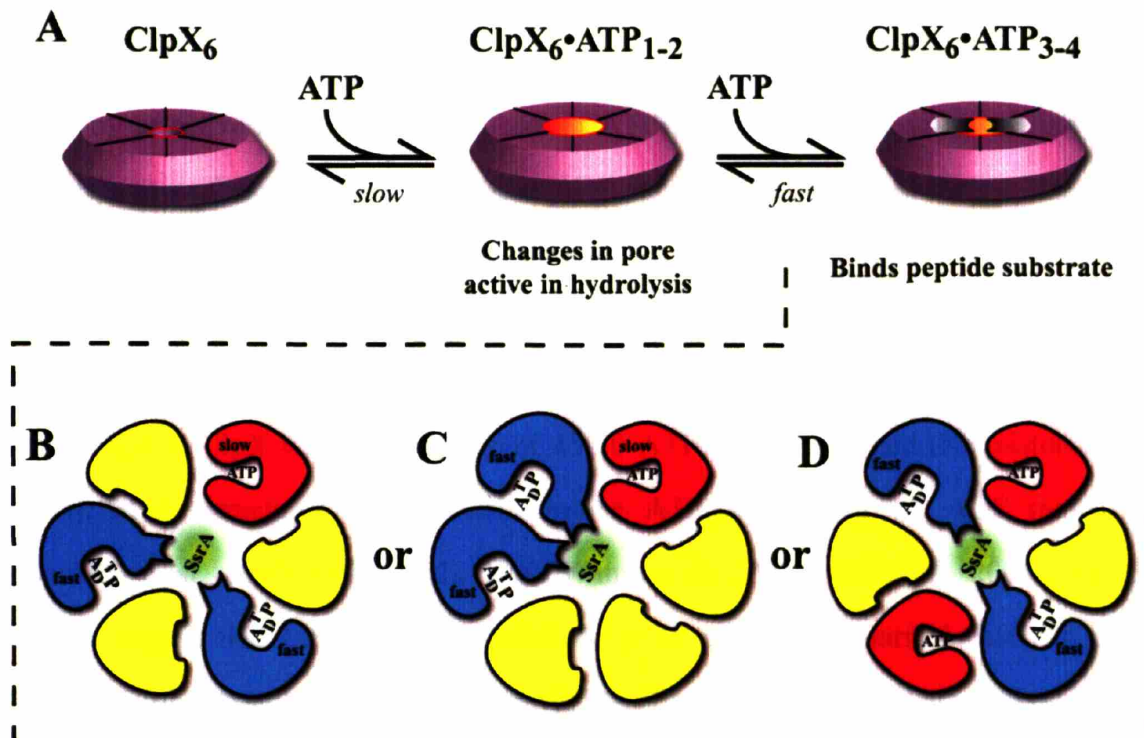
Figure 6. Models for ClpX binding to ATP and the ssrA tag of substrates. (**A**) Sequential model in which binding of 1-2 ATPs propagates structural changes to the central pore of ClpX, and binding of 1-2 additional ATPs stabilize the conformation that binds the ssrA tag. (**B-D**) Cartoons depicting potential arrangements of subunits in ClpX hexamers saturated with ATP. In each cartoon, yellow subunits do not bind ATP, ATP binding to red subunits is required before ATP binding to blue subunits, red subunits release ATP more slowly than blue subunits, blue subunits contact the ssrA tag of substrates, and binding of either ADP or ATP to blue subunits supports ssrA-tag binding. ATP binds more strongly to the blue than the red subunits, even though the blue sites release ATP faster.

SsrA-tag binding and linkage to the ATPase cycle

A critical step for all AAA+ machines is recognition of the proper macromolecular substrates. For ClpX, binding to the ssrA tag of substrates represents the initial step in the eventual unfolding and translocation of these protein molecules. ClpX binds the ssrA tag in the presence of Mg^{++}/ATP but not Mg^{++}/ADP. As noted above, occupancy of three or more nucleotide-binding sites also appears to be a prerequisite for this interaction. Interestingly, however, when ATP is bound in the "slow" class of sites, then ADP in the remaining sites can also support ssrA-tag binding.

ClpX hexamers with a mixture of bound ATP and ADP could arise during the ATPase cycle by selective hydrolysis of a subset of ATPs, for example those in the fast sites. Subsequent exchange of ATP for these ADP molecules could then restore the ATP-saturated enzyme without ever passing through an "all" ADP state. An attractive feature of this model is maintenance of strong contacts with the ssrA tag of a substrate over many cycles of ATP hydrolysis. In fact, recent results suggest that native ssrA-tagged substrates stay bound to ClpX while an average of 15-20 ATPs are hydrolyzed (Kenniston et al., 2005). Many structures of hexameric AAA+ ATPases contain six ADP molecules (Bochtler et al., 2000; Sousa et al., 2000; Wang et al., 2001a; Gai et al., 2004), but our results suggest that $ClpX_6 \cdot ADP_6$ is unlikely to be part of the normal catalytic cycle because ClpX hexamers with six bound Mg^{++}/ATPs never form and there is no evidence for hexamers with ATP bound to some sites and ADP bound to all of the remaining sites.

Models for ATP binding to ClpX

Cartoons depicting some possible arrangements of nucleotide-bound subunits in an ATP-saturated ClpX hexamer are shown in Fig. 6b, 6c, and 6d. In each case, there are ATP-bound subunits (red or blue) and empty subunits (yellow). To account for multiple classes of ATP-binding sites, the red subunits release ATP slowly and the blue subunits release ATP rapidly. Positive cooperativity requires that ATP binding to the lower-affinity red subunits creates or allows access to the sites of higher-affinity binding in the blue subunits. To explain the need to fill 3 or 4 sites before ssrA tag binding, we suggest that contacts between two blue subunits and the ssrA tag (green) are required for strong ssrA tag binding. To explain the ability of ADP in some sites to support ssrA-tag binding, we propose that either bound ADP or ATP allows blue subunits to interact with the ssrA tag. It may seem odd that the high-affinity blue subunits in our models release ATP faster than the low-affinity red subunits. However, this feature is easily explained if ATP binds

much more rapidly to the high-affinity blue subunits than to the red subunits, as the ratio of the association and dissociation rates determines affinity.

There are structural precedents for some aspects of the Fig. 6 models. For example, the alternating arrangement of ATP-bound subunits (Fig. 6b) shares similarities with the 1do2 crystal structure of $HslU_6$, in which empty and nucleotide-bound subunits alternate (Bochtler et al., 2000). The trimer-of-dimers 1do2 $HslU_6$ arrangement is symmetric, however, whereas the Fig. 6b model lacks cyclic symmetry. A different $HslU_6$ structure (1do0) is a dimer-of-trimers, in which two subunits of each trimer bind nucleotide (one with Mg^{++}) and one subunit is nucleotide free (Bochtler et al., 2000). This crystal structure is most similar to the ClpX model shown in Fig. 6d. Whether the nucleotides bound in these HslU structures are nucleoside triphosphates or diphosphates is controversial (Wang et al., 2001b). Nevertheless, HslU can clearly adopt conformations in which nucleotides bind to only a subset of the six subunits.

Similarities with other AAA+ enzymes

It is important to note that mechanism has not been rigorously established for any AAA+ ATPase or related enzyme and that major differences exist in many of the models proposed for these machines. For example, recent structural studies of the AAA+ SV40 LTag helicase have been interpreted as favoring a concerted hydrolysis model that involves a hexamer with ATP bound to each subunit (Gai et al., 2004). By contrast, for several other hexameric AAA+ machines (Rho helicase, RuvB translocase, and p97) and related enzymes (T7 gene 4 helicase), ATP binds only to a subset of potential nucleotide-binding sites or binds to sites that display distinct functional properties, leading to models similar to those shown in Fig. 6 (Stitt, 1988; Marrione and Cox, 1995; Patel and Hingorani, 1995; Marrione and Cox, 1996; Singleton et al., 2000; Putnam et al., 2001; Stitt, 2001; Jeong et al., 2002; Zalk and Shoshan-Barmatz, 2003; Hishida et al., 2004).

For instance, the structure of T7 helicase reveals a hexamer with four Mg^{++}/AMPPNPs bound, and has been used to support a dimer-of-trimers model (like the Fig. 6d cartoon) with adjacent ATP, ADP, and empty sites (Singleton et al., 2000). Hence, the existence of distinct types of ATP-binding subunits in homo-hexamers seems to be a property shared by many different types of ATP-dependent machines.

This theme of subunit specialization is also reflected in heteromeric AAA+ enzymes, including the replicative sliding-clamp loader, the Mcm2-7 helicase, and dynein. Individual subunits or modules in these machines have evolved to play specialized roles and only a subset are catalytically active (Jeruzalmi et al., 2001; Schwacha and Bell, 2001; Kon et al., 2004). In the F_1 ATPase, which is more distantly related, subunits also have dedicated functions (Boyer, 1997). Catalytically active α-subunits and inactive β-subunits alternate in the F_1 hexamer; moreover, each of the three α-subunits can assume distinct properties with respect to ATP binding and hydrolysis.

For ClpX, it will be important to determine how the different classes of nucleotide-binding sites are actually arranged in a hexamer, how individual subunits communicate with each other, what function is served by each subset of subunits, whether ATP hydrolysis is coordinated among different sites, and how the occupancy, structure, and functional roles of individual subunits change during a complete enzymatic and mechanical cycle. Our findings that subunits of ClpX can adopt at least three conformations with distinct ATP-binding properties, that occupancy of two classes of sites is linked to binding to the ssrA tag, and that subunits communicate in both positive and negative allosteric fashions both constrains detailed models of mechanism and sets the stage for future studies. Finally, parallels between our results for the ClpX protein unfoldase and results obtained for hexameric helicases and translocases suggest that these

enzymes may use a common mechanism to perform mechanical work on dramatically different macromolecular substrates.

Methods

Solutions

PD buffer contains 25 mM HEPES-KOH (pH 7.6), 5 mM KCl, 5 mM MgCl$_2$, 0.032% NP-40, and 10% glycerol. Buffer A contains 50 mM Tris (pH 8.0), 100 mM KCl, 1 mM MgCl$_2$, and 10% glycerol. Buffer B contains 10 mM Tris (pH 7.6), 50 mM KCl.

Proteins and peptides

ClpX mutants were constructed using overlap extension mutagenesis and verified by DNA sequencing. GFP-ssrA, *E. coli* ClpX and variants, and *E. coli* ClpP and His$_6$-ClpP were expressed and purified by published procedures (Kim et al., 2000). The ssrA peptide fluorescein-NKKGRHGAANDENYALAA-COOH was synthesized by the M.I.T. Biopolymers Laboratory and purified on a Shimadzu LC-10AD-VP HPLC column. SspB$_2$-ssrA was generated in the background of a designed YGFM/SLA SspB heterodimer, in which one subunit was disulfide cross-linked to a cysteine-containing ssrA peptide and the other subunit was labeled with a fluorescent dye to monitor binding to ClpX (Bolon et al., 2004a). Each SspB subunit was purified separately as described (Bolon et al., 2004b). The YGFM subunit also contained the A73Q mutation, which abrogates binding to ssrA peptide, and the D147C mutation to allow labeling. This subunit (150 μM) was incubated with 3 mM 5-iodoacetamidofluorescein from Molecular Probes (Eugene, OR) in 6 M GuHCl, 100 mM potassium phosphate (pH 7.0) for 2 hr at 22 °C. The reaction was stopped by addition of 100 mM 2-mercaptoethanol. The SLA

subunit contained the Y44C mutation to allow disulfide cross-linking to an ssrA peptide containing the A2C mutation (Bolon et al., 2004a). Equal amounts of the fluorescein labeled YGFM-A73Q/D147C subunit and SLA-Y44C subunit were mixed in 6 M GuHCl. After gel filtration to remove small molecules and denaturant, the A2C ssrA peptide was cross-linked to the heterodimer and the $SspB_2$-ssrA molecule was purified as described (Bolon et al., 2004a).

Protein concentrations were determined by UV absorbance at 280 nm, using extinction coefficients of 84480 $M^{-1}cm^{-1}$ ($ClpX_6$ or $ClpX_6$ E185Q), 118080 $M^{-1}cm^{-1}$ ($ClpX_6$ V154W/E185Q) and 125160 $M^{-1}cm^{-1}$ ($ClpP_{14}$). The concentration of the ssrA peptide was determined in basic ethanol (pH ~10) using an extinction coefficient of 92300 $M^{-1}cm^{-1}$ at 500 nm. Sodium salts of ATP and ADP were purchased from Sigma (St. Louis, MI), dissolved in water, and the pH was adjusted to 7.0 by addition of NaOH. ATP/ADP concentrations were determined by absorbance at 259 nm using an extinction coefficient of 15400 $M^{-1}cm^{-1}$. Both ATP and ADP were free of contaminating nucleotide as assayed by thin-layer chromatography. ATPγS was purchased from Roche Diagnostics (Indianapolis, IN) and dissolved in water.

Assays

Unless noted, assays were performed at 23 °C. ClpXP degradation of GFP-ssrA was performed as described (Kim et al., 2000). Fluorescence was measured using a PTI QM-20000-4SE spectrofluorometer (Lawrenceville, NJ). Binding of mant-ADP to E185Q ClpX was assayed in buffer A by changes in fluorescence intensity (excitation: 360 nm;

emission 440 nm), which was averaged for $\approx$100 s and corrected for any dilution. Binding of fluorescein-labeled ssrA peptide or SspB$_2$-ssrA to ClpX were assayed by changes in anisotropy (excitation: 467 nm; emission: 511 nm) using motorized Glan Thompson polarizers. Data were collected over 200 s and averaged. The fluorescence emission spectrum (310-375 nm; excitation 295 nm) of E185Q/Y154W ClpX was collected with an emission polarizing filter perpendicular to the plane of excitation to minimize the effects of Raman scattering. ATP hydrolysis assays were performed at 30 °C using a coupled assay (Burton et al., 2001).

ClpP pull-down assays were performed by a modification of a published protocol (Joshi et al., 2004). Reactions (50 μL) contained 1 μM His$_6$-ClpX$_6$ E185Q (if present), 1 μM ClpP$_{14}$, 10 mM imidazole, 1 mM nucleotide, and PD buffer. Components were equilibrated for 10 min, and then mixed with Ni^{++}-NTA resin (in the same buffer) for another 10 min. The mixture was loaded into a Spin-X® centrifuge tube filter with a 0.45 μm nylon filter (Corning, NY) and centrifuged briefly to near dryness. The resin was washed with 0.5 mL PD buffer, 10 mM imidazole, and 1 mM nucleotide and bound protein was eluted with 0.5 M imidazole in buffer A and analyzed by SDS-PAGE. Gels were stained with Sypro Orange (Molecular Probes) and visualized using a Syngene GeneGenius Bioimaging system (Frederick, MD).

BA85 nitrocellulose filters (25 mm; 0.45 μm; Schleicher & Schuell GmbH) were soaked in 0.5 M KOH for 20 min and rinsed with water until the pH was approximately neutral. After this treatment, filters were stored in buffer B at 4 °C for up to two weeks. A stock

solution of radiolabeled ATP was prepared by mixing [^{32}P]-γ-ATP (10 mCi/mL at 1.67 μM) with a 10-fold (v/v) excess of unlabeled 30 μM ATP. For equilibrium binding, 20 μL samples of appropriate dilutions of ATP and protein were allowed to equilibrate for five min. Samples were then diluted into 4 mL of ice-cold buffer A without glycerol and passed through a nitrocellulose filter using a FH225V vacuum filtration unit (Pharmacia Biotech, San Francisco, CA). Filters were counted in scintillation vials with 4 mL of scintillation fluid. For assays of ATP dissociation kinetics, 0.4 μM of E185Q ClpX was ~90% saturated with [^{32}P]-γ-ATP (5 μM) in a total volume of 100 μL. 1.5 mL of either unlabeled ADP or ATP was added, and 10 μL samples were used per each time point. Data from 3-4 independent dissociation experiments were combined to construct plots.

Fitting of equilibrium and kinetic data was performed in KALEIDAGRAPH (Synergy Software, Reading, PA). Kinetic trajectories were fit to single- or double-exponential functions. Equilibrium data were fit to equations for 1:1 or cooperative binding. In the latter case, the function was $\max/(1+K^n/[\text{ATP}]^n)$, where max represents binding at saturation, [ATP] is the total ATP concentration, K is the ATP concentration at half-maximal binding, and n is the Hill constant. Rates of ATP hydrolysis were fit to the corresponding function $V_{max}/(1+K_M^n/[\text{ATP}]^n)$. In experiments where [ATP]$_{total}$ was significantly greater than [ATP]$_{free}$, the Hill constant represents a lower limit and K must be corrected for the amount of bound ligand to calculate a true equilibrium constant.

Isothermal titration calorimetry was performed in buffer A using a Microcal VP-ITC calorimeter (Amherst, MA). After degassing, ATP (107 μM) was loaded into a 300 μL

syringe and injected in 7.5 μl aliquots at 13 min intervals into a 1.4-mL cell containing 3.6 μM E185Q ClpX. Integration and fitting of ITC data were performed with ORIGIN (Microcal) software.

References

Bochtler, M., Hartmann, C., Song, H. K., Bourenkov, G. P., Bartunik, H. D., and Huber, R. (2000). The structures of HsIU and the ATP-dependent protease HsIU-HsIV. Nature *403*, 800-805.

Bolon, D. N., Grant, R. A., Baker, T. A., and Sauer, R. T. (2004a). Nucleotide-dependent substrate handoff from the SspB adaptor to the AAA+ ClpXP protease. Mol Cell *16*, 343-350.

Bolon, D. N., Wah, D. A., Hersch, G. L., Baker, T. A., and Sauer, R. T. (2004b). Bivalent tethering of SspB to ClpXP is required for efficient substrate delivery: a protein-design study. Mol Cell *13*, 443-449.

Boyer, P. D. (1997). The ATP synthase--a splendid molecular machine. Annu Rev Biochem *66*, 717-749.

Burton, R. E., Baker, T. A., and Sauer, R. T. (2003). Energy-dependent degradation: Linkage between ClpX-catalyzed nucleotide hydrolysis and protein-substrate processing. Protein Sci *12*, 893-902.

Burton, R. E., Baker, T. A., and Sauer, R. T. (2005). Nucleotide-dependent substrate recognition by the AAA+ HslUV protease. Nat Struct Mol Biol *12*, 245-251.

Burton, R. E., Siddiqui, S. M., Kim, Y. I., Baker, T. A., and Sauer, R. T. (2001). Effects of protein stability and structure on substrate processing by the ClpXP unfolding and degradation machine. Embo J *20*, 3092-3100.

Flynn, J. M., Levchenko, I., Seidel, M., Wickner, S. H., Sauer, R. T., and Baker, T. A. (2001). Overlapping recognition determinants within the ssrA degradation tag allow modulation of proteolysis. Proc Natl Acad Sci U S A *98*, 10584-10589.

Gai, D., Zhao, R., Li, D., Finkielstein, C. V., and Chen, X. S. (2004). Mechanisms of conformational change for a replicative hexameric helicase of SV40 large tumor antigen. Cell *119*, 47-60.

Glover, J. R., and Tkach, J. M. (2001). Crowbars and ratchets: hsp100 chaperones as tools in reversing protein aggregation. Biochem Cell Biol *79*, 557-568.

Gottesman, S., Roche, E., Zhou, Y., and Sauer, R. T. (1998). The ClpXP and ClpAP proteases degrade proteins with carboxy-terminal peptide tails added by the SsrA-tagging system. Genes Dev *12*, 1338-1347.

Guo, F., Maurizi, M. R., Esser, L., and Xia, D. (2002). Crystal structure of ClpA, an Hsp100 chaperone and regulator of ClpAP protease. J Biol Chem *277*, 46743-46752.

Hishida, T., Han, Y. W., Fujimoto, S., Iwasaki, H., and Shinagawa, H. (2004). Direct evidence that a conserved arginine in RuvB AAA+ ATPase acts as an allosteric effector for the ATPase activity of the adjacent subunit in a hexamer. Proc Natl Acad Sci U S A *101*, 9573-9577.

Jeong, Y. J., Kim, D. E., and Patel, S. S. (2002). Kinetic pathway of dTTP hydrolysis by hexameric T7 helicase-primase in the absence of DNA. J Biol Chem *277*, 43778-43784.

Jeruzalmi, D., Yurieva, O., Zhao, Y., Young, M., Stewart, J., Hingorani, M., O'Donnell, M., and Kuriyan, J. (2001). Mechanism of processivity clamp opening by the delta subunit wrench of the clamp loader complex of E. coli DNA polymerase III. Cell *106*, 417-428.

Joshi, S. A., Hersch, G. L., Baker, T. A., and Sauer, R. T. (2004). Communication between ClpX and ClpP during substrate processing and degradation. Nat Struct Mol Biol *11*, 404-411.

Kenniston, J. A., Baker, T. A., and Sauer, R. T. (2005). Partitioning between unfolding and release of native domains during ClpXP degradation determines substrate selectivity and partial processing. Proc Natl Acad Sci U S A *102*, 1390-1395.

Kenniston, J. A., Burton, R. E., Siddiqui, S. M., Baker, T. A., and Sauer, R. T. (2004). Effects of local protein stability and the geometric position of the substrate degradation tag on the efficiency of ClpXP denaturation and degradation. J Struct Biol *146*, 130-140.

Kim, D. Y., and Kim, K. K. (2003). Crystal structure of ClpX molecular chaperone from Helicobacter pylori. J Biol Chem *278*, 50664-50670.

Kim, Y. I., Burton, R. E., Burton, B. M., Sauer, R. T., and Baker, T. A. (2000). Dynamics of substrate denaturation and translocation by the ClpXP degradation machine. Mol Cell *5*, 639-648.

Kon, T., Nishiura, M., Ohkura, R., Toyoshima, Y. Y., and Sutoh, K. (2004). Distinct functions of nucleotide-binding/hydrolysis sites in the four AAA modules of cytoplasmic dynein. Biochemistry *43*, 11266-11274.

Lee, S., Sowa, M. E., Watanabe, Y. H., Sigler, P. B., Chiu, W., Yoshida, M., and Tsai, F. T. (2003). The structure of ClpB: a molecular chaperone that rescues proteins from an aggregated state. Cell *115*, 229-240.

Marrione, P. E., and Cox, M. M. (1995). RuvB protein-mediated ATP hydrolysis: functional asymmetry in the RuvB hexamer. Biochemistry *34*, 9809-9818.

Marrione, P. E., and Cox, M. M. (1996). Allosteric effects of RuvA protein, ATP, and DNA on RuvB protein-mediated ATP hydrolysis. Biochemistry *35*, 11228-11238.

Orelle, C., Dalmas, O., Gros, P., Di Pietro, A., and Jault, J. M. (2003). The conserved glutamate residue adjacent to the Walker-B motif is the catalytic base for ATP hydrolysis in the ATP-binding cassette transporter BmrA. J Biol Chem *278*, 47002-47008.

Ortega, J., Singh, S. K., Ishikawa, T., Maurizi, M. R., and Steven, A. C. (2000). Visualization of substrate binding and translocation by the ATP-dependent protease, ClpXP. Mol Cell *6*, 1515-1521.

Patel, S. S., and Hingorani, M. M. (1995). Nucleotide binding studies of bacteriophage T7 DNA helicase-primase protein. Biophys J *68*, 186S-189S; discussion 189S-190S.

Piszczek, G., Rozycki, J., Singh, S. K., Ginsburg, A., and Maurizi, M. R. (2005). The molecular chaperone, ClpA, has a single high affinity peptide binding site per hexamer. J Biol Chem *280*, 12221-12230.

Putnam, C. D., Clancy, S. B., Tsuruta, H., Gonzalez, S., Wetmur, J. G., and Tainer, J. A. (2001). Structure and mechanism of the RuvB Holliday junction branch migration motor. J Mol Biol *311*, 297-310.

Sauer, R. T., Bolon, D. N., Burton, B. M., Burton, R. E., Flynn, J. M., Grant, R. A., Hersch, G. L., Joshi, S. A., Kenniston, J. A., Levchenko, I., *et al.* (2004). Sculpting the proteome with AAA(+) proteases and disassembly machines. Cell *119*, 9-18.

Schwacha, A., and Bell, S. P. (2001). Interactions between two catalytically distinct MCM subgroups are essential for coordinated ATP hydrolysis and DNA replication. Mol Cell *8*, 1093-1104.

Segel, I. (1976). Biochemical Calculations, 2nd edn, John Wiley & Sons).

Siddiqui, S. M., Sauer, R. T., and Baker, T. A. (2004). Role of the processing pore of the ClpX AAA+ ATPase in the recognition and engagement of specific protein substrates. Genes Dev *18*, 369-374.

Singleton, M. R., Sawaya, M. R., Ellenberger, T., and Wigley, D. B. (2000). Crystal structure of T7 gene 4 ring helicase indicates a mechanism for sequential hydrolysis of nucleotides. Cell *101*, 589-600.

Smith, P. C., Karpowich, N., Millen, L., Moody, J. E., Rosen, J., Thomas, P. J., and Hunt, J. F. (2002). ATP binding to the motor domain from an ABC transporter drives formation of a nucleotide sandwich dimer. Mol Cell *10*, 139-149.

Sousa, M. C., Trame, C. B., Tsuruta, H., Wilbanks, S. M., Reddy, V. S., and McKay, D. B. (2000). Crystal and solution structures of an HslUV protease-chaperone complex. Cell *103*, 633-643.

Stitt, B. L. (1988). Escherichia coli transcription termination protein rho has three hydrolytic sites for ATP. J Biol Chem *263*, 11130-11137.

Stitt, B. L. (2001). Escherichia coli transcription termination factor Rho binds and hydrolyzes ATP using a single class of three sites. Biochemistry *40*, 2276-2281.

Vale, R. D. (2000). AAA proteins. Lords of the ring. J Cell Biol *150*, F13-19.

Wah, D. A., Levchenko, I., Baker, T. A., and Sauer, R. T. (2002). Characterization of a specificity factor for an AAA+ ATPase: assembly of SspB dimers with ssrA-tagged proteins and the ClpX hexamer. Chem Biol *9*, 1237-1245.

Wang, J., Hartling, J. A., and Flanagan, J. M. (1997). The structure of ClpP at 2.3 A resolution suggests a model for ATP-dependent proteolysis. Cell *91*, 447-456.

Wang, J., Song, J. J., Franklin, M. C., Kamtekar, S., Im, Y. J., Rho, S. H., Seong, I. S., Lee, C. S., Chung, C. H., and Eom, S. H. (2001a). Crystal structures of the HslVU peptidase-ATPase complex reveal an ATP-dependent proteolysis mechanism. Structure (Camb) *9*, 177-184.

Wang, J., Song, J. J., Seong, I. S., Franklin, M. C., Kamtekar, S., Eom, S. H., and Chung, C. H. (2001b). Nucleotide-dependent conformational changes in a protease-associated ATPase HslU. Structure (Camb) *9*, 1107-1116.

Zalk, R., and Shoshan-Barmatz, V. (2003). ATP-binding sites in brain p97/VCP (valosin-containing protein), a multifunctional AAA ATPase. Biochem J *374*, 473-480.

APPENDIX

Communication between ClpX and ClpP during substrate processing and degradation

Portions published: Shilpa A. Joshi, Greg L. Hersch, Tania A. Baker, and Robert T. Sauer (2004). Communication between ClpX and ClpP during substrate processing and degradation. Nat Struct Mol Biol 11, 404-411. The latter part of the discussion in this paper has been rewritten based on the results discussed in the previous chapter.

SUMMARY

In the ClpXP compartmental protease, ring hexamers of the AAA+ ClpX ATPase bind, denature, and then translocate protein substrates into the degradation chamber of the double-ring $ClpP_{14}$ peptidase. A key question is the extent to which functional communication between ClpX and ClpP occurs and is regulated during substrate processing. Here, we show that ClpX-ClpP affinity varies with ClpX's protein-processing task and with the catalytic engagement of ClpP's active sites. Functional communication between symmetry-mismatched ClpXP rings depends on ClpX's ATPase activity and appears to be transmitted through structural changes in its IGF loops which contact ClpP. A conserved arginine in ClpX's sensor-II helix links the nucleotide state of ClpX to both the binding of ClpP and protein substrates. A simple model explains the observed relationships between ATP binding, ATP hydrolysis, and functional interactions between ClpX, protein substrates, and ClpP.

Note: The experiments in this appendix were performed by a former graduate student, Shilpa A. Joshi and me. I conducted the experiments with "loopless" ClpX in Figure 2, and developed the model depicted in Figure 8.

AAA+ ATPases function as essential components of energy-dependent compartmental proteases in all biological . For example, the 19S portion of the eukaryotic proteasome consists predominantly of AAA ATPases, which help recognize and translocate substrates to an associated 20S protease (Glickman et al., 1998). In bacteria, the ClpXP and ClpAP proteases consist of either the ClpX or ClpA ATPase and the ClpP peptidase, and the HslUV protease consists of the HslU ATPase and the HslV peptidase (Gottesman et al., 1997a; Gottesman et al., 1997b; Ogura and Wilkinson, 2001). In each of these energy-dependent proteases, the active sites for polypeptide cleavage are sequestered in a degradation chamber formed by a multi-subunit complex with a barrel-like shape (Bochtler et al., 1997; Groll et al., 1997; Wang et al., 1997; Wang et al., 1998; Bochtler et al., 2000; Groll et al., 2000; Sousa et al., 2000; Whitby et al., 2000; Sousa and McKay, 2001; Wang et al., 2001a). Entry portals, too small to admit native proteins, provide access to this chamber. The ATPases of compartmentalized proteases from bacteria form ring hexamers which bind appropriate protein substrates, unfold these molecules, and translocate them through a central protein-processing pore and into the peptidase chamber for degradation (Gottesman et al., 1997a; Gottesman et al., 1997b; Ogura and Wilkinson, 2001). The interaction of ATP and its γ-phosphate with these proteolytic ATPases is mediated in part by evolutionarily conserved sensor I and II sequence motifs (Guenther et al., 1997; Neuwald et al., 1999).

One key question for all energy-dependent proteases is how interactions between the ATPase and the peptidase coordinate substrate processing and degradation. For HslUV, the peptidase and ATPase are both six-fold symmetric and structures of the complex in

different nucleotide-bound states are known (Bochtler et al., 2000; Sousa et al., 2000; Wang et al., 2001a; Wang et al., 2001b; Sousa et al., 2002). Nucleotide binding modulates the size of the protein-processing pore and the entry portal and also alters contacts between HslU and HslV, propagating structural changes to the peptidase active sites and mediating communication between the ATPase and peptidase (Yoo et al., 1996; Seol et al., 1997; Sousa et al., 2000; Wang et al., 2001b; Ramachandran et al., 2002; Seong et al., 2002; Sousa et al., 2002).

For ClpXP **(Fig. 1)** and ClpAP (Wang et al., 1997; Beuron et al., 1998; Grimaud et al., 1998; Wang et al., 1998; Ortega et al., 2000), docking of the ATPase and peptidase involves a symmetry mismatch between a hexameric ATPase ring and a heptameric ClpP ring. Although high-resolution structures of these complexes have not been solved, flexible surface loops in both ClpX and ClpA, which contain an IGF or IGL motif, have been implicated in ClpP binding (Kim et al., 2001; Singh et al., 2001; Guo et al., 2002; Kim and Kim, 2003). Despite the symmetry mismatch, coordination between the activities of the 6-fold symmetric ATPase and 7-fold symmetric peptidase must occur, as binding of ClpA activates ClpP peptidase activity (Thompson et al., 1994), proteins trapped in the degradation chamber of inactive ClpP can be released in a reaction that depends upon ATP hydrolysis by ClpX (Kim et al., 2000), and the ATPase activities of ClpA and ClpX are depressed upon binding to ClpP (Hwang et al., 1988; Kim et al., 2001).
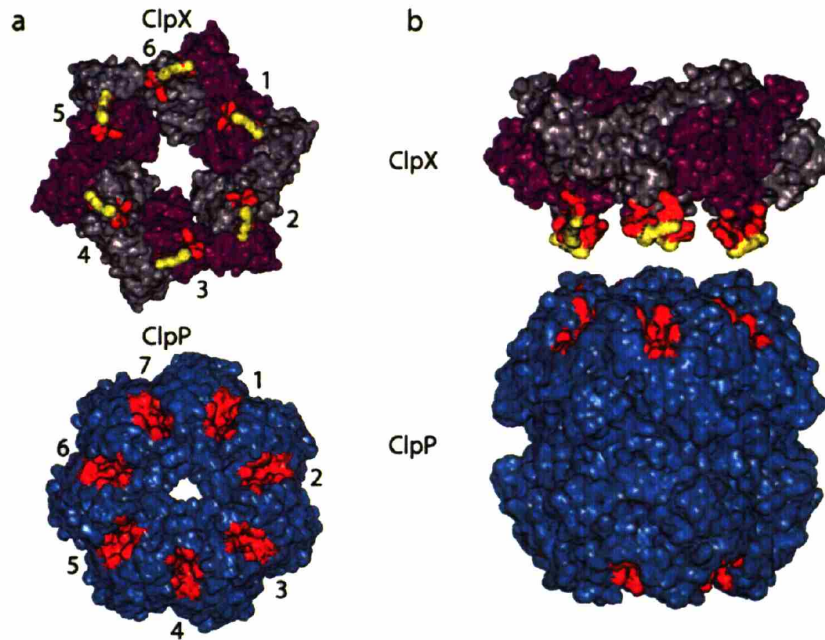
Figure 1 Symmetry mismatch between ClpX and ClpP. (a) Axial views of the interaction surfaces of ClpX and ClpP are shown (Wang et al., 1997; Kim and Kim, 2003). Subunits in ClpX$_6$ are colored purple or gray, whereas subunits in the visible heptameric ring of ClpP$_{14}$ are turquoise. Part of the ClpX loop that mediates ClpP binding is colored red and the signature tripeptide at its tip is yellow. Hydrophobic clefts in ClpP are also colored red. (b) Side view showing how the IGF loops of ClpX might align with the hydrophobic clefts of ClpP.

To probe functional communication between the ClpX and ClpP enzymes of *Escherichia coli*, we have used changes in ATPase activity to monitor and quantify the strength of the ClpX-ClpP interaction. We find that ClpP binds most tightly to ClpX when the ATPase is denaturing protein substrates, less tightly during translocation of substrates, and least tightly in the absence of substrates. ClpX is also able to detect the catalytic status of the ClpP active sites, as evidenced by a significant increase in affinity when the active-site serines of ClpP are modified. ClpP binding suppresses the protein-unfolding defects of ClpX variants with mutations at an intersubunit interface, but rescue occurs at the expense of binding affinity and reverses the response to substrate processing. This result suggests that subunit-subunit interactions in wild-type ClpX play an important role in the

unfolding of protein substrates by preventing quaternary distortions in ClpX that prevent substrate denaturation and weaken ClpP binding. Finally, we demonstrate that a conserved arginine in ClpX's sensor-II motif links ATP binding to conformational changes required for ClpP and protein substrate binding.

RESULTS

Substrate design. Protein substrates had ssrA tags to target them to ClpX (Gottesman et al., 1998). Unfolding of GFP-ssrA by ClpX or degradation by ClpXP results in loss of fluorescence (Kim et al., 2000; Singh et al., 2000). Unlabelled and ^{35}S-labelled variants of the human titin-I27-ssrA protein were degraded by ClpXP either as native proteins or as denatured, carboxymethylated (CM) molecules (Kenniston et al., 2003).

ClpP interaction requires more than two IGF loops. The IGF loop (residues 264–278) of *E. coli* ClpX mediates binding to ClpP (Kim et al., 2001; Singh et al., 2001). We constructed and purified ClpX loopless, a variant in which this loop was replaced with a short linker. As expected, ClpX loopless did not support degradation of an ssrA-tagged substrate in the presence of ClpP **(Fig. 2a)**, and did not bind His$_6$-ClpP in Ni^{++}-NTA pull-down assays (not shown). ClpX loopless was, however, as active as wild-type ClpX in unfolding GFP-ssrA as monitored by loss of native GFP fluorescence **(Fig. 2b)**. Moreover, ClpX loopless formed stable ternary complexes with GFP-ssrA and the delivery protein SspB during gel filtration in the presence of ATPγS **(Fig. 2c)**. These mutant complexes chromatographed at the same position as wild-type complexes, suggesting that ClpX loopless, like ClpX, is hexameric under these conditions(Wah et al.,

2002). We conclude that ClpX loopless fails to interact with ClpP but otherwise

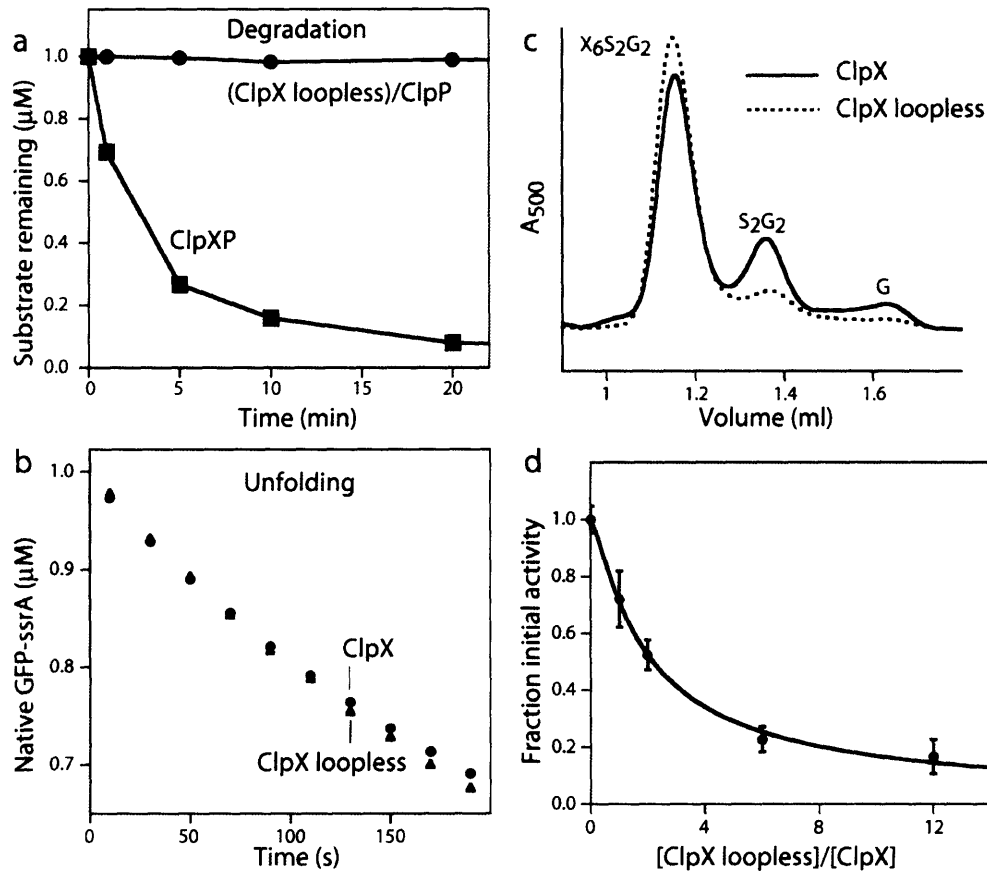assembles normally and is active in binding and denaturing ssrA-tagged substrates.

Figure 2 Properties of ClpX loopless. (a) ClpX$_6$ loopless (100 nM) did not support degradation of CM-titin-V13P-ssrA (1 μM) in the presence of ClpP$_{14}$ (300 nM), whereas wild-type ClpX mediated efficient degradation under these conditions. (b) GFP-ssrA (1 μM) in the presence of SspB$_2$ (1 μM) was unfolded at essentially the same rate by ClpX$_6$ or ClpX$_6$ loopless (300 nM) as assayed by loss of native GFP-ssrA fluorescence. (c) ClpX loopless forms stable ternary complexes. ClpX$_6$ or ClpX$_6$ loopless (6 μM), SspB$_2$ (3 μM), GFP-ssrA (6 μM), and ATPγS (5 mM) were chromatographed and the elution position of GFP-ssrA was monitored by A$_{500}$. Positions of the ternary complex (X$_6$S$_2$G$_2$), binary complex of SspB and GFP-ssrA (S$_2$G$_2$), and free GFP-ssrA (G) are shown. (d) Degradation of titin-V4A-ssrA (5 μM) by wild-type ClpXP (100 nM ClpX$_6$; 2 μM ClpP$_{14}$) was inhibited by addition of ClpX loopless. The solid line is a fit to eq. 3 (see Methods) with a bias factor of 0.99, an A$_{21}$ value of 0.63, and an A$_{12}$ value of 0.003.

It is not known how many IGF loops in a ClpX hexamer (a trimer of stable dimers

(Wojtyra et al., 2003)) are required for functional collaboration with ClpP. An IGF-loop

peptide bound ClpP very weakly (K_d>200 μM; not shown), suggesting that stable ClpP

binding requires several IGF loops and/or requires the loop to be held in a specific conformation by ClpX. To test the activity of hexamers containing mixtures of wild-type and loopless dimers, we added ClpX loopless to wild-type ClpX and assayed degradation of an ssrA-tagged substrate in the presence of excess ClpP. As shown in **Figure 2d**, a modest excess of ClpX loopless inhibited degradation, with the data fitting a model in which hexamers with only one wild-type dimer have less than 1% activity, those with two wild-type dimers are roughly 60% active, and mixing of wild-type and mutant dimers is unbiased. Pull-down experiments confirmed that wild-type and loopless ClpX form mixed multimers (not shown). We conclude that functional interactions between ClpX and ClpP require IGF loops in at least two of the dimers that comprise the ClpX hexamer.

ATPase assay for ClpX-ClpP affinity. ClpP binding decreases the rate of ATP hydrolysis by ClpX (Kim et al., 2001). ATP turnover by 50 nM $ClpX_6$ or $ClpX_6$ loopless was assayed in the presence of $ClpP_{14}$ at concentrations ranging from 0 to 2.5 μM. No significant changes in ATPase activity were observed for the ClpX loopless control. In contrast, for wild-type ClpX, changes in rate fit well to a simple binding isotherm **(Fig. 3a)**. These experiments confirm the importance of the IGF loop in binding ClpP and indicate that the changes in ATP hydrolysis when ClpP binds ClpX are mediated by the same region of the protein that permits collaboration in protein degradation. Assays performed with 200 nM $ClpX_6$ gave similar results, with the combined data obtained for the two ClpX concentrations fitting a 1:1 binding model in which $ClpX_6$ and $ClpP_{14}$ interact with an apparent equilibrium dissociation constant (K_{app}) of 92 ± 17 nM **(Fig. 3b)**. These results indicate that ClpX hexamers do not dissociate significantly in the 50–

200 nM concentration range. Nevertheless, it is important to note that K_{app} reflects a population-weighted average of the K_d values of ClpP for the ClpX hexamer in each of its different enzymatic and conformational states as it passes through its cycles of ATP hydrolysis and coupled conformational changes.
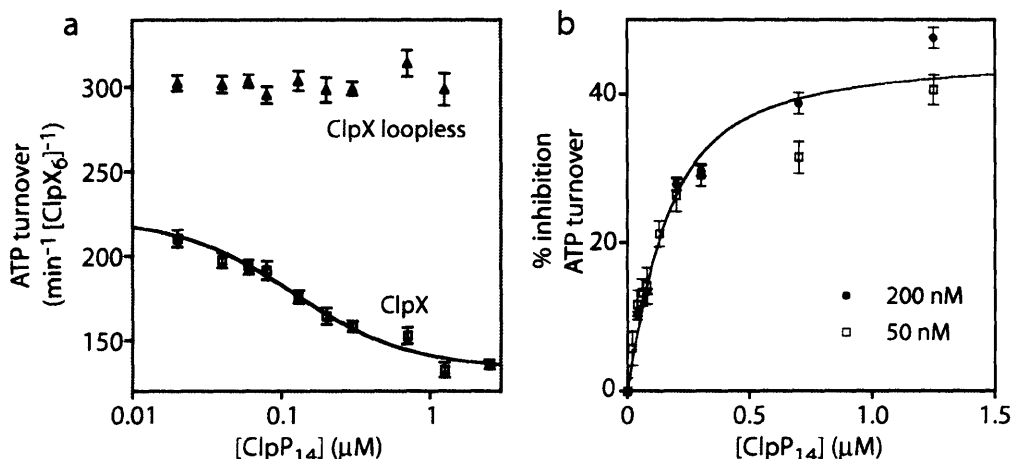

Figure 3 An assay for ClpX-ClpP interaction in solution. **(a)** Changes in the ATP hydrolysis rate of 50 nM ClpX$_6$ or ClpX$_6$ loopless as a function of ClpP concentration. Data in linear form were fit to eq. 1 and then plotted in semi-log form. **(b)** Percent inhibition of ATP turnover as a function of ClpP concentration with two different ClpX$_6$ concentrations. The fitted line is that expected for a one-to-one binding reaction (eq. 1) with an apparent affinity of 92 ± 17 nM.

Substrate processing strengthens ClpX-ClpP affinity. Studies using titin-ssrA substrates with a range of stabilities showed that ClpX denatures these molecules at different rates but translocates the denatured proteins to ClpP at the same rate (Kenniston et al., 2003). Hence, we reasoned that assaying ClpX-ClpP affinity during degradation of these titin substrates should reveal whether the processes of protein denaturation and translocation affect this interaction. ATPase assays were used to monitor ClpP affinity in the presence of concentrations of titin-ssrA substrates that ensured approximately 90% saturation of ClpX. When ClpP was titrated against ClpX in the presence of the most

141

stable native substrate, wild-type titin-ssrA, K_{app} was 19 ± 5 nM, a decrease of roughly five-fold compared to the absence of substrate (**Figs. 3a** and **4a**). In the presence of less stable native variants, K_{app} values were 27 ± 3 nM (V15P) and 53 ± 9 nM (V13P). When a denatured titin substrate (CM-V13P) was present, K_{app} was 78 ± 9 nM. With other denatured substrates (CM-titin; CM-V15P), K_{app} values were within error of the CM-V13P value (not shown). These results show that the apparent affinity for ClpP is stronger when ClpX is processing titin-ssrA substrates, with the strongest binding observed for native substrates that are denatured most slowly.

K_{app} for ClpX-ClpP binding in the presence of different titin-ssrA substrates was linearly correlated (R = 0.99) with the rate constants for degradation (**Fig. 4b**). Although more complicated models are possible, this relationship is explained simply if ClpX has one affinity for ClpP while denaturing titin-ssrA substrates and a different, weaker affinity while translocating these substrates. Indeed, the linear fit in **Figure 4b** represents a model in which K_{app} is 16 nM during denaturation and 70 nM during translocation (see Methods). These results suggest the existence of a mechanism by which ClpP can detect the protein-processing task in which ClpX is engaged. The ClpX-ClpP affinities were also well correlated with the rates of ATP turnover by ClpXP and ClpX in the presence of the titin-ssrA substrates (**Fig. 4c**). Based on these observations, we suggest that the ATPase rate of ClpX during substrate processing, which depends on the average time required for denaturation and translocation, controls its apparent affinity for ClpP.
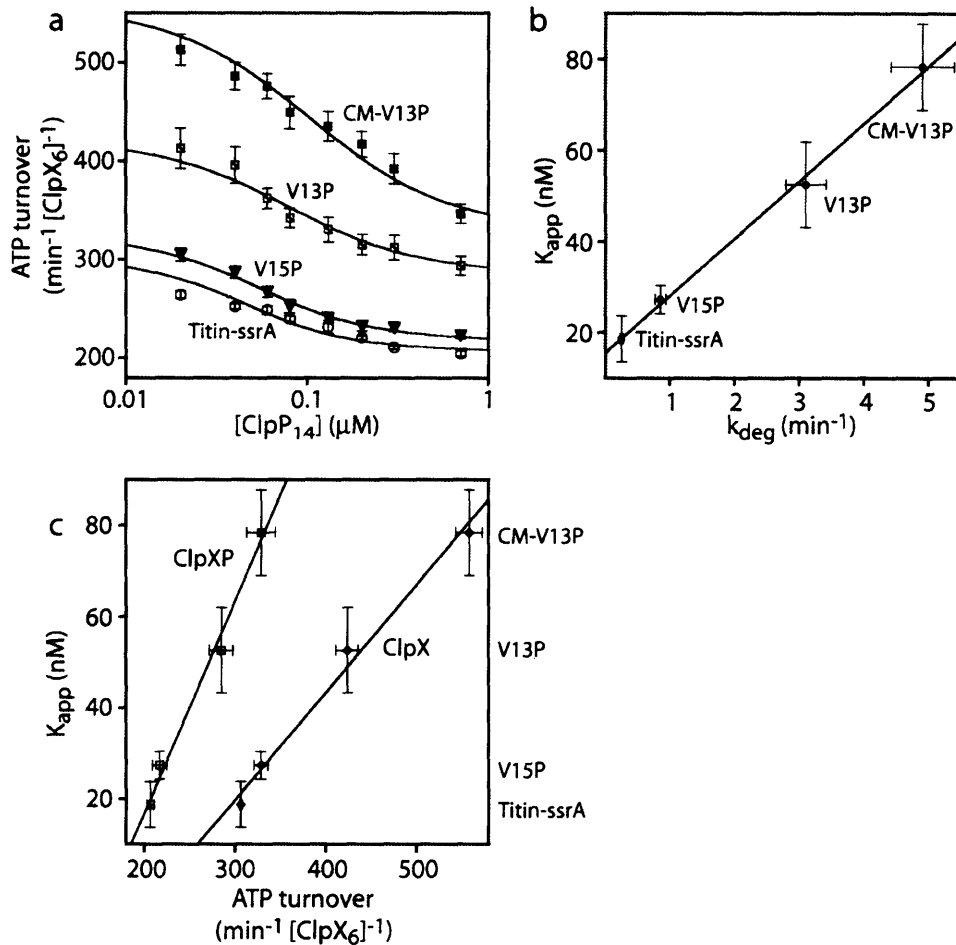
Figure 4 ClpX-ClpP affinity changes in an ATPase-dependent fashion during substrate denaturation and translocation. (a) Binding of ClpP to 50 nM $ClpX_6$ in the presence of 15 μM concentrations of four variants of titin-ssrA. The fits represent K_{app} values of 19 ± 5 nM for wild-type titin-I27-ssrA, 27 ± 3 nM for the native V15P mutant, 53 ± 9 nM for the native V13P variant, and 78 ± 9 nM for the denatured CM-V13P protein. (b) K_{app} values for the ClpX-ClpP interaction in the presence of titin-ssrA substrates vary linearly with the rate constant for ClpXP degradation of these substrates (Kenniston et al., 2003). The line is a fit to eq. 2 (see Methods), with affinities of 16 and 70 nM, respectively, when ClpXP is denaturing or translocating titin-ssrA substrates. (c) K_{app} for the ClpX-ClpP interaction correlates linearly (R = 0.99) with the ATPase rates of ClpXP and ClpX during the processing of different titin-ssrA substrates. ClpXP ATPase rates are values obtained with saturating concentrations of ClpP.

Active-site communication between ClpP and ClpX. If ClpP can detect whether ClpX

is processing protein substrates, then ClpX may be able to detect whether ClpP is

degrading substrates. To address this possibility, we used DFP-ClpP, a variant in which

the active-site serines (S97) were covalently modified by reaction with di-isopropyl-

fluorophosphate (Kim et al., 2000). Although DFP-ClpP is inactive in degradation, the

143

modification mimics the acyl-enzyme intermediate in peptide-bond hydrolysis. Moreover, a DFP oxygen binds in the oxyanion hole of the active site, mimicking the carbonyl oxygen of a peptide substrate (Wang et al., 1997). DFP-ClpP bound ClpX so strongly that the bound and total concentrations of ClpX were essentially the same (**Fig. 5**). This "stoichiometric binding" indicates that the affinity constant is less than or equal to 5 nM. Hence, ClpX appears to be capable of sensing whether the ClpP active sites are engaged with substrate. To ensure that the tighter ClpX binding observed for DFP-ClpP was caused by modification of the active-site S97, we assayed binding of a ClpP S97A mutant after treatment with DFP (Flynn et al., 2003). DFP-treated ClpP S97A bound ClpX like wild-type ClpP and much more weakly than DFP-ClpP (**Fig. 5**). We conclude that the strong ClpX binding observed for DFP-ClpP results from acylation of the active-site serines and/or from concomitant substrate-like interactions of the covalent modification.
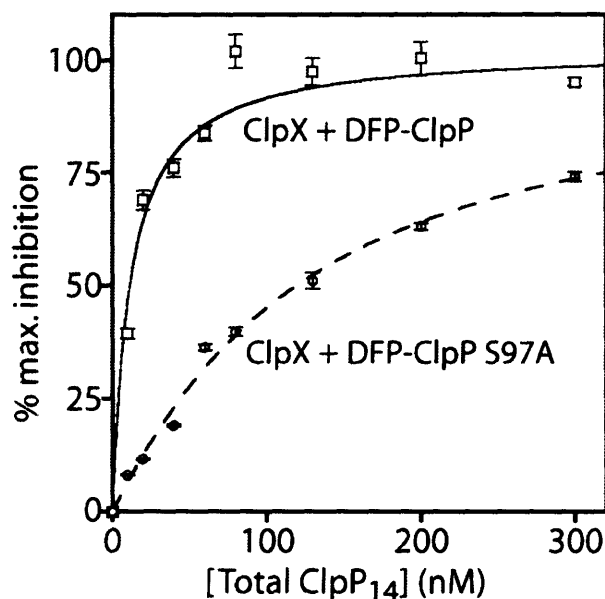

Figure 5 Modification of the ClpP active sites strengthens ClpX binding. DFP-ClpP bound tightly to 50 nM $ClpX_6$ as assayed by changes in ATP hydrolysis. $ClpP_{14}$ can bind two ClpX hexamers and, at half-maximal binding, the total concentration of DFP-$ClpP_{14}$ was roughly 15 nM and the concentration of bound $ClpX_6$ was 25 nM. Although an accurate K_{app} cannot be determined from these data, the upper limit for this constant is ≈ 5 nM. K_{app} for the interaction of ClpX with DFP-treated ClpP S97A (94 nM) was similar to that for wild-type ClpP, confirming that the tight binding of DFP-ClpP results from modification of the active-site S97 side chain.

ClpP rescues the unfolding defects of ClpX mutants. Mutations in the C-terminal portion of the ClpX sensor-II helix, which forms part of the interface between the C-domain of one subunit and the ATPase domain of an adjacent subunit, cause defects in substrate unfolding but not in substrate binding (Joshi et al., 2003). Because ClpP binds more tightly when ClpX is denaturing substrates, we reasoned that ClpP binding might suppress the unfolding defects of these sensor-II mutants. This result was observed. By themselves, ClpX L381K and ClpX D382K had undetectable activities in unfolding GFP-ssrA **(Fig. 6a)**. In the presence of DFP-ClpP, however, the same mutants catalyzed efficient unfolding of GFP-ssrA **(Fig. 6b)**. Unmodified ClpP also suppressed the unfolding defects of these sensor-II mutants (not shown). Because DFP-ClpP suppressed most efficiently the unfolding defect of ClpX D382K, we selected this ClpX variant for more detailed studies.

In the absence of substrate, ClpP bound ClpX D382K (K_{app} = 0.12 ± 0.05 μM; **Fig. 6c**) only slightly more weakly than wild-type ClpX. When substrate was present, however, the affinity of ClpP for this mutant was substantially worse. K_{app} was almost 20-fold weaker (2.3 ± 0.5 μM) in the presence of the native V13P variant of titin-ssrA and about 10-fold weaker (1.1 ± 0.4 μM) in the presence of denatured CM-titin-ssrA **(Fig. 6d)**. Thus, whereas the affinity of ClpP for wild-type ClpX strengthens during the processing of protein substrates, the opposite is true for the D382K mutant. These data suggest that when ClpX D382K engages a protein substrate, it must assume a conformation poorly suited for binding ClpP and substrate unfolding. Although ClpP can stabilize ClpX D382K in an active conformation, the energy used for this conformational change

145

reduces affinity. Unusually, addition of ClpP to ClpX D382K **(Fig. 6d)** increased the

ATP hydrolysis rate in the presence of protein substrates. By contrast, ClpP binding

reduced ATPase activity for ClpX D382K without substrate **(Fig. 6c)** and for wild-type

ClpX under all conditions **(Figs. 3a and 4a)**. These results are consistent with a distorted

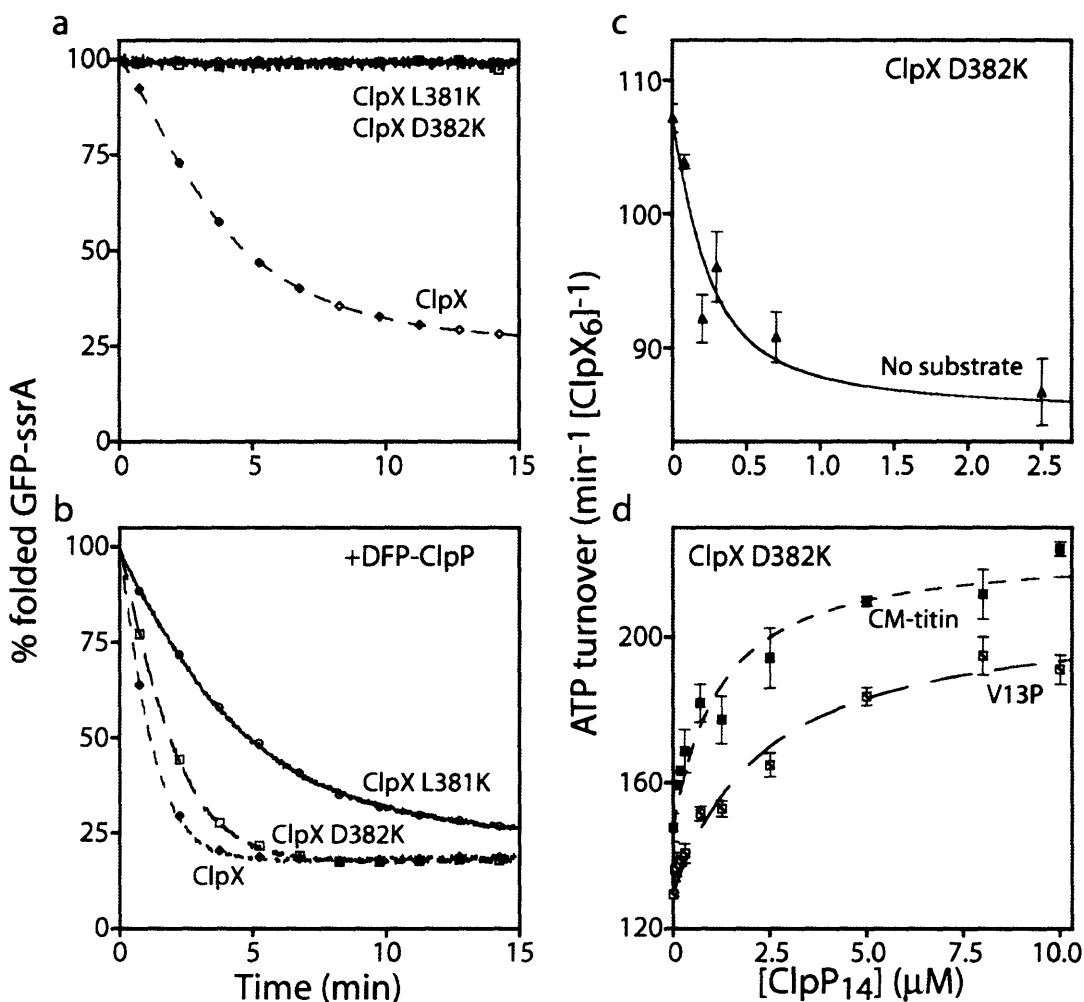conformation for complexes between ClpX D382K and substrates.

Figure 6 ClpP rescues the unfolding defects of ClpX mutants. The sensor-II helix mutants, ClpX D382K and ClpX L381K, fail to unfold GFP-ssrA (310 nM) by themselves (panel **a**) but unfold this substrate efficiently in the presence of 800 nM DFP-ClpP$_{14}$ (panel **b**). In these experiments, the concentrations of mutant or wild-type ClpX$_6$ were 260 nM, and 460 nM SspB was present. ClpP binds 200 nM ClpX$_6$ D382K with an apparent affinity of 120 ± 50 nM in the absence of substrate (panel **c**) but binds more weakly in the presence of a denatured substrate (13.1 μM CM-titin-ssrA; K_{app} = 1.1 ± 0.4 μM) or a native substrate (15 μM titin-V13P-ssrA; K_{app} = 2.3 ± 0.5 μM) (panel **d**).
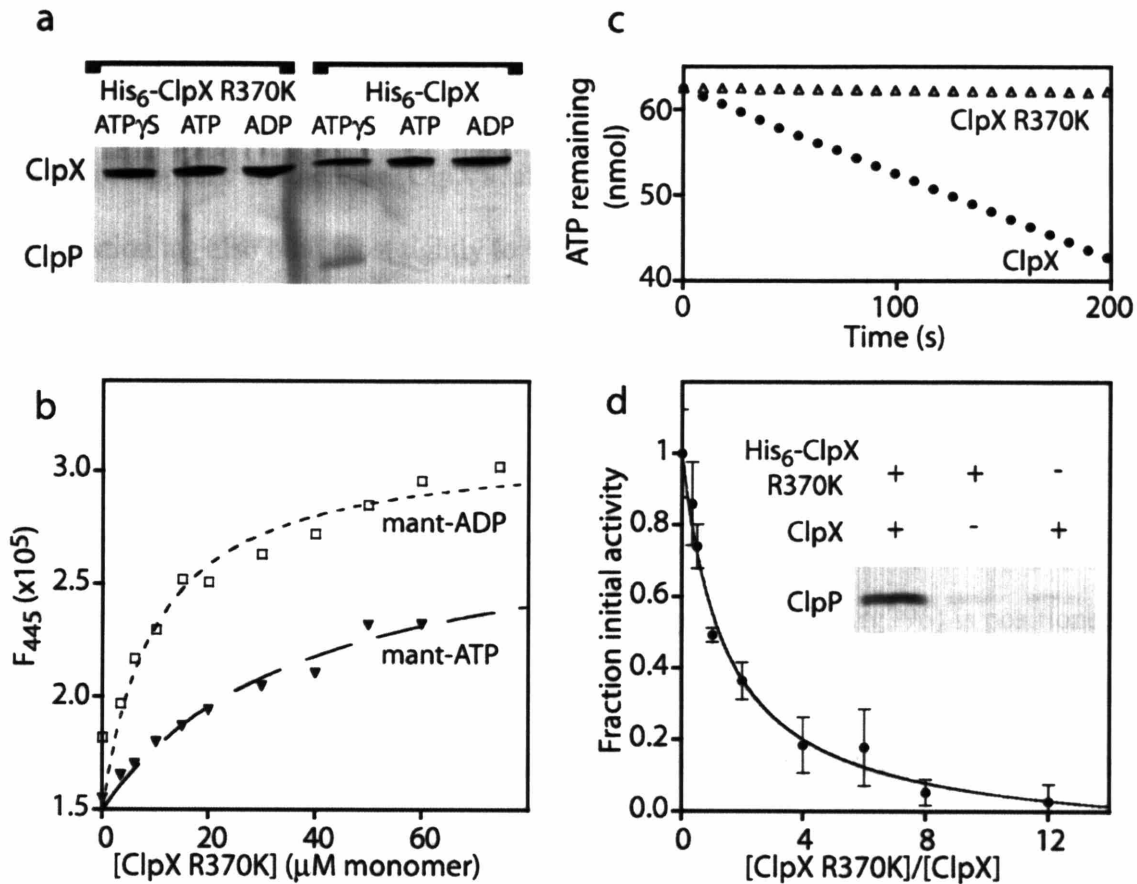
Figure 7 The "ATP" state of ClpX is required for strong ClpP interactions. **(a)** Untagged ClpP bound Ni^{++}-NTA in the presence of His_6-ClpX and $ATP\gamma S$; weak binding was observed with ATP or ADP in some experiments but is not visible here. No binding of ClpP to His_6-ClpX R370K was detected with any nucleotide. **(b)** Binding of ClpX R370K to 1 μM mant-ADP or mant-ATP assayed by changes in fluorescence in the absence of magnesium. The fitted lines are for K_d's of 39 μM (mant-ATP) and 18 μM (mant-ADP). **(c)** $ClpX_6$ R370K (400 nM) hydrolyzed ATP at less than 1% of the rate of wild-type $ClpX_6$ (400 nM) as determined in a coupled spectrophotometric assay (Karon et al., 1994). **(d)** Degradation of GFP-ssrA (7 μM) by wild-type ClpXP (100 nM $ClpX_6$; 2.7 μM $ClpP_{14}$) was inhibited by addition of the ClpX R370K mutant. The solid line is a fit to eq. 4 (see Methods) with a bias factor of 0.33. **Inset**— untagged ClpP binds Ni^{++}-NTA in the presence of a mixture of His_6-ClpX R370K and untagged wild-type ClpX, but much less in the presence of either single species. All pull-down reactions contained $ATP\gamma S$.

Nucleotide state of ClpX controls ClpP binding. The experiments presented above suggest that ClpX ATPase activity is linked to interactions with ClpP. In pull-down assays, untagged ClpP bound Ni^{++}-NTA in the presence of His_6-ClpX and $ATP\gamma S$ but did not bind well when ATP or ADP were present **(Fig. 7a)**. Because ATP hydrolysis by ClpX is rapid, ClpX hexamers contain some bound ADP even with excess ATP if ADP

release is slow. By contrast, ATPγS is hydrolyzed slowly by ClpX (Burton et al., 2003), and thus ClpX•ATPγS is probably the best mimic of the "ATP" state. ATP binding therefore appears to increase ClpX's affinity for ClpP. Peptides containing the ssrA degradation tag also bind most tightly to ClpX in the ATP-bound state (Wah et al., 2002).

To test if contacts between ClpX and ATP play a role in stabilizing ClpP binding, we constructed and purified a ClpX mutant in which Arg370 was mutated to lysine. This highly conserved side chain resides in the N-terminal portion of the sensor-II helix; the corresponding residue in the crystal structure of *H. pylori* ClpX (Arg396) is positioned to contact bound nucleotide but is distant from the ClpP binding surface (Kim and Kim, 2003). ClpX R370K purified like wild-type ClpX and bound the fluorescent nucleotides mant-ATP (K_d=39 μM) and mant-ADP (K_d=18 μM) with affinities within a few fold of those for wild-type ClpX (Burton et al., 2003 and **Fig. 7b**; not shown). Moreover, ATPγS and ATP competed equally well for binding of mant-ADP to ClpX R370K (R. Burton, personal communication). Hence, ClpX R370K shows no significant defect in ATP binding. Nevertheless, this mutant failed to hydrolyze ATP **(Fig. 7c)** and did not bind ClpP in pull-down assays containing ATPγS, ATP, or ADP **(Fig. 7a)**. In addition, ClpX R370K did not show detectable binding to a fluorescent ssrA peptide in the presence of ATPγS (K_d>20 μM; wild-type K_d≈3 μM (Wah et al., 2002)), did not unfold GFP-ssrA, and did not degrade GFP-ssrA when ClpP was present (not shown). These results suggest that interactions between Arg370 and bound ATP are required to stabilize a ClpX conformation that possesses a high affinity for both ClpP and for ssrA-tagged substrates.

To determine whether the mutant R370K and wild-type subunits co-assemble, we titrated increasing quantities of ClpX R370K against a fixed quantity of wild-type ClpX and excess ClpP and assayed degradation of GFP-ssrA **(Fig. 7d)**. Addition of the mutant in 12-fold excess caused nearly complete inhibition. We also observed inhibition by ClpX R370K of ClpXP degradation of denatured CM-titin-ssrA and of ClpX unfolding of GFP-ssrA (not shown). Hence, mixed hexamers with one wild-type dimer and two ClpX R370K dimers must be inactive in these assays. The best fit of the **Figure 7d** inhibition data was obtained from a model in which the 2:1 and 1:2 mixed hexamers were both inactive, and wild-type dimers had a 3-fold preference for assembling with themselves rather than with mutant dimers. Untagged ClpP bound Ni^{++}-NTA resin following incubation with His_6-ClpX R370K, untagged wild-type ClpX, and ATPγS **(Fig. 7d inset)**. This result demonstrates that ClpX R370K and wild-type subunits co-assemble and show that at least one species of mixed hexamer can bind ClpP. With a 6-fold excess of ClpX R370K, the ATPase activity of wild-type ClpX was only reduced ~30% (not shown). Hence, mixed hexamers containing wild-type and R370K subunits retain some ATPase activity but are unable to bind and/or to process protein substrates.

DISCUSSION

The studies presented here provide strong evidence for functional communication between ClpX and ClpP during the processing and degradation of protein substrates. For example, ClpP affinity improved during substrate processing by ClpX. Like other molecular machines, the conformation of ClpX must change during the ATPase cycle. Results from the previous chapter suggest that ClpX hydrolyzes only a fraction of its

bound nucleotide at a time to avoid experiencing an all ADP conformation that cannot bind strongly to peptidase, as demonstrated in **Figure 7**, or substrate (Hersch et al., 2005). If each ClpX subunit contributes individually to ClpP affinity, our results suggest that ClpX subunits with bound ATP will stabilize ClpX•ClpP complex formation. Therefore, alterations in the ATPase rate and thus the time spent by each subunit bound to ATP versus ADP would modulate ClpX-ClpP affinity. This model is illustrated in **Figure 8**. For simplicity, only three subunits are shown and those that do not bind nucleotide are omitted. Prior studies have shown that the ATPase rate of ClpXP is roughly 4-fold higher during translocation than denaturation of titin-ssrA substrates (Kenniston et al., 2003). Hence, the ATP-bound states in the **Figure 8** model would be more highly populated when ClpX is engaged in denaturing native titin-ssrA, whereas the mixed ATP/ADP-bound state, which has a weaker affinity for ClpP, would predominate during translocation. This model explains why the apparent affinity of the ClpX-ClpP interaction correlates with the degradation rates of different titin-ssrA substrates and with the ATPase rates during the processing of these substrates. The model could also be expanded to include ClpX states with more than one ADP bound.

ClpX bound much more tightly when the active-site serines of ClpP were acylated by reaction with DFP. Previous studies also suggest that ClpA binds more strongly to DFP-ClpP than to the unmodified enzyme (Singh et al., 1999). Because the DFP-modified residues are located within the degradation chamber of ClpP (Wang et al., 1997), they cannot affect interactions with the ATPases directly. We suggest that DFP-modification of the ClpP active sites lowers the energy required for a conformational change that
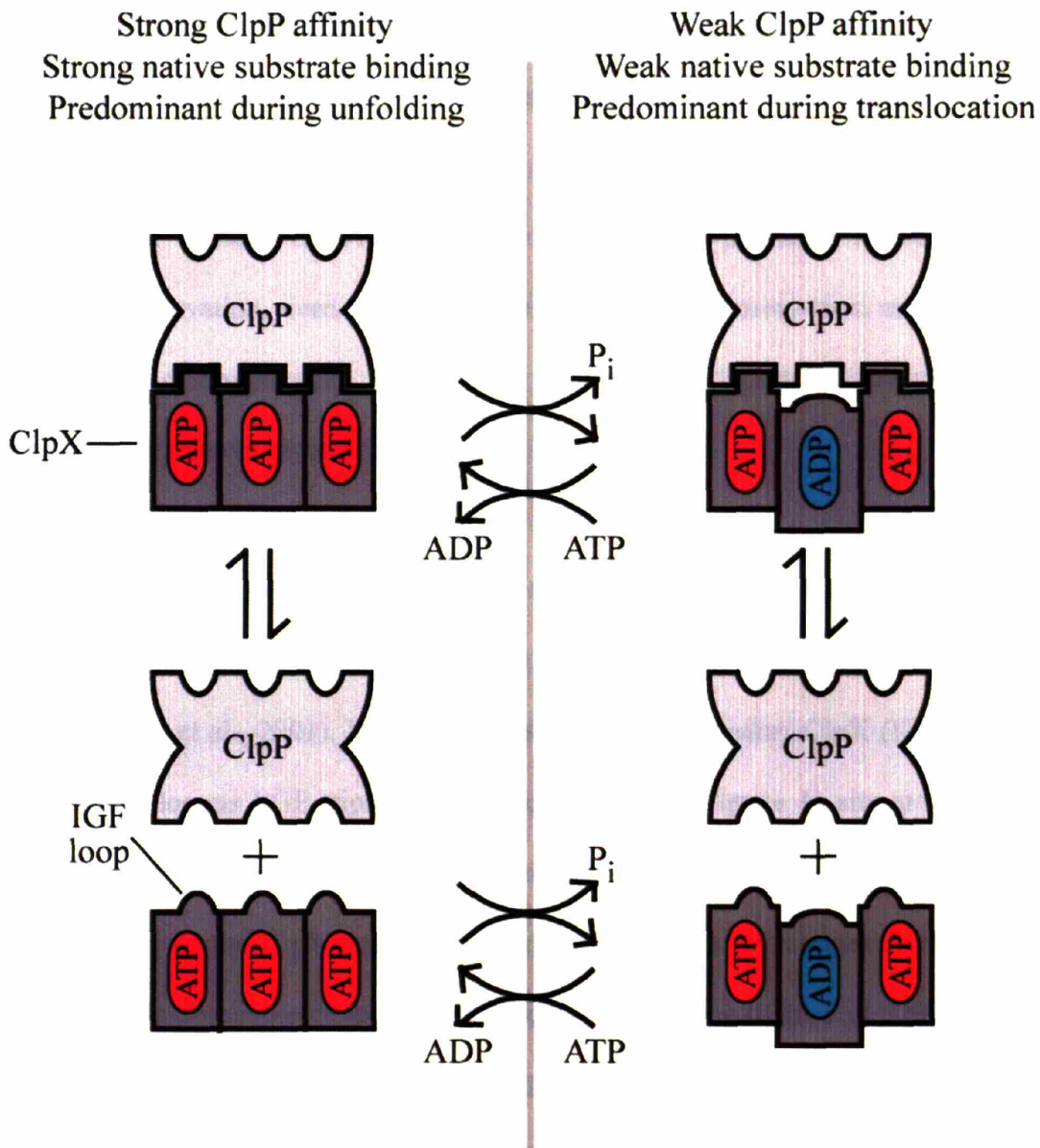
Figure 8 Model for the interaction of ClpX and ClpP. Cartoon depiction of ClpX and ClpXP in all-ATP-bound (ClpX•ATP) mixed ATP/ADP-bound states. ClpX•ATP binds ClpP more strongly than ClpX•ATP/ADP. The depression of ClpX's ATPase activity upon ClpP binding occurs because of conformation changes or restraints in the IGF loops. Bound native protein substrates (not shown) affect the ATPase activity of ClpX independently and increase apparent ClpP affinity by binding preferentially to the all-ATP-bound enzymes. During the processing of protein substrates (not shown), the all-ATP-bound enzymes are stabilized during denaturation, whereas the mixed ATP/ADP-bound enzymes are more highly populated during translocation. ClpX R370K is trapped in an all ADP conformation, even when ATP is bound, explaining its inability to bind ClpP or native substrates. DFP-modification of the active sites of ClpP stabilizes the ClpX-bound conformation of the peptidase relative to its free conformation.

occurs upon binding to ClpX. In the model of **Figure 8**, this would increase ClpX-ClpP affinity by allowing more of the interaction energy to drive the binding reaction. Despite the fact that the ClpP and HslV peptidases have unrelated structures and active-site architectures, it is notable that ClpXP and HslUV both have mechanisms that allow communication between the ATPase active sites and the peptidase active sites. This functional conservation, even in the absence of structural conservation, emphasizes the importance of communication between the processing and protease compartments of these energy-dependent proteases.

The IGF loop of *E. coli* ClpX appears to be the major determinant of ClpP binding and related peptide motifs are found in all of the AAA+ ATPases that collaborate with ClpP homologs (Kim et al., 2001). In the crystal structure of *H. pylori* ClpX (Kim and Kim, 2003), a homologous LGF tripeptide (colored yellow in **Figure 1**) sits at the tip of a surface loop that extends away from the protease-proximal surface. Alignment of the symmetry axes of the ClpX and ClpP rings positions these tripeptides from the ClpX hexamer near hydrophobic clefts on the surface of a ClpP ring (Kim et al., 2001). In each ClpX subunit (Kim and Kim, 2003), the IGF/LGF loop is preceded by a short α-helix that connects directly to the sensor-I portion of the ATP/ADP binding site. In ClpA, the corresponding loop is disordered but is also connected to the sensor-I portion of an active site for ATP hydrolysis (Guo et al., 2002). As illustrated in **Figure 8**, changes in the conformation of the IGF loops upon ClpP binding and/or changes in the number of loops that contact ClpP could regulate ClpX-ClpP affinity in a manner dependent on the nucleotide state of ClpX. ClpX with bound ADP and ClpA crystallize not as ring

hexamers but in "lock washer" conformations in which subunits are related by a screw axis (Guo et al., 2002; Kim and Kim, 2003). If the ADP states of these ATPases resembled this lock-washer conformation, then only a subset of the IGF loops would be positioned to contact a ClpP ring.

Our results suggest that one role of the sensor-II helix in ClpX is to link ATP binding with structural changes required for the "ATP" conformation. The ClpX R370K sensor-II mutant binds but cannot hydrolyze ATP, has low affinity for ClpP and ssrA-tagged substrates, and has no GFP-ssrA unfolding or degradation activity. We propose that the defects of this mutant arise because it is trapped in the "ADP" state irrespective of the identity of the bound nucleotide. Failure to adopt the "ATP" conformation would explain the absence of ATPase activity for the R370K mutant as well as its inability to bind strongly to ssrA-tagged substrates or to ClpP. The protein-processing defects of this mutant are easily explained by the ssrA-tag binding and ATP hydrolysis defects. Based on the *H. pylori* ClpX structure (Kim and Kim, 2003), the Arg370 side chain is positioned to contact bound ATP and these interactions could be needed to adopt or stabilize the "ATP" conformation. The inactivity in protein processing of ClpX hexamers containing mixtures of R370K and wild-type dimers suggests that the conformations and/or ATPase activities of different subunits must be coordinated in some fashion. ATPγS, which is hydrolyzed slowly, does not support unfolding of stable protein substrates by wild-type ClpX (Burton et al., 2003), again suggesting that proper coordination of ATP hydrolysis by different ClpX subunits is important.

Mutations at the C-terminal end of the sensor-II helix disrupt subunit-subunit packing in the hexamer and result in ClpX enzymes that bind but fail to unfold ssrA-tagged substrates (Joshi et al., 2003). ClpP binding suppresses the substrate processing defects of several of these sensor-II mutants, including ClpX D382K. ClpP binding to ClpX D382K is similar to wild-type ClpX in the absence of protein substrates but becomes much weaker in the presence of native substrates. These results suggest that when ClpX D382K binds to and attempts to unfold a native ssrA-tagged substrate, it becomes trapped in a conformation that is inactive for protein unfolding and binds ClpP poorly. Hence, maintenance of proper subunit-subunit contacts within ClpX appears to be essential both for substrate unfolding and for strong ClpP interactions. We propose that subunit-subunit contacts mediated by D382 and surrounding residues in *E. coli* ClpX resist tension that is generated when the enzyme applies an unfolding force to a native substrate. Such tension would be a natural consequence of the unfolding force applied to a protein substrate, as this process must create an equal and opposite force. If this tension results in quaternary distortions of ClpX D382K, then ClpP binding could stabilize the active ATPase conformation, allowing it to resist distortion and use the energy of ATP hydrolysis for productive conformational changes that drive substrate unfolding.

.

What role is served by communication between ClpX and ClpP during substrate processing? The total ClpX$_6$ concentration in *E. coli* is estimated to be within a few fold of K_{app} for the ClpX-ClpP interaction in the absence of substrate. Thus, substrate binding to free ClpX hexamers would be expected to drive assembly of ClpXP complexes. Because ClpP in the cell can associate with either ClpX or ClpA, this tightening could

provide a mechanism to distribute the peptidase based on whether substrates for one ATPase or the other were most prevalent. Communication may also facilitate translocation of denatured substrates from ClpX to ClpP by coordinating changes in the diameters of the ATPase processing pore and the peptidase entry portal. This coordination of conformational changes could allow efficient substrate transfer during the power stroke associated with each cycle of ATP hydrolysis and prevent slippage or dissociation during the recovery phase. It is also possible that coordination is required to allow efficient release of cleaved peptides from the degradation chamber at the same time that uncleaved polypeptide chains are entering the chamber. Finally, when ClpX hexamers are docked with both peptidase rings of ClpP, a situation expected when ClpX is in excess over ClpP, translocation appears to occur exclusively from one ClpX hexamer rather than simultaneously from both hexamers (Ortega et al., 2002). Communication between ClpX and ClpP would obviously be critical for regulating substrate traffic under these circumstances.

METHODS

Solutions. *Buffer A*: 43 mM Hepes-KOH (pH 7.6), 8.5 mM Tris-HCl (pH 8.0), 142 mM KCl, 15% (v/v) glycerol, 1.1 mM DTT, 5.4 mM $MgCl_2$, 420 μM EDTA, 36 μM $ZnSO_4$, 36 μM ATP, 0.032% (v/v) NP-40, and 0.004% (v/v) Triton X-100. *Buffer B*: 35 mM Hepes-KOH (pH 7.6), 4.4 mM Tris-HCl (pH 7.6), 1.5 mM Tris-HCl (pH 8.0), 95 mM KCl, 14% (v/v) glycerol, 660 μM DTT, 7.4 mM $MgCl_2$, 85 μM EDTA, 19 μM $ZnSO_4$, 19 μM ATP, 0.16% (v/v) NP-40, and 0.002% (v/v) Triton X-100. *Buffer L*: contains 50 mM Tris-HCl (pH 7.6), 10% (v/v) glycerol, 1 mM DTT, and 0.5 mM EDTA. *Buffer M*:

47 mM Tris-HCl (pH 7.6), 284 mM KCl, 9.5% (v/v) glycerol, 4.7 mM DTT, 95 µM

MgCl$_2$, and 10 mM EDTA. *Buffer N*: 50 mM sodium phosphate (pH 8.0), 300 mM NaCl,

and 250 mM imidazole. *Buffer S*: 50 mM Tris-HCl (pH 8.0), 300 mM KCl, 10% (v/v)

glycerol, 3 mM DTT, and 10 mM MgCl$_2$. *ATP mix I*: 5 mM ATP, 16 mM creatine

phosphate, and 0.32 mg ml^{-1} creatine phosphokinase. *ATP mix III*: 2.5 mM ATP, 1 mM

NADH, 7.5 mM phosphoenolpyruvate, 0.05 mg ml^{-1} pyruvate kinase, and 0.025 mg ml^{-1}

lactate dehydrogenase.

Strains, Plasmids, and Proteins. *E. coli* strain CF150, an X90 derivative, in which a *cat*

gene replaces the *clpP*, *clpX*, and *lon* genes, was provided by C. Farrell (MIT). A plasmid

expressing His$_6$-ClpX R370K (pSJ62) was produced using overlap extension mutagenesis

(Joshi et al., 2003). A plasmid expressing ClpX loopless (pGH003) was constructed from

pET-3a-ClpX (Levchenko et al., 1995) by polymerase chain reaction. In ClpX loopless, a

GSGSG sequence replaces wild-type residues 264–278. The synthetic peptide sequence

containing ClpX's IGF loop was fluorescein-NH-KKGRYTGSG<u>IGF</u>GATVKAK-

CONH$_2$.

ClpX loopless and wild-type ClpX were purified as described (Burton et al., 2003), as

were GFP-ssrA and His$_6$-tagged variants of ClpP, ClpX, and titin-I27-ssrA (Kim et al.,

2000; Joshi et al., 2003; Kenniston et al., 2003). ^{35}S-titin-ssrA variants were gifts from J.

Kenniston (MIT), and SspB was provided by D. Wah (MIT). His$_6$-ClpP S97A was

purified from *E. coli* strain CF150 containing pYK162 (Flynn et al., 2003) using a

published protocol (Kim et al., 2000) with modifications. After Mono Q chromatography,

ClpP S97A fractions were applied to a HiPrep 16/60 Sephacryl S-300HR column (Amersham Biosciences) equilibrated in buffer S. Purified protein fractions were pooled and stored at −80 °C. Carboxymethylation of titin-ssrA variants and acylation of ClpP variants with DFP were performed as described (Kim et al., 2000; Kenniston et al., 2003). Chemically modified proteins were dialyzed extensively before use.

E. coli ClpP was purified using a published protocol (Levchenko et al., 1997) with modifications. Cells were resuspended in 3 ml of buffer L plus 150 mM KCl for each gram of cells, lysed by French press, and centrifuged at 15,000 rpm in a SA-600 rotor for 60 min. The supernatant was filtered, ammonium sulfate was added to 30% (w/v) saturation, and the supernatant containing ClpP was retained after centrifugation. Ammonium sulfate was added to this supernatant to 60% (w/v) saturation, and the pellet containing ClpP was recovered by centrifugation. The pellet was resuspended, desalted into buffer L plus 150 mM KCl using a PD-10 column (Amersham Biosciences), and loaded onto a HiLoad 16/10 Q Sepharose HP column (Amersham Biosciences) equilibrated in buffer L with 150 mM KCl. ClpP was eluted with a 200 ml linear gradient from 150 mM to 400 mM KCl in buffer L and concentrated by ammonium sulfate precipitation (60% (w/v) saturation). The pellet containing ClpP was resuspended, desalted into buffer L plus 100 mM KCl, and loaded onto a HiPrep 16/60 Sephacryl S-300HR column equilibrated in this buffer. Fractions containing purified ClpP were pooled, concentrated by chromatography on a HiLoad 16/10 Q Sepharose HP column, and stored in aliquots at −80 °C.

Nucleotide hydrolysis and binding assays. ATP hydrolysis by ClpX in buffer A was measured at 30 °C using a coupled assay (Kim et al., 2001). ClpX and ClpP were incubated for two min before addition of substrate and/or ATP mix III. Except where noted, 50 nM $ClpX_6$ was used for all assays. K_{app} values for ClpX-ClpP binding were determined by plotting ATPase rates (R_{obs}) versus the total ClpP concentration (PT) and fitting to equation 1: $R_{obs} = R0 \pm (R1*((XT + PT + K_{app}) - SQRT((XT + PT + K_{app})^2 - (4*XT*PT))))/(2*XT)$, where $R0$ is the ATPase rate without ClpP, $R1$ is the ATPase rate with saturating ClpP, and XT is the total ClpX concentration (Segel, 1975). Mant-ADP or mant-ATP binding to ClpX R370K was assayed at 4 °C in buffer M (Burton et al., 2003).

Substrate unfolding, degradation, and binding assays. GFP-ssrA unfolding or degradation (Kim et al., 2000) was performed in buffer B plus ATP mix I at 30 °C. In mixing experiments with ClpX R370K, wild-type and mutant ClpX were preincubated for 5 min at 30 °C, ClpP and ATP mix I were added, and GFP-ssrA was added two min later to start the reaction. Degradation of ^{35}S-titin-ssrA substrates was assayed by TCA-soluble peptide release (Gottesman et al., 1998; Kenniston et al., 2003). For ClpXP degradation of titin-ssrA substrates at saturating concentrations, the slow steps are denaturation (k_{den}) and translocation (k_{trans}), with $1/k_{deg} = 1/k_{den} + 1/k_{trans}$ and $\tau_{deg} = \tau_{den} + \tau_{trans}$ (Kenniston et al., 2003). K_{app} for the ClpX-ClpP interaction during substrate processing can be expressed as $(\tau_{den}/\tau_{deg}) \cdot K_{app}^{den} + (\tau_{trans}/\tau_{deg}) \cdot K_{app}^{trans}$. The value of k_{trans} for different titin-ssrA substrates is essentially constant (4.3 min^{-1}). Substitution of $\tau_{deg} - \tau_{trans}$ for τ_{den} and rearrangement of terms yields the linear equation $K_{app} = \tau_{trans} \cdot (K_{app}^{trans} - K_{app}^{den}) \cdot k_{deg} + K_{app}^{den}$ (eq. 2). The general equation for inhibition by mixed hexamer

158

formation between active and inactive dimers of ClpX is $A = (1 + 3 \cdot A_{21} \cdot B \cdot R + 3 \cdot A_{12} \cdot B^2 \cdot R^2)/(1 + B \cdot R)^2$ (eq. 3) where A is the fractional activity of fully active hexamers, A_{21} is the fractional activity of a hexamer with two active and one inactive dimer, A_{12} is the activity of a hexamer with one active and two inactive dimers, R is the ratio of total inactive to total active subunits, and B is the mixing bias. $B=1$ indicates unbiased mixing of active and inactive dimers; $B<1$ indicates a preference of active dimers to associate with other active dimers rather than inactive dimers. If three active dimers are required for activity, eq. 3 simplifies to $A = (1 + B \cdot R)^{-2}$ (eq. 4). Binding of a fluorescent ssrA peptide to ClpX or ClpX R370K was assayed by changes in fluorescence anisotropy as described (Wah et al., 2002).

Pull-down and ternary complex assays. ClpXP pull-down assays were performed using a published protocol with modifications (Kim et al., 2001). Each reaction (30 μL) contained 300 nM His_6-$ClpX_6$ (wild-type or R370K) and 300 nM untagged $ClpP_{14}$. Some reactions also contained 300 nM untagged wild-type $ClpX_6$. 3 mM nucleotide (ATPγS, ATP, or ADP) was present during initial complex formation and in washes after binding to Ni^{++}-NTA agarose. Protein was eluted in 30 μL buffer N and subjected to SDS-PAGE. Gels were stained with Sypro Orange (Molecular Probes) and visualized using a FluorImager 595 (Molecular Dynamics). Assays for ternary complexes of ClpX, SspB, and GFP-ssrA were performed by gel-filtration chromatography on a Superdex 200 column (Amersham Biosciences) as described (Wah et al., 2002).

References

Beuron, F., Maurizi, M. R., Belnap, D. M., Kocsis, E., Booy, F. P., Kessel, M., and Steven, A. C. (1998). At sixes and sevens: characterization of the symmetry mismatch of the ClpAP chaperone-assisted protease. J Struct Biol *123*, 248-259.

Bochtler, M., Ditzel, L., Groll, M., and Huber, R. (1997). Crystal structure of heat shock locus V (HslV) from Escherichia coli. Proc Natl Acad Sci U S A *94*, 6070-6074.

Bochtler, M., Hartmann, C., Song, H. K., Bourenkov, G. P., Bartunik, H. D., and Huber, R. (2000). The structures of HsIU and the ATP-dependent protease HsIU-HsIV. Nature *403*, 800-805.

Burton, R. E., Baker, T. A., and Sauer, R. T. (2003). Energy-dependent degradation: Linkage between ClpX-catalyzed nucleotide hydrolysis and protein-substrate processing. Protein Sci *12*, 893-902.

Flynn, J. M., Neher, S. B., Kim, Y. I., Sauer, R. T., and Baker, T. A. (2003). Proteomic discovery of cellular substrates of the ClpXP protease reveals five classes of ClpX-recognition signals. Mol Cell *11*, 671-683.

Glickman, M. H., Rubin, D. M., Coux, O., Wefes, I., Pfeifer, G., Cjeka, Z., Baumeister, W., Fried, V. A., and Finley, D. (1998). A subcomplex of the proteasome regulatory particle required for ubiquitin-conjugate degradation and related to the COP9-signalosome and eIF3. Cell *94*, 615-623.

Gottesman, S., Maurizi, M. R., and Wickner, S. (1997a). Regulatory subunits of energy-dependent proteases. Cell *91*, 435-438.

Gottesman, S., Roche, E., Zhou, Y., and Sauer, R. T. (1998). The ClpXP and ClpAP proteases degrade proteins with carboxy-terminal peptide tails added by the SsrA-tagging system. Genes Dev *12*, 1338-1347.

Gottesman, S., Wickner, S., and Maurizi, M. R. (1997b). Protein quality control: triage by chaperones and proteases. Genes Dev *11*, 815-823.

Grimaud, R., Kessel, M., Beuron, F., Steven, A. C., and Maurizi, M. R. (1998). Enzymatic and structural similarities between the Escherichia coli ATP-dependent proteases, ClpXP and ClpAP. J Biol Chem *273*, 12476-12481.

Groll, M., Bajorek, M., Kohler, A., Moroder, L., Rubin, D. M., Huber, R., Glickman, M. H., and Finley, D. (2000). A gated channel into the proteasome core particle. Nat Struct Biol *7*, 1062-1067.

Groll, M., Ditzel, L., Lowe, J., Stock, D., Bochtler, M., Bartunik, H. D., and Huber, R. (1997). Structure of 20S proteasome from yeast at 2.4 A resolution. Nature *386*, 463-471.

Guenther, B., Onrust, R., Sali, A., O'Donnell, M., and Kuriyan, J. (1997). Crystal structure of the delta' subunit of the clamp-loader complex of E. coli DNA polymerase III. Cell *91*, 335-345.

Guo, F., Maurizi, M. R., Esser, L., and Xia, D. (2002). Crystal structure of ClpA, an Hsp100 chaperone and regulator of ClpAP protease. J Biol Chem *277*, 46743-46752.

Hersch, G. L., Burton, R. E., Bolon, D. N., Baker, T. A., and Sauer, R. T. (2005). Asymmetric interactions of ATP with the AAA+ ClpX6 unfoldase: allosteric control of a protein machine. Cell, (in press).

Hwang, B. J., Woo, K. M., Goldberg, A. L., and Chung, C. H. (1988). Protease Ti, a new ATP-dependent protease in Escherichia coli, contains protein-activated ATPase and proteolytic functions in distinct subunits. J Biol Chem *263*, 8727-8734.

Joshi, S. A., Baker, T. A., and Sauer, R. T. (2003). C-terminal domain mutations in ClpX uncouple substrate binding from an engagement step required for unfolding. Mol Microbiol *48*, 67-76.

Karon, B. S., Mahaney, J. E., and Thomas, D. D. (1994). Halothane and cyclopiazonic acid modulate Ca-ATPase oligomeric state and function in sarcoplasmic reticulum. Biochemistry *33*, 13928-13937.

Kenniston, J. A., Baker, T. A., Fernandez, J. M., and Sauer, R. T. (2003). Linkage between ATP consumption and mechanical unfolding during the protein processing reactions of an AAA+ degradation machine. Cell *114*, 511-520.

Kim, D. Y., and Kim, K. K. (2003). Crystal Structure of ClpX Molecular Chaperone from Helicobacter pylori. J Biol Chem *278*, 50664-50670.

Kim, Y. I., Burton, R. E., Burton, B. M., Sauer, R. T., and Baker, T. A. (2000). Dynamics of substrate denaturation and translocation by the ClpXP degradation machine. Mol Cell *5*, 639-648.

Kim, Y. I., Levchenko, I., Fraczkowska, K., Woodruff, R. V., Sauer, R. T., and Baker, T. A. (2001). Molecular determinants of complex formation between Clp/Hsp100 ATPases and the ClpP peptidase. Nat Struct Biol *8*, 230-233.

Levchenko, I., Luo, L., and Baker, T. A. (1995). Disassembly of the Mu transposase tetramer by the ClpX chaperone. Genes Dev *9*, 2399-2408.

Levchenko, I., Yamauchi, M., and Baker, T. A. (1997). ClpX and MuB interact with overlapping regions of Mu transposase: implications for control of the transposition pathway. Genes Dev *11*, 1561-1572.

Neuwald, A. F., Aravind, L., Spouge, J. L., and Koonin, E. V. (1999). AAA+: A class of chaperone-like ATPases associated with the assembly, operation, and disassembly of protein complexes. Genome Res *9*, 27-43.

Ogura, T., and Wilkinson, A. J. (2001). AAA+ superfamily ATPases: common structure-diverse function. Genes Cells *6*, 575-597.

Ortega, J., Lee, H. S., Maurizi, M. R., and Steven, A. C. (2002). Alternating translocation of protein substrates from both ends of ClpXP protease. Embo J *21*, 4938-4949.

Ortega, J., Singh, S. K., Ishikawa, T., Maurizi, M. R., and Steven, A. C. (2000). Visualization of substrate binding and translocation by the ATP-dependent protease, ClpXP. Mol Cell *6*, 1515-1521.

Ramachandran, R., Hartmann, C., Song, H. K., Huber, R., and Bochtler, M. (2002). Functional interactions of HslV (ClpQ) with the ATPase HslU (ClpY). Proc Natl Acad Sci U S A *99*, 7396-7401.

Segel, I. H. (1975). Enzyme kinetics : behavior and analysis of rapid equilibrium and steady state enzyme systems (New York, Wiley).

Seol, J. H., Yoo, S. J., Shin, D. H., Shim, Y. K., Kang, M. S., Goldberg, A. L., and Chung, C. H. (1997). The heat-shock protein HslVU from Escherichia coli is a protein-activated ATPase as well as an ATP-dependent proteinase. Eur J Biochem *247*, 1143-1150.

Seong, I. S., Kang, M. S., Choi, M. K., Lee, J. W., Koh, O. J., Wang, J., Eom, S. H., and Chung, C. H. (2002). The C-terminal tails of HslU ATPase act as a molecular switch for activation of HslV peptidase. J Biol Chem *277*, 25976-25982.

Singh, S. K., Grimaud, R., Hoskins, J. R., Wickner, S., and Maurizi, M. R. (2000). Unfolding and internalization of proteins by the ATP-dependent proteases ClpXP and ClpAP. Proc Natl Acad Sci U S A *97*, 8898-8903.

Singh, S. K., Guo, F., and Maurizi, M. R. (1999). ClpA and ClpP remain associated during multiple rounds of ATP-dependent protein degradation by ClpAP protease. Biochemistry *38*, 14906-14915.

Singh, S. K., Rozycki, J., Ortega, J., Ishikawa, T., Lo, J., Steven, A. C., and Maurizi, M. R. (2001). Functional domains of the ClpA and ClpX molecular chaperones identified by limited proteolysis and deletion analysis. J Biol Chem *276*, 29420-29429.

Sousa, M. C., Kessler, B. M., Overkleeft, H. S., and McKay, D. B. (2002). Crystal structure of HslUV complexed with a vinyl sulfone inhibitor: corroboration of a proposed mechanism of allosteric activation of HslV by HslU. J Mol Biol *318*, 779-785.

Sousa, M. C., and McKay, D. B. (2001). Structure of Haemophilus influenzae HslV protein at 1.9 A resolution, revealing a cation-binding site near the catalytic site. Acta Crystallogr D Biol Crystallogr *57*, 1950-1954.

Sousa, M. C., Trame, C. B., Tsuruta, H., Wilbanks, S. M., Reddy, V. S., and McKay, D. B. (2000). Crystal and solution structures of an HslUV protease-chaperone complex. Cell *103*, 633-643.

Thompson, M. W., Singh, S. K., and Maurizi, M. R. (1994). Processive degradation of proteins by the ATP-dependent Clp protease from Escherichia coli. Requirement for the multiple array of active sites in ClpP but not ATP hydrolysis. J Biol Chem *269*, 18209-18215.

Wah, D. A., Levchenko, I., Baker, T. A., and Sauer, R. T. (2002). Characterization of a Specificity Factor for an AAA+ ATPase. Assembly of SspB Dimers with ssrA-Tagged Proteins and the ClpX Hexamer. Chem Biol *9*, 1237-1245.

Wang, J., Hartling, J. A., and Flanagan, J. M. (1997). The structure of ClpP at 2.3 A resolution suggests a model for ATP-dependent proteolysis. Cell *91*, 447-456.

Wang, J., Hartling, J. A., and Flanagan, J. M. (1998). Crystal structure determination of Escherichia coli ClpP starting from an EM-derived mask. J Struct Biol *124*, 151-163.

Wang, J., Song, J. J., Franklin, M. C., Kamtekar, S., Im, Y. J., Rho, S. H., Seong, I. S., Lee, C. S., Chung, C. H., and Eom, S. H. (2001a). Crystal structures of the HslVU peptidase-ATPase complex reveal an ATP-dependent proteolysis mechanism. Structure (Camb) *9*, 177-184.

Wang, J., Song, J. J., Seong, I. S., Franklin, M. C., Kamtekar, S., Eom, S. H., and Chung, C. H. (2001b). Nucleotide-dependent conformational changes in a protease-associated ATPase HslU. Structure (Camb) *9*, 1107-1116.

Whitby, F. G., Masters, E. I., Kramer, L., Knowlton, J. R., Yao, Y., Wang, C. C., and Hill, C. P. (2000). Structural basis for the activation of 20S proteasomes by 11S regulators. Nature *408*, 115-120.

Wojtyra, U. A., Thibault, G., Tuite, A., and Houry, W. A. (2003). The N-terminal zinc binding domain of ClpX is a dimerization domain that modulates the chaperone function. J Biol Chem *278*, 48981-48990.

Yoo, S. J., Seol, J. H., Shin, D. H., Rohrwild, M., Kang, M. S., Tanaka, K., Goldberg, A. L., and Chung, C. H. (1996). Purification and characterization of the heat shock proteins HslV and HslU that form a new ATP-dependent protease in Escherichia coli. J Biol Chem *271*, 14035-14040.

Acknowledgments